

Vibration Analysis of Thickness- and Width- Tapered Laminated Composite Beams using Hierarchical Finite Element Method

Mohammad Amin Fazili

A thesis

in

the Department

of

Mechanical and Industrial Engineering

Presented in Partial Fulfillment of the Requirements

For the Degree of

Master of Applied Science (Mechanical Engineering) at

Concordia University

Montreal, Quebec, Canada

September 2013

©Mohammad Amin Fazili 2013

CONCORDIA UNIVERSITY
School of Graduate Studies

This is to certify that the Thesis prepared,

By: **Mohammad Amin Fazili**

Entitled: **Vibration Analysis of Thickness- and Width-Tapered Laminated Composite Beams using Hierarchical Finite Element Method**

and submitted in partial fulfillment of the requirements for the Degree of

Master of Applied Science (Mechanical Engineering)

complies with the regulations of this University and meets the accepted standards with respect to originality and quality.

Signed by the final Examining Committee:

_____	Chair
Dr. Z.C. Chen	
_____	Examiner
Dr. S.V. Hoa	
_____	Examiner (external)
Dr. Y. Shayan	
_____	Supervisor
Dr. R. Ganesan	

Approved by: _____
Chair of Department or Graduate Program Director

Dean of Faculty

Date: **September 30, 2013**

ABSTRACT

Vibration Analysis of Thickness- and Width-Tapered Laminated Composite Beams using Hierarchical Finite Element Method

Mohammad Amin Fazili

Tapered laminated composite beams provide stiffness-tailoring and mass-tailoring design capabilities. They are increasingly and widely being used in engineering applications including robotic manipulators, aircraft wings, space structures, helicopter blades and yokes, turbine blades, and civil infrastructure. In the present work, the free and the forced vibration response of symmetric linear-thickness-and-width-tapered laminated composite beams are considered. Considering a variety of tapered configurations according to different types of plies drop-off configurations both conventional and hierarchical finite element formulations are developed based on cylindrical laminated beam bending theory. Natural frequencies, mode shapes and forced vibration response of different types of internally-tapered composite beams are determined. Comparison of the hierarchical finite element solution with the Rayleigh-Ritz and a higher-order finite element solution is performed. A parametric study is conducted to investigate the effects of boundary conditions, width-ratio, taper configurations, thickness-tapering angle, laminate configuration, compressive axial force and damping on the free and forced vibration response of thickness- and width-tapered laminated composite beams.

ACKNOWLEDGEMENTS

It is my great pleasure to show my appreciation to many people who made this thesis possible.

First and foremost, I would like to dedicate this accomplishment to my dearest parents, Dr. Amir Fazili and Dr. Fariba Zahedi, and thank them for all their endless love, priceless guidance and unconditional support.

Then, I offer my sincerest gratitude to my supervisor, Dr. Rajamohan Ganesan, who has supported me, throughout my thesis research with his kind attention, inspiring guidance, patience and immense knowledge.

I am also thankful to all my friends at graduate research office EV 13.167 who supported me by sharing ideas and discussion during my research studies.

Last but not least, I would like to dedicate this thesis to my dear aunt Farangis Zahedi and my beloved cousin Amir Karimi who have always encouraged me to achieve high academic success throughout my life.

Thank You.

Table of Contents

ABSTRACT.....	iii
ACKNOWLEDGEMENTS.....	iv
Table of Contents.....	v
List of Figures.....	viii
List of Tables.....	xv
Nomenclature.....	xviii
1. Introduction, literature review and scope of the thesis.....	1
1.1 Vibration analysis in mechanical design.....	1
1.2 Composite materials and structures.....	2
1.3 Finite element method.....	4
1.4 Literature survey.....	5
1.4.1 Vibration analysis of uniform laminated composite beams.....	5
1.4.2 Vibration analysis of tapered composite beams.....	6
1.4.3 Finite Element Method.....	7
1.5 Objectives of the thesis.....	8
1.6 Layout of the thesis.....	8
2. Finite element formulation and free vibration analysis of uniform composite beams.....	10
2.1 Introduction.....	10

2.2	Cylindrical bending of laminated composite beams	11
2.3	Conventional Finite Element Method (CFEM) formulation.....	13
2.4	Hierarchical Finite Element Method (HFEM) formulation	16
2.5	Free vibration analysis of a uniform laminated composite beam.....	18
2.6	Summary	23
3.	Free vibration analysis of tapered composite beams	24
3.1	Introduction	24
3.2	Free vibration analysis of width-tapered laminated composite beams	25
3.2.1	Effect of boundary conditions on natural frequencies	25
3.2.2	Effect of width-ratio on natural frequencies	27
3.2.3	Effect of taper angle (or equivalently length of the beam) on natural frequencies....	29
3.2.4	Effect of laminate configuration on natural frequencies.....	31
3.2.5	Effect of axial force on natural frequencies	34
3.3	Free vibration analysis of thickness-tapered laminated composite beams.....	36
3.3.1	Effect of boundary condition on natural frequencies.....	37
3.3.2	Effect of taper angle (or equivalently length of the beam) on natural frequencies....	39
3.3.3	Effect of laminate configuration on natural frequencies.....	42
3.3.4	Effect of taper configuration on natural frequencies	44
3.3.5	Effect of axial force on natural frequencies	46
3.4	Free vibration analysis of thickness- and width-tapered laminated composite beams ..	48
3.4.1	Effect of boundary condition on natural frequencies.....	48
3.4.2	Effect of taper angle (or equivalently length of the beam) on natural frequencies....	50

3.4.3	Effect of laminate configuration on natural frequencies.....	52
3.4.4	Effect of width-ratio on natural frequencies	54
3.4.5	Effect of taper configuration on natural frequencies	56
3.4.6	Effect of axial force on natural frequencies.....	58
3.4.7	Effect of damping on natural frequencies	60
3.5	Summary	65
4.	Forced vibration analysis of tapered composite beams.....	68
4.1	Introduction	68
4.2	Undamped Forced vibration analysis.....	69
4.2.1	Formulation.....	69
4.2.2	Forced vibration response of uniform composite beams	71
4.2.3	Forced vibration response of thickness- and width-tapered composite beams.....	77
4.2.3.1	Effect of taper configuration on forced vibration response.....	80
4.2.3.2	Effect of width-ratio on forced vibration response.....	85
4.3	Damped forced vibration analysis.....	94
4.3.1	Formulation.....	94
4.3.2	Damped forced vibration response of uniform composite beams.....	95
4.3.3	Damped forced vibration response of thickness- and width-tapered composite beams	99
4.4	Summary	109
5.	Conclusion and future work	111
5.1	Major contributions	111

5.2	Conclusions	112
5.3	Recommendations for future work.....	116
	BIBLIOGRAPHY.....	117
	APPENDIX A.....	122
	APPENDIX B.....	144

List of Figures

Figure 1.1	Applications of tapered composite structures.....	3
Figure 2.1	Global coordinate system	11
Figure 2.2	Element's nodal degrees of freedom	13
Figure 3.1	Width-tapered composite beam	25
Figure 3.2	Boundary conditions.....	26
Figure 3.3	Effect of width-ratio on the first natural frequency of the width-tapered composite beam	27
Figure 3.4	Effect of width-ratio on the second natural frequency of the width-tapered composite beam	28
Figure 3.5	Effect of width-ratio on the third natural frequency of the width-tapered composite beam	28
Figure 3.6	Effect of length on the first natural frequency of the width-tapered composite beam	30

Figure 3.7 Effect of length on the second natural frequency of the width-tapered composite beam	30
Figure 3.8 Effect of length on the third natural frequency of the width-tapered composite beam	31
Figure 3.9 LC1, LC2, LC3 and LC4 laminate configurations	32
Figure 3.10 Effect of laminate configuration on the first natural frequency of the width-tapered composite beam	32
Figure 3.11 Effect of laminate configuration on the second natural frequency of the width-tapered composite beam	33
Figure 3.12 Effect of laminate configuration on the third natural frequency of the width-tapered composite beam	33
Figure 3.13 Effect of compressive axial force on the first natural frequency of the width-tapered composite beam	34
Figure 3.14 Effect of compressive axial force on the second natural frequency of the width-tapered composite beam	35
Figure 3.15 Effect of compressive axial force on the third natural frequency of the width-tapered composite beam	35
Figure 3.16 Taper Configurations	37
Figure 3.17 Effect of the length on the first natural frequency of the thickness-tapered composite beam	40
Figure 3.18 Effect of the laminate configuration on the first natural frequency of thickness-tapered composite beam	43

Figure 3.19 Effect of taper configuration on the first natural frequency of the thickness-tapered composite beam	44
Figure 3.20 Effect of taper configuration on the second natural frequency of the thickness-composite tapered beam	45
Figure 3.21 Effect of taper configuration on the third natural frequency of the thickness-tapered composite beam	45
Figure 3.22 Effect of compressive axial force on the first natural frequency of the thickness-tapered composite beam	47
Figure 3.23 Effect of the length on the first natural frequency of the thickness- and width-tapered composite beams ($b_R/b_L=0.5$)	51
Figure 3.24 Effect of laminate configuration on the first natural frequency of the thickness- and width-tapered composite beam ($b_R/b_L=0.5$)	53
Figure 3.25 Effect of width-ratio on the first natural frequency of the thickness- and width-tapered composite beam	55
Figure 3.26 Effect of taper configuration on the first natural frequency of the thickness- and width-tapered composite beam ($b_R/b_L=0.5$)	56
Figure 3.27 Effect of taper configuration on the second natural frequency of the thickness- and width-tapered composite beam ($b_R/b_L=0.5$)	57
Figure 3.28 Effect of taper configuration on the third natural frequency of the thickness- and width-tapered composite beam ($b_R/b_L=0.5$)	57
Figure 3.29 Effect of compressive axial force on the first natural frequency of the thickness- and width-tapered composite beam ($b_R/b_L=0.5$)	59

Figure 4.1 Element’s nodal degrees of freedom	71
Figure 4.2 Location of the forces and the moments and the response points for different boundary conditions for uniform laminated composite beam	72
Figure 4.3 First three mode shapes of uniform laminated composite beams with different boundary conditions	74
Figure 4.4 Forced vibration response (maximum deflection) of the uniform composite beams for different boundary conditions.....	75
Figure 4.5 Forced vibration response (maximum rotation) of the uniform composite beams for different boundary conditions.....	76
Figure 4.6 Location of the forces and the moments and the response points for different boundary conditions	78
Figure 4.7 First three mode shapes of thickness- and width-tapered laminated composite beams with different boundary conditions.....	79
Figure 4.8 Forced vibration response of the thickness- and width-tapered simply supported composite beams with different taper configurations.....	81
Figure 4.9 Forced vibration response of the thickness- and width-tapered clamped-clamped composite beams with different taper configurations.....	82
Figure 4.10 Forced vibration response of the thickness- and width-tapered clamped-free composite beams with different taper configurations.....	83
Figure 4.11 Forced vibration response of the thickness- and width-tapered free-clamped composite beams with different taper configurations.....	84

Figure 4.12 Effect of width-ratio (b_R/b_L) on forced vibration response in terms of maximum deflection of the thickness- and width-tapered composite beam with taper configuration A.....	86
Figure 4.13 Effect of width-ratio (b_R/b_L) on forced vibration response in terms of maximum deflection of the thickness- and width-tapered composite beam with taper configuration B.....	87
Figure 4.14 Effect of width-ratio (b_R/b_L) on forced vibration response in terms of maximum deflection of the thickness- and width-tapered composite beam with taper configuration C.....	88
Figure 4.15 Effect of width-ratio (b_R/b_L) on forced vibration response in terms of maximum deflection of the thickness- and width-tapered composite beam with taper configuration D.....	89
Figure 4.16 Effect of width-ratio (b_R/b_L) on forced vibration response in terms of maximum rotation of the thickness- and width-tapered composite beam with taper configuration A...	90
Figure 4.17 Effect of width-ratio (b_R/b_L) on forced vibration response in terms of maximum rotation of the thickness- and width-tapered composite beam with taper configuration B...	91
Figure 4.18 Effect of width-ratio (b_R/b_L) on forced vibration response in terms of maximum rotation of the thickness- and width-tapered composite beam with taper configuration C...	92
Figure 4.19 Effect of width-ratio (b_R/b_L) on forced vibration response in terms of maximum rotation of the thickness- and width-tapered composite beam with taper configuration D...	93
Figure 4.20 Undamped vs. damped forced response in terms of maximum deflection for the uniform composite beam with different boundary conditions	97

Figure 4.21 Undamped vs. damped forced response in terms of maximum rotation for the uniform composite beam with different boundary conditions	98
Figure 4.22a Effect of damping on forced vibration response in terms of maximum deflection of the simply supported composite beams with different taper configurations	101
Figure 4.22b Magnified views of plots given in Figure 4.22a near 1 st resonance	102
Figure 4.23a Effect of damping on forced vibration response in terms of maximum deflection of the clamped-clamped composite beams with different taper configurations	103
Figure 4.23b Magnified views of plots given in Figure 4.23a near 1 st resonance	104
Figure 4.24a Effect of damping on forced vibration response in terms of maximum deflection of the clamped-free composite beams with different taper configurations.....	105
Figure 4.24b Magnified views of plots given in Figure 4.24a near 1 st resonance	106
Figure 4.25a Effect of damping on forced vibration response in terms of maximum deflection of the free-clamped composite beams with different taper configurations.....	107
Figure 4.25b Magnified views of plots given in Figure 4.25a near 1 st resonance	108
Figure A.1 Effect of the length on the second natural frequency of the thickness-tapered composite beam	130
Figure A.2 Effect of the length on the third natural frequency of the thickness-tapered composite beam	131
Figure A.3 Effect of the laminate configuration on the second natural frequency of the thickness-tapered composite beam	132
Figure A.4 Effect of the laminate configuration on the third natural frequency of the thickness-tapered composite beam	133

Figure A.5 Effect of compressive axial force on the second natural frequency of the thickness-tapered composite beam	134
Figure A.6 Effect of compressive axial force on the third natural frequency thickness-tapered composite beam	135
Figure A.7 Effect of the length on the second natural frequency of the thickness- and width-tapered composite beam	136
Figure A.8 Effect of the length on the third natural frequency of the thickness- and width-tapered composite beam	137
Figure A.9 Effect of laminate configuration on the second natural frequency of the thickness- and width-tapered composite beam	138
Figure A.10 Effect of laminate configuration on the third natural frequency of thickness- and width-tapered composite beam	139
Figure A.11 Effect of width-ratio on the second natural frequency of the thickness- and width-tapered composite beam	140
Figure A.12 Effect of width-ratio on the third natural frequency of the thickness- and width-tapered composite beam	141
Figure A.13 Effect of compressive axial force on the second natural frequency of the thickness- and width-tapered composite beam	142
Figure A.14 Effect of compressive axial force on the third natural frequency of the thickness- and width-tapered composite beam	143

List of Tables

Table 2.1 Mechanical properties of ply.....	18
Table 2.2 Mechanical properties of resin material.....	18
Table 2.3 Boundary condition coefficients for the uniform composite beams.....	20
Table 2.4 The comparison between CFEM and HFEM and the exact value of the first three natural frequencies for simply supported uniform composite beams.....	20
Table 2.5 The comparison between CFEM and HFEM and the exact value of the first three natural frequencies for clamped-clamped uniform composite beams.....	21
Table 2.6 The comparison between CFEM and HFEM and the exact value of the first three natural frequencies for clamped-free uniform composite beams.....	21
Table 3.1 Natural frequencies of width-tapered composite beam for different boundary conditions.....	26
Table 3.2 First natural frequencies (rad/s) of thickness-tapered composite beams.....	38
Table 3.3 Second natural frequencies (rad/s) of thickness-tapered composite beams.....	38
Table 3.4 Third natural frequencies (rad/s) of thickness-tapered composite beams.....	38
Table 3.5 First natural frequency (rad/s) of the thickness- and width-tapered composite beams for different boundary conditions ($b_R/b_L = 0.5$).....	49
Table 3.6 Second natural frequency (rad/s) of the thickness- and width-tapered composite beams for different boundary conditions ($b_R/b_L = 0.5$).....	49
Table 3.7 Third natural frequency (rad/s) of the thickness- and width-tapered composite beams for different boundary conditions ($b_R/b_L=0.5$).....	50

Table 3.8 Effect of damping on natural frequencies of thickness- and width-tapered composite beam with the taper configuration A ($b_R/b_L=0.5$).....	61
Table 3.9 Effect of damping on natural frequencies of thickness- and width-tapered composite beam with the taper configuration B ($b_R/b_L=0.5$).....	62
Table 3.10 Effect of damping on natural frequencies of thickness- and width-tapered composite beam with the taper configuration C ($b_R/b_L=0.5$).....	63
Table 3.11 Effect of damping on natural frequencies of thickness- and width-tapered composite beam with the taper configuration D ($b_R/b_L=0.5$).....	64
Table A.1 The first three natural frequencies of a width-tapered composite beam for different width ratios - A comparison between HFEM, HOFEM and R-R methods ($b_R/b_L= 0.01$) ..	122
Table A.2 The first three natural frequencies of a width-tapered composite beam for different width ratios - A comparison between HFEM, HOFEM and R-R methods ($b_R/b_L= 0.02$) ..	123
Table A.3 The first three natural frequencies of a width-tapered composite beam for different width ratios - A comparison between HFEM, HOFEM and R-R methods ($b_R/b_L= 0.05$) ..	124
Table A.4 The first three natural frequencies of a width-tapered composite beam for different width ratios - A comparison between HFEM, HOFEM and R-R methods ($b_R/b_L= 0.1$)	125
Table A.5 The first three natural frequencies of a width-tapered composite beam for different width ratios - A comparison between HFEM, HOFEM and R-R methods ($b_R/b_L= 0.4$)	126
Table A.6 The first three natural frequencies of a width-tapered composite beam for different width ratios - A comparison between HFEM, HOFEM and R-R methods ($b_R/b_L= 0.6$)	127
Table A.7 The first three natural frequencies of a width-tapered composite beam for different width ratios - A comparison between HFEM, HOFEM and R-R methods ($b_R/b_L= 0.8$)	128

Table A.8 The first three natural frequencies of a width-tapered composite beam for different width ratios - A comparison between HFEM, HOFEM and R-R methods ($b_R/b_L = 1.0$)	129
Table B.1 Assembly algorithm of K and M matrices in CFEM	144
Table B.2 Assembly algorithm of K and M matrices in HFEM with one hierarchical term	145

Nomenclature

H	Height of the laminate
H_p	Equivalent height of the ply in element
H_r	Equivalent height of the resin in element
t_i	Thickness of the i -th ply
L	Length of the beam
l_e	Length of the element
B	Uniform width of the beam
b_L, b_R	Width at the left section and the right section of the beam
$b(x)$	Width of the beam at coordinate x
b_R/b_L	Width-ratio
x	Longitudinal direction of the laminated beam
y	Transverse direction of the laminated beam
z	Thickness direction of the laminated beam
u	The longitudinal displacement
v	The transverse displacement
w	The displacement along thickness direction
E_1	Longitudinal modulus
E_2	Transverse modulus
G_{12}	In-plane shear modulus
ρ	Density
ρ_p	Density of ply

ρ_r	Density of resin
E	Elastic Modulus of resin
G	Shear modulus of resin
ν	Poisson's ratio of resin
ν_{12}	Major Poisson's ratio of ply
ν_{21}	Minor Poisson's ratio of ply
$[N^w]$	Shape functions of the beam
$[N^d]$	First derivatives of shape functions of the beam
$[N^M]$	Second derivatives of shape functions of the beam
LC	Laminate configuration
N	Number of hierarchical terms
θ	Rotation about the y-axis
A_i	Hierarchical degrees-of-freedom
B_i	Hierarchical force terms
$[k]$	Element stiffness matrix
$[K]$	Global stiffness matrix
$\{u\}$	Nodal displacement matrix of the beam
D_{11}	Coefficient of bending stiffness
\overline{Q}_{11}	Coefficient of transformed reduced stiffness matrix
N_x	Axial force per unit width along the x-axis
$[m]$	Element mass matrix
$[M]$	Global mass matrix
$[C]$	Global damping matrix

$[c]$	Interpolation functions' coefficient's matrix
λ	Square of the natural frequency of the beam
$\{\phi\}$	Eigenvector
ξ	Damping ratio
$\{y\}$	Vector of displacements in the transformed coordinates
$\{F\}$	Force vector
ω_i	i -th Natural frequency
ω_{di}	i -th Damped natural frequency
ω	Frequency of excitation
t	Time
FEM	Finite Element Method
CFEM	Conventional Finite Element Method
HFEM	Hierarchical Finite Element Method
HOFEM	Higher-Order Finite Element Method
R-R	Rayleigh-Ritz method
φ	Thickness-tapering angle
$[\tilde{P}]$	Orthonormal eigenvector matrix
α	Mass proportional Rayleigh damping constant
β	Stiffness proportional Rayleigh damping constant
P_{cr}	Critical buckling load

1. Introduction, literature review and scope of the thesis

1.1 Vibration analysis in mechanical design

Mechanical vibration is a time-dependent phenomenon which deals with the repetitive motion of an object relative to a stationary frame of reference. Mostly, vibration is undesirable, not only because of the waste of energy and unwanted resultant motions but also because of unwanted sound and noise. Vibration may also lead to fatigue and unpredictable failure of the structure or machine due to the created dynamic stresses in the structure. Hence in order to reduce or prevent the above-mentioned problems caused by vibration often the problem of controlling the vibration of the structure is encountered.

The vibration of a system may occur due to an excitation generated by initial displacement and/or initial velocity of the mass (free vibration) or may occur due to an excitation created by harmonically excited force (forced vibration). In free vibration mechanical system will vibrate at one or more of its natural frequencies. In this case, damping or friction from material itself or surrounding medium will cause the vibration to stop. In forced vibration, the system is forced to vibrate at the same frequency as that of the exciting harmonic force. In this case if the frequency of exciting force gets close to the natural frequencies of the system, the structure will undergo a vibration resonance in which the system will respond at greater amplitude than it does at other frequencies. There are many examples of structures failing or not meeting objectives or heavily reduced lifetime due to vibration resonances, fatigue or high noise levels in the system which can be avoided by proper vibration analysis.

1.2 Composite materials and structures

Composite material refers to material that is created by the synthetic assembly of two or more organic or inorganic materials in order to obtain specific material properties such as high strength and high stiffness to weight ratio, corrosion resistance, thermal properties, fatigue life and wear resistance and increased tolerance to damage [1]. Development and design of polymer composite materials and structures is the fastest growing segment of lightweight (durable and sustainable) construction and product engineering. Since fifteen years for each five years period the world market volume of advanced polymer composites was doubled. For the first decade of this millennium a growth of at least 700 percent was foreseen. The majority of structural parts in novel aircraft and space platform designs will be materialized in polymer composite materials. In case of fireproof interiors including floors and supporting structures (beams and brackets) the applied volume of composites are reaching the maximum of almost 100 percent and for the high performance and durable exterior shell structures almost 80 percent by volume is within the reach. The same trends and developments are true for inshore and offshore wind turbine blade designs and the development of the latest fast transport systems varying from trains, cars, ferries, trucks to ships and yachts, shows similar tendencies [2].

In some specific applications of composite structures such as helicopter yoke, robot arms, turbine blades and satellite antenna, the laminates need to be stiff at one location and flexible at another location. For example in a helicopter yoke, a progressive variation in the thickness of the yoke is required to provide high stiffness at the hub and flexibility at the middle of yoke length to accommodate for flapping. This type of structure is created by terminating or dropping off selected plies at specific locations to reduce the stiffness which is called as the tapered composite structure

[3]. Moreover, tapered composite structures are also being used in the sports industry (hockey blades, lacrosse shafts and etc.) because of their mass and stiffness tailoring properties. Figure 1.1 shows some applications of tapered composite structures.



Tapered hockey blade and shaft



Wind turbine blade



Helicopter yoke and blade



Aircraft wing

Figure 1.1 Applications of tapered composite structures [38 - 42]

1.3 Finite element method

Finite element method is a numerical technique derived from variational method for finding approximate solutions to problems. This method overcomes the disadvantage of the traditional variational methods by providing a systematic procedure for the derivation of the approximation functions over subregions of the domain. The method has three basic features that account for its superiority over other competing methods. First, a geometrically complex domain of the problem is represented as a collection of geometrically simple subdomains, called finite elements. Second, over each finite element, the approximation functions are derived using the basic idea that any continuous function can be represented by a linear combination of algebraic polynomials. Third, algebraic relations among undetermined coefficients (i.e., nodal values) are obtained by satisfying the governing equations, often in a weighted-integral sense, over each element. Thus, the finite element method can be viewed, in particular, as an element-wise application of the Rayleigh-Ritz or weighted-residual methods. The finite element method is one of the most powerful numerical techniques ever devised for solving differential (and integral) equations of initial and boundary-value problems in geometrically complicated regions [4]. The greatest advantage of the finite element method is its ability to analyze systems with all kinds of shapes, geometry, boundary conditions and non-linearities. As a result, it is one of the most accurate and powerful tools used to analyze complex mechanical structures such as the vibration of tapered laminated composite beams.

The convergence and accuracy of the results determined using finite element formulation depend strongly on the selected type of element. The type of element that is considered for the finite element formulation in this study has two degrees of freedom per node (deflection and

rotation) and two nodes per element. In Hierarchical Finite Element Method (HFEM) a number of trigonometric terms are added to the interpolation functions and therefore the corresponding hierarchical degrees of freedom will be added to each element. However, they are non-physical degrees of freedom and serve the purpose of keeping the stiffness matrix and mass matrix in hierarchical forms.

1.4 Literature survey

In this section an up-to-date and comprehensive literature survey on the important works done on the free and forced vibration response of uniform and tapered laminated composite beams is presented. There has been a lot of studies completed on the subject of vibration analyses of laminated composite plates and shells. However, there has been a rare amount of literature on vibration analysis of laminated composite beams despite their applicability in various industrial and commercial structures. Moreover, the works that have been done using HFEM on the analysis of the beams and plates are confined to homogeneous materials. The following is an up-to-date survey categorized by the subject:

1.4.1 Vibration analysis of uniform laminated composite beams

A free vibration analysis of uniform laminated composite beams without considering the effects of shear deformation and rotary inertia was conducted by Abarcar and Caniff [5]. Chandrashekhara et al. [6] have studied the free vibrations and obtained the natural frequencies of advanced composite beams. They have considered the effect of rotary inertia and shear deformation in the free vibration analysis of the beams. Miller and Adams [7] studied the vibration characteristics of the orthotropic clamped-free uniform beams using the classical laminate theory

without including the effect of shear deformation. Chen and Yang [8] studied the static and dynamic formulation of symmetrically laminated composite beams. Vinson and Sierakowski [9] determined the exact natural frequencies of a simply-supported uniform composite beam based on classical laminate theory. The free vibration analysis of composite beams using exact integration method was conducted by Hodges et al. [10]. Khdeir [11] have studied the free vibration of cross-ply laminated beams with arbitrary boundary conditions. Reddy [12], Berthelot [13], Whitney [14] and Jones [15] have found the exact solutions for the free vibrations of uniform laminated composite beams. Marur and Kant [16] conducted the free vibration analysis of uniform laminated composite beams using finite element formulation. Singh and Abdelnassar [17] examined the forced vibration response of composite beams considering a third order shear deformation theory.

1.4.2 Vibration analysis of tapered composite beams

Roy and Ganesan [18] have studied the response of a tapered composite beam with general boundary conditions. He et al. [19] have conducted a review of the works on tapered laminated composite structures with focus on interlaminar failures and three-dimensional stress analyses. Thickness-tapered laminated composite beams have been studied for their response in the works of Ganesan and Zabihollah [20, 21] using an advanced finite element formulation and parametric study. Ahmed [3] has studied and conducted experiments for free and forced vibration response of tapered composite beams including the effects of axial force and damping. Badagi [22] conducted the free and forced vibration analysis of thickness-tapered width-tapered laminated composite beams using Rayleigh-Ritz method. Farghaly and Gadelrab [23] have studied the free vibration of stepped uniform-width thickness-tapered Timoshenko composite beams using finite element

method. Salajegheh [36] has studied the vibrations of thickness-and-width tapered laminated composite beams with rigid and elastic supports using a higher-order finite element method.

1.4.3 Finite Element Method

Zienkiewicz [24], Cook [25] and Reddy [4] have used conventional finite element method to analyze the vibration of beams. Nabi and Ganesan [26] developed a general finite element formulation based on FSDT with 16 degrees of freedom per element to study the free vibration characteristics of laminated composite beams. They also conducted a parametric study on the influence of beam geometry and boundary conditions on the natural frequencies of the beam. Chen [27] has studied the free vibration response of tapered composite beams using hierarchical finite element method and Rayleigh-Ritz method. Lees and Thomas [28] conducted a modal analysis on a clamped-clamped Timoshenko beam using hierarchical finite element method (HFEM). They used two nodes per element with two degrees of freedom that are the deflection and cross section rotation, on each node. Bardell [29] conducted a free vibration analysis of a rectangular plate using the HFEM considering ten boundary conditions. Yu et al. [30] studied a multivariable hierarchical finite element for static and vibration analysis of beams. Ribeiro and Petyt [31] studied the non-linear free and forced vibration of composite laminated plates using HFEM and harmonic balance method. Han and Petyt [32, 33] conducted a study on free and forced vibration of isotropic and symmetrically laminated rectangular plates using HFEM. They found that with far fewer degrees-of-freedom than conventional finite element method, accurate results may be produced using the HFEM.

1.5 Objectives of the thesis

The main objectives of the present study are the following:

1. To investigate the free vibration response of uniform, width-tapered, thickness-tapered and thickness- and width-tapered laminated composite beams using the hierarchical finite element method.
2. To conduct a comprehensive parametric study on the effects of boundary condition, width-ratio, thickness-tapering angle, taper configuration, laminate configurations and compressive axial force on the free vibration frequency response of the composite beams.
3. To study the forced vibration response of undamped and damped thickness- and width-tapered laminated composite beams using hierarchical finite element method (HFEM) and to conduct a comprehensive parametric study on the effects of boundary condition, width-ratio, taper configuration, laminate configuration, compressive axial force and damping on the forced vibration response (the amplitudes of deflection and rotation).

The response of tapered laminated composite beams is determined based on classical laminated beam theory and cylindrical bending theory.

1.6 Layout of the thesis

The present chapter provides a brief introduction and literature review on free and forced vibrations of tapered laminated composite beams.

In chapter 2, the elastic behavior of composite beams is presented based on cylindrical bending theory. Then Finite Element Method (FEM) and Hierarchical Finite Element Method (HFEM) formulations of the composite beams are presented. At the end of the chapter free vibration analysis of the uniform laminated composite beams is conducted using FEM and HFEM,

the frequency response is determined and the accuracy and convergence of HFEM is investigated compared to FEM.

Chapter 3 contains a thorough parametric study on the free vibration frequency response of three types of tapered laminated composite beams that are width-tapered, thickness-tapered and width- and thickness- tapered composite beams. For each type, the effects of boundary condition, width-ratio, thickness-tapering angle, laminate configuration, taper configuration and compressive axial force on frequency response are determined and presented through tables and figures.

In chapter 4, the forced vibration analysis of undamped and damped uniform and thickness- and width-tapered composite beams is carried out. Moreover, a parametric study on the effects of boundary condition, width-ratio and taper configuration on forced vibration response in terms of maximum deflection and maximum rotation is conducted.

Finally in chapter 5, the main contributions made in the present study, overall conclusions and the recommendations for future work are presented.

2. Finite element formulation and free vibration analysis of uniform composite beams

2.1 Introduction

Laminated composite beams are increasingly and widely being used in engineering applications including robotic manipulators, aircraft wings, space structures, helicopter blades and yokes, turbine blades and civil infrastructure due to their high stiffness-to-weight and strength-to-weight ratios. Finite element method is one of the most accurate and powerful tools used to predict the behavior of complex mechanical structures such as the vibration of tapered laminated composite beams. In this chapter free vibration analysis of uniform-thickness uniform-width laminated composite beams is conducted. Two degrees of freedom (deflection w , rotation θ) per node and two nodes per element are considered in the finite element formulations. Simply supported, clamped-clamped and clamped-free boundary conditions are considered. The material chosen in this study is NCT-301 graphite-epoxy prepreg [34] which is available in the laboratory of Concordia Centre for Composites (CONCOM). The mechanical properties of the ply and the resin are given in the Tables 2.1 and 2.2. Symmetric laminate is considered in all problems. In this chapter the elastic behavior of composite beams is presented in section 2.2. In sections 2.3 and 2.4 the conventional finite element method (CFEM) and hierarchical finite element method (HFEM) formulations are presented. Finally, in section 2.5 free vibration analysis of a uniform laminated composite beam is presented.

2.2 Cylindrical bending of laminated composite beams

The classical laminate theory considers the effect of pure bending on stresses and deformations. The basic assumption of this theory is that the cross-sections of the beam remain plane and normal to the deformed longitudinal axis and the changes in dimensions of the cross-section are negligible. The rotation is about a neutral axis that passes through the centroid of the cross-section. It is also assumed that transverse shear stresses have no effect on beam deformations and the material has a linear elastic isotropic behavior. There are two approaches in deriving the equations of motion of the laminated composite beams which are the cylindrical bending theory and one-dimensional beam theory. Considering the fact that the composite beam that is being used in this study has a large length-to-thickness ratio as shown in Figure 2.1 the cylindrical bending theory is employed [13]. It is also assumed that the beam is symmetric.

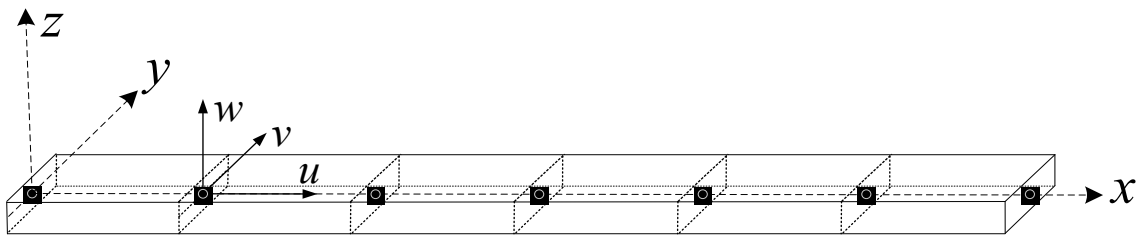


Figure 2.1 Global coordinate system

By writing the equations of potential and kinetic energies and applying the Hamilton principle and cylindrical bending assumptions [27], one can get the equation of motion for a laminated composite beam as:

$$\int_0^L b(x) D_{11}(x) \left(\frac{d^2 w}{dx^2} \right) \left(\frac{d^2 \delta w}{dx^2} \right) dx - \int_0^L b(x) N_x \left(\frac{dw}{dx} \right) \left(\frac{d\delta w}{dx} \right) dx - \omega^2 \int_0^L \int_{-H/2}^{H/2} \rho b(x) w \delta w dx dz = 0 \quad (2.1)$$

In equation (2.1) L is the length of the laminated composite beam, N_x is the compressive axial force (if present), and $D_{11}(x)$ is the coefficient of bending stiffness of the laminated composite beam. Considering the cylindrical bending, $D_{11}(x)$ is defined as [13]:

$$D_{11}(x) = \int_{-H/2}^{H/2} \overline{Q_{11}} z^2 dz \quad (2.2)$$

in which $\overline{Q_{11}}$ is the coefficient of the transformed reduced stiffness of the beam and H is the total thickness of the beam. Also, $b(x)$ is the width of the beam which is defined as:

$$b(x) = \frac{(b_R - b_L)x}{L} + b_L \quad (2.3)$$

In which b_L is the width at the wide section of the beam and b_R is the width at the narrow section of the beam. In case of the uniform-width beam, $b(x)$ is a constant value that is denoted by b . It is also assumed that the deflection in z -direction is:

$$w(x, t) = W(x)e^{i\omega t} \quad (2.4)$$

2.3 Conventional Finite Element Method (CFEM) formulation

In Conventional Finite Element Method (CFEM) the system is divided into a number of elements. Each element has a number of nodes, which are the critical points. The displacements or forces or any other desired variable within the element are defined as a function of those variables in the nodes. For example for an element with two nodes, the displacement of any desired point within the element could be defined as a function of displacements of the two nodes. This function is called Interpolation or Shape function. In this study two nodes per element and two degrees of freedom per node are used in the formulation as shown in Figure 2.2.

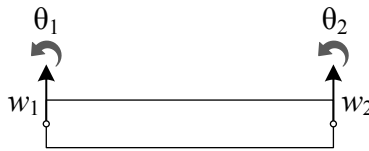


Figure 2.2 Element's nodal degrees of freedom

In Figure 2.2, w_1 and w_2 represent the deflections in the thickness direction at the first and the second node respectively and θ_1 and θ_2 denote the rotations about the y-axis at the first and the second node respectively. Having two degrees of freedom per node and four degrees of freedom per element, a third-order polynomial is required for the expression of deflection to satisfy the boundary conditions as below:

$$W(x) = c_1 + c_2x + c_3x^2 + c_4x^3 \quad (2.5)$$

or:

$$W = [K_w][c] \quad (2.6)$$

in which:

$$[K_w] = [1 \ x \ x^2 \ x^3] \quad (2.7)$$

$$[c] = \begin{bmatrix} c_1 \\ c_2 \\ c_3 \\ c_4 \end{bmatrix} \quad (2.8)$$

The rotation at the node can be defined as the first derivative of deflection:

$$\theta = [K_\theta][c] \quad (2.9)$$

in which:

$$[K_\theta] = \frac{d([K_w])}{dx} = [0 \ 1 \ 2x \ 3x^2] \quad (2.10)$$

Applying the boundary conditions considering the first node at $x_{(1)} = 0$ and $x_{(2)} = l_e$ in which, l_e is the length of the element one will have the nodal displacement matrix $\{u\}$ as:

$$\{u\} = \begin{Bmatrix} w_1 \\ \theta_1 \\ w_2 \\ \theta_2 \end{Bmatrix} = [K_u]\{c\} \quad (2.11)$$

in which:

$$[K_u] = \begin{bmatrix} 1 & 0 & 0 & 0 \\ 0 & 1 & 0 & 0 \\ 1 & l_e & l_e^2 & l_e^3 \\ 0 & 1 & 2l_e & 3l_e^2 \end{bmatrix} \quad (2.12)$$

In order to define a relation between local displacement matrix $\{u\}$ and global displacement (W), from Equation (2.11) one can write:

$$\{c\} = [K_u]^{-1}\{u\} \quad (2.13)$$

Combining Equations (2.6) and (2.13) gives:

$$W = [K_w][K_u]^{-1}\{u\} \quad (2.14)$$

Then by defining Interpolation function matrix $[N^w]$ as:

$$[N^w] = [K_w][K_u]^{-1} \quad (2.15)$$

one can define the relation between local displacement matrix $\{u\}$ and global displacement (W) as:

$$W = [N^w]\{u\} \quad (2.16)$$

Moreover by using the following notations:

$$[N^d] = \frac{d[N^w]}{dx} \quad (2.17)$$

$$[N^M] = \frac{d^2[N^w]}{dx^2} \quad (2.18)$$

and substituting Equation (2.16 – 2.18) into Equation (2.1), the governing equation of motion of the laminated composite beam is derived as:

$$\left[\int_0^{l_e} b(x) \left[D_{11}[N^M]^T[N^M] - N_x[N^d]^T[N^d] \right] dx - \omega^2 \int_0^{l_e} b(x)(\rho_p H_p + \rho_r H_r)[N^w]^T[N^w] dx \right] \{u\} = 0 \quad (2.19)$$

Stiffness $[k]$ and mass $[m]$ matrices are defined for each element as:

$$[k] = \int_0^{l_e} b(x) \left[D_{11}(x)[N^M]^T[N^M] - N_x[N^d]^T[N^d] \right] dx \quad (2.20)$$

$$[m] = \int_0^{l_e} b(x)(\rho_p H_p + \rho_r H_r)[N^w]^T[N^w] dx \quad (2.21)$$

In equation (2.21) the term $(\rho_p H_p + \rho_r H_r)$ is defined as:

$$\int_{-H/2}^{H/2} \rho dz = \rho_p H_p + \rho_r H_r \quad (2.22)$$

in which ρ_p is the density of the ply , ρ_r is the density of resin, H is the thickness of the laminated composite beam and H_p and H_r are the equivalent thicknesses of the resin and ply in each element.

As it was mentioned above, equations (2.20) and (2.21) provide the stiffness and mass matrices for each element. By using an assembly algorithm that is presented in Appendix B, one

can assemble global stiffness $[K]$ and mass $[M]$ matrices of the beam. As a result equation (2.19) transforms into:

$$[[K] - \omega^2[M]]\{u\} = 0 \quad (2.23)$$

Equation (2.23) is an eigenvalue problem and can be solved to determine the natural frequencies of the beam. It should be noted that in Equations (2.20) and (2.21) H_p and H_r are specifically calculated for each element.

2.4 Hierarchical Finite Element Method (HFEM) formulation

In the CFEM formulation a cubical displacement function was assumed in Equation (2.5). In the Hierarchical Finite Element Method (HFEM) the displacement function is modified by adding trigonometric or polynomial functions at the end of the equation [35]. In this study the trigonometric hierarchical functions are used as:

$$W(x) = c_1 + c_2x + c_3x^2 + c_4x^3 + \sum_{i=1}^N c_{i+4} \sin \frac{i\pi x}{l_e}, \quad i = 1,2,3, \dots \quad (2.24)$$

in which l_e is the length of the element and N is the number of hierarchical terms.

Equation (2.24) can be expressed as:

$$W = [K_w][c] \quad (2.25)$$

$$K_w = \left[1 \quad x \quad x^2 \quad x^3 \quad \sin \frac{\pi x}{l_e} \quad \dots \quad \sin \frac{N\pi x}{l_e} \right] \quad (2.26)$$

$$[c] = \begin{bmatrix} c_1 \\ c_2 \\ c_3 \\ c_4 \\ c_5 \\ \vdots \\ c_{N+4} \end{bmatrix} \quad (2.27)$$

In the same manner rotation (θ) can be expressed as:

$$\theta = [K_\theta][c] \quad (2.28)$$

$$K_\theta = \frac{d(K_w)}{dx} = \left[0 \ 1 \ 2x \ 3x^2 \ \frac{\pi}{l_e} \cos \frac{\pi x}{l_e} \dots \frac{N\pi}{l_e} \cos \frac{N\pi x}{l_e} \right] \quad (2.29)$$

The displacement matrix in local coordinate system is:

$$\{u\} = \begin{Bmatrix} w_1 \\ \theta_1 \\ w_2 \\ \theta_2 \\ A_1 \\ \vdots \\ A_N \end{Bmatrix} = [K_u]\{c\} \quad (2.30)$$

in which A_i are the hierarchical degrees of freedom corresponding to hierarchical terms.

The procedure to determine the stiffness $[k]$ and mass $[m]$ matrices for each element is the same as that described for CFEM in section 2.3. The algorithm to assemble the global stiffness $[K]$ and global mass $[M]$ matrices is described in Appendix B.

$$[K_u] = \begin{bmatrix} 1 & 0 & 0 & 0 & 0 & \dots & 0 \\ 0 & 1 & 0 & 0 & \frac{\pi}{l_e} & \dots & \frac{N\pi}{l_e} \\ 1 & l_e & l_e^2 & l_e^3 & 0 & \dots & 0 \\ 0 & 1 & 2l_e & 3l_e^2 & -\frac{\pi}{l_e} & \dots & (-1)^N \frac{N\pi}{l_e} \\ 0 & 0 & 0 & 0 & 1 & \dots & 0 \\ \vdots & \vdots & \vdots & \vdots & \vdots & \ddots & \vdots \\ 0 & 0 & 0 & 0 & 0 & \dots & 1 \end{bmatrix} \quad (2.31)$$

2.5 Free vibration analysis of a uniform laminated composite beam

A laminated composite beam made of NCT-301 graphite-epoxy composite material with the mechanical properties mentioned in Tables 2.1 and 2.2 is considered. The beam has $[0/90]_{9s}$ laminate configuration and a length (L) of 25 cm. The thickness and the width of the beam are constant throughout the length of the beam and therefore it is called a “uniform beam”. The beam is composed of 36 plies. Individual ply thickness (t_i) is 0.125 mm and the beam thickness (H) is 4.5 mm. The beam has a width of 15 mm.

Table 2.1 Mechanical properties of ply [22]

Longitudinal modulus (E_1)	113.9 GPa
Transverse modulus (E_2)	7.9856 GPa
$E_3 = E_2$	7.9856 GPa
In-plane shear modulus (G_{12})	3.138 GPa
Major Poisson's ratio (ν_{12})	0.288
Minor Poisson's ratio (ν_{21})	0.178
Density of ply (ρ_p)	1480 kg/m ³

Table 2.2 Mechanical properties of resin material [22]

Elastic modulus (E)	3.93 GPa
Shear modulus (G)	1.034 GPa
Poisson's ratio (ν)	0.37
Density of resin (ρ_r)	1000 kg/m ³

In order to validate the HFEM formulation, free vibration analysis is carried out using both CFEM and HFEM for three boundary conditions that are simply supported, clamped-clamped and clamped- free, as shown in Figure 2.3.

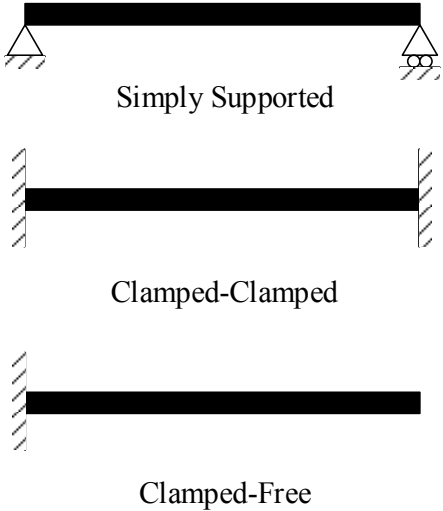


Figure 2.3 Boundary conditions

The first three natural frequencies are given in Table 2.4 alongside the exact values of the natural frequencies that can be calculated as [13]:

$$\omega_i = \frac{\gamma_i}{l^2} \sqrt{\frac{D_{11}}{\rho H}}$$

The values of γ_i for different boundary conditions are given in Table 2.3.

As it is shown in Tables 2.4 - 2.6, HFEM provides a better accuracy than CFEM with less number of elements that will significantly reduce the time required for the computations. It can also be shown that there is no significant difference between the results when the second

hierarchical term is added. As a result, in this study HFEM with one trigonometric hierarchical term is considered.

Table 2.3 Boundary condition coefficients for the uniform composite beams

Boundary Condition	γ_1	γ_2	γ_3
Simply Supported	9.867	39.478	88.826
Clamped - Clamped	22.373	61.673	120.90
Clamped - Free	3.516	22.034	61.701

Table 2.4 The comparison between CFEM and HFEM and the exact value of the first three natural frequencies for simply supported uniform composite beams

		2E*	4E	6E	12E	Exact Value
ω_1 (rad/s)	HFEM(1)**	1366.79	1366.69	1366.68	1366.68	1366.68
	HFEM(2)***	1366.70	1366.69	1366.68	1366.68	
	CFEM	1372.08	1367.04	1366.76	1366.69	
ω_2 (rad/s)	HFEM(1)	5468.92	5467.16	5466.79	5466.75	5466.69
	HFEM(2)	5466.85	5466.80	5466.76	5466.74	
	CFEM	6067.64	5488.33	5471.18	5467.03	
ω_3 (rad/s)	HFEM(1)	12662.91	12309.21	12301.12	12300.21	12300.12
	HFEM(2)	12314.15	12300.48	12300.29	12300.19	
	CFEM	15251.52	12524.94	12348.73	12303.38	

* 2E means 2 Elements ** (1) means one hierarchical term *** (2) means two hierarchical terms

Table 2.5 The comparison between CFEM and HFEM and the exact value of the first three natural frequencies for clamped-clamped uniform composite beams

		2E	4E	6E	12E	Exact Value
ω_1 (rad/s)	HFEM(1)	3100.43	3098.16	3098.13	3098.13	3098.08
	HFEM(2)	3098.28	3098.14	3098.13	3098.13	
	CFEM	3148.35	3102.24	3098.95	3098.18	
ω_2 (rad/s)	HFEM(1)	8550.15	8542.06	8540.30	8540.11	8540.06
	HFEM(2)	8540.34	8540.29	8540.15	8540.11	
	CFEM	11351.52	8619.10	8556.87	8541.18	
ω_3 (rad/s)	HFEM(1)	17240.57	16781.70	16744.70	16742.08	16741.55
	HFEM(2)	16821.05	16743.05	16742.29	16742.05	
	CFEM	-	17099.59	16861.99	16750.06	

Table 2.6 The comparison between CFEM and HFEM and the exact value of the first three natural frequencies for clamped-free uniform composite beams

		2E	4E	6E	12E	Exact Value
ω_1 (rad/s)	HFEM(1)	486.88	486.87	486.87	486.87	486.87
	HFEM(2)	486.88	486.87	486.87	486.87	
	CFEM	487.11	486.89	486.88	486.88	
ω_2 (rad/s)	HFEM(1)	3055.35	3051.28	3051.22	3051.21	3051.14
	HFEM(2)	3051.34	3051.22	3051.21	3051.21	
	CFEM	3077.11	3054.77	3051.97	3051.26	
ω_3 (rad/s)	HFEM(1)	8578.80	8546.55	8543.78	8543.49	8543.44
	HFEM(2)	8546.43	8543.65	8543.53	8543.49	
	CFEM	10407.33	8609.63	8559.12	8544.55	

2.6 Summary

In this chapter the elastic behavior of composite beams was presented in section 2.2. In sections 2.3 and 2.4 the Conventional Finite Element Method (CFEM) and Hierarchical Finite Element Method (HFEM) were presented and in section 2.5 free vibration analysis of a uniform composite beam was conducted. A summary of observations is given below:

- Clamped-Clamped boundary condition has the largest natural frequencies among all boundary conditions. Simply supported and clamped-free beams have the second and the third largest natural frequencies respectively.
- It was noted that HFEM gives more accurate results with same number of elements compared to CFEM. Also it reaches the exact value with much less number of elements compared to CFEM.
- Moreover, it was noted that adding the second hierarchical trigonometric term does not make a significant improvement in the accuracy nor the number of elements required to reach the exact values. As a result, in this study HFEM with one trigonometric hierarchical term is considered.

3. Free vibration analysis of tapered composite beams

3.1 Introduction

In order to reduce the cost and the use of extra-material while preserving the desired properties of composite beams, different types of tapering are being developed. In this chapter, the study of free vibration frequency response of composite beams considering three types of tapering is presented. In section 3.2 the free vibration analysis of a width-tapered laminated composite beam is conducted. In section 3.3 the free vibration analysis of a thickness-tapered laminated composite beam is conducted. In section 3.4 the free vibration analysis of a thickness- and width-tapered laminated composite beam is conducted. In all the parametric studies presented in this chapter NCT-301 graphite-epoxy composite material is used, which is available in the laboratory of Concordia Centre for Composites. The mechanical properties of the ply and the resin are given in Tables 2.1 and 2.2. Cylindrical bending theory and Hierarchical Finite Element Method (HFEM) are used for all the formulations. In each section, the effects of different parameters such as boundary condition, taper angle, width-ratio, laminate configuration, taper configuration and axial force, on natural frequencies of the beam are analyzed and presented through figures and tables in corresponding subsections. An interpretation of each figure is given at the end of each subsection and at the end of the chapter a summary of observations and discussion is presented.

3.2 Free vibration analysis of width-tapered laminated composite beams

In the current section, a width-tapered composite beam as it is shown in Figure 3.1 is analyzed. In the following subsections, parametric studies are conducted to study the effects of boundary condition, width-ratio, taper angle (or equivalently length of the beam), laminate configuration and compressive axial force on the natural frequencies of the beam. The beam has uniform thickness and is assumed to be symmetric about its mid-plane and therefore only the upper-half of the beam is considered in all of the calculations.

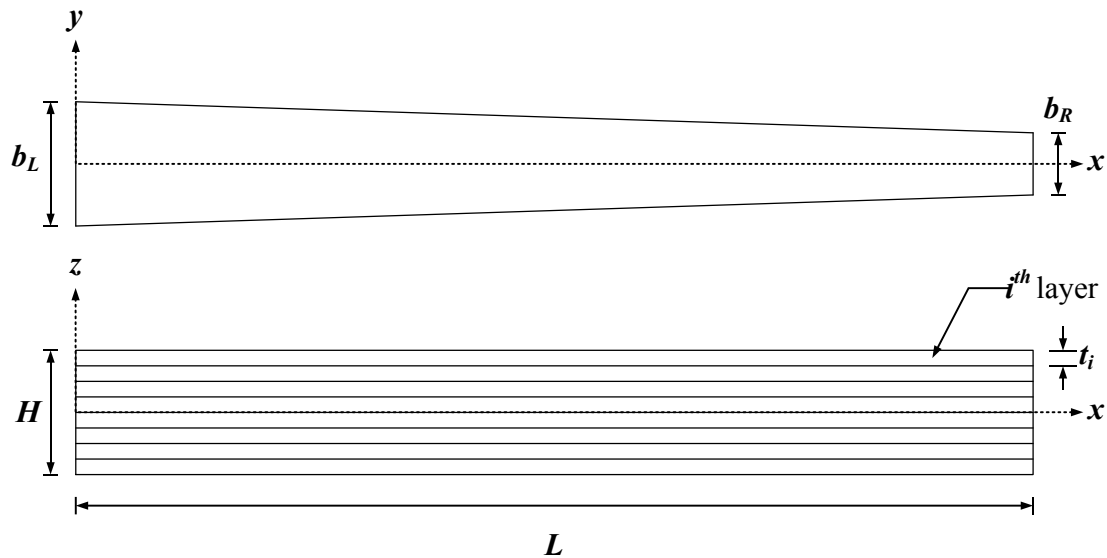


Figure 3.1 Width-tapered composite beam

3.2.1 Effect of boundary conditions on natural frequencies

A laminated composite beam made of NCT-301 graphite-epoxy composite material with the mechanical properties mentioned in Tables 2.1 and 2.2 is considered. The beam has $[0/90]_{9s}$ laminate configuration and a length (L) of 25 cm. The beam is composed of 36 plies. Individual

ply thickness (t_i) is 0.125 mm and the beam thickness (H) is 4.5 mm. The beam has a width of 15 mm at the wide section (b_L) and 7.5 mm at the narrow section (b_R), which leads to a width-ratio (b_R/b_L) of 0.5. Free vibration analysis is carried out for four boundary conditions that are simply supported, clamped-clamped, clamped-free and free-clamped, as shown in Figure 3.2. The first three natural frequencies are given in Table 3.1.

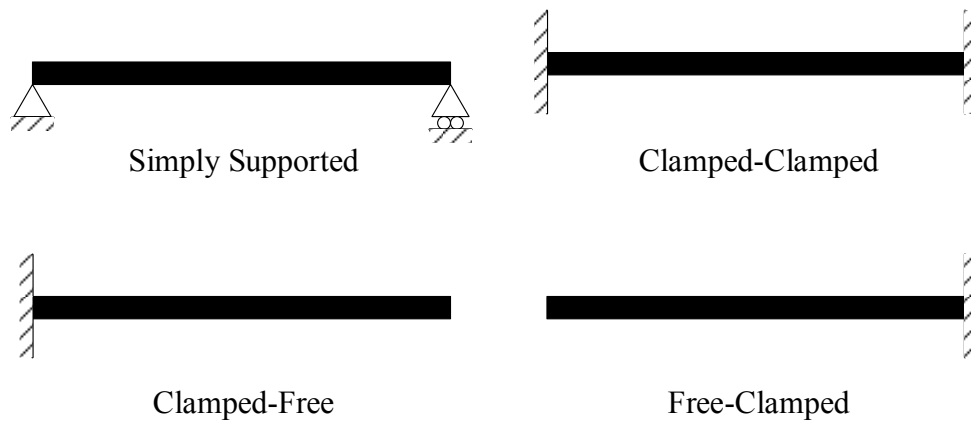


Figure 3.2 Boundary conditions

Table 3.1 Natural frequencies of width-tapered composite beam for different boundary conditions

	Simply Supported	Clamped-Clamped	Clamped-Free	Free-Clamped
ω_1 (rad/s)	1360.53	3071.59	597.54	393.22
ω_2 (rad/s)	5472.06	8503.50	3256.82	2857.78
ω_3 (rad/s)	12309.99	16703.78	8751.79	8358.53

It can be observed from Table 3.1 that the highest natural frequency is for clamped-clamped boundary condition because the stiffness of the beam increases in this condition. The lowest natural frequency is for free-clamped beam since there is no support at one end and the stiffness decreases accordingly. Simply supported beam has the second highest natural frequencies and clamped-free beam has slightly higher natural frequencies than free-clamped beam and comes in third. One can say that since the support is at the wide section of the width-tapered beam (compared to free-clamped beam), the clamped-free beam has a higher stiffness.

3.2.2 Effect of width-ratio on natural frequencies

Width-ratio (b_R/b_L) is the ratio of width of the beam at the narrow end (b_R), over the width of the beam at the wide end (b_L). The beam in section 3.2.1 is considered with width-ratios of 0.01, 0.02, 0.05, 0.1, 0.2, 0.4, 0.6, 0.8 and 1.0. The first three natural frequencies for four different boundary conditions are illustrated through Figures 3.3 - 3.5.

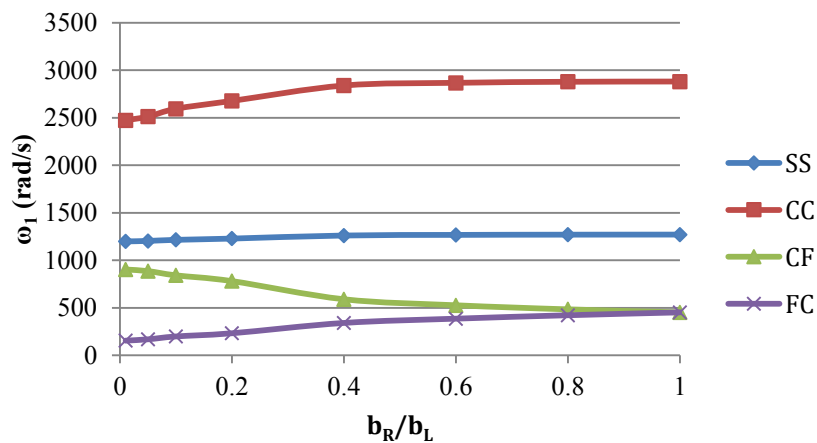


Figure 3.3 Effect of width-ratio on the first natural frequency of the width-tapered composite beam

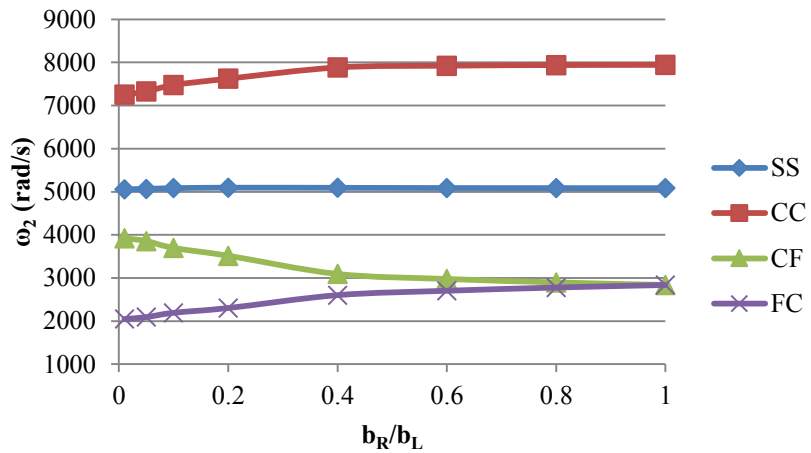


Figure 3.4 Effect of width-ratio on the second natural frequency of the width-tapered composite beam

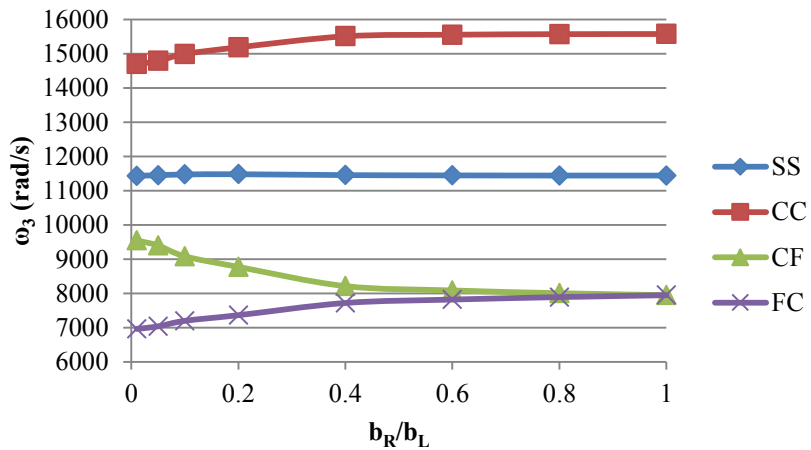


Figure 3.5 Effect of width-ratio on the third natural frequency of the width-tapered composite beam

It can be seen from Figures 3.3 - 3.5 that by increasing the width-ratio from 0.01 to 1.0, the first three natural frequencies increase for simply supported, clamped-clamped and free-clamped beams but they decrease for clamped-free beam. The reason is that for the clamped-free boundary

condition by increasing the width-ratio, material on the free side is being added up. Therefore, the beam becomes more resistant to vibrate and that leads to reduction of natural frequencies. Also it is evident that the highest natural frequency is for clamped-clamped boundary condition, while the lowest is for free-clamped boundary condition.

In Tables A.1 - A.8, the values of the first three natural frequencies are presented alongside the results obtained using R-R (Rayleigh-Ritz method) [22] and HOFEM (Higher-Order Finite Element Method) [36]. The comparison shows that HFEM (Hierarchical Finite Element Method) provides accurate results within 0.2% of difference from the above-mentioned methods, which is very acceptable.

3.2.3 Effect of taper angle (or equivalently length of the beam) on natural frequencies

The same tapered composite beam considered in section 3.2.1 is used with width-ratio of 0.5. The beam is considered to have taper angles (ϕ) of 0.86° , 0.573° , 0.43° and 0.344° (corresponding lengths are 0.1 m, 0.15 m, 0.2 m and 0.25 m). The first three natural frequencies for four different boundary conditions are illustrated through Figures 3.6 - 3.8.

As it is shown in Figures 3.6 - 3.8, by increasing the length of the tapered beam or equivalently decreasing the taper angle, all the first three natural frequencies will decrease. It is evident that natural frequencies are affected more significantly by changes in length (or equivalently taper angle), for beams with clamped-clamped and simply supported boundary conditions. Comparing among different boundary conditions, clamped-clamped boundary condition has the highest natural frequencies. The second and third highest natural frequencies correspond to simply supported and clamped-free boundary conditions, respectively. Clamped-

free boundary condition has a slightly higher frequency response than free-clamped boundary condition, which has the lowest natural frequencies.

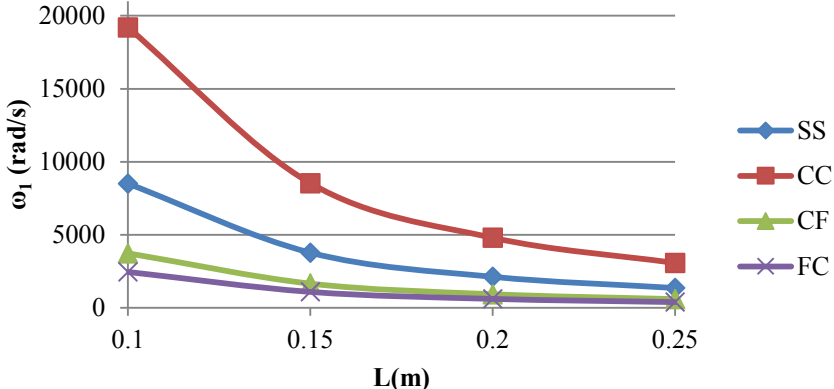


Figure 3.6 Effect of length on the first natural frequency of the width-tapered composite beam

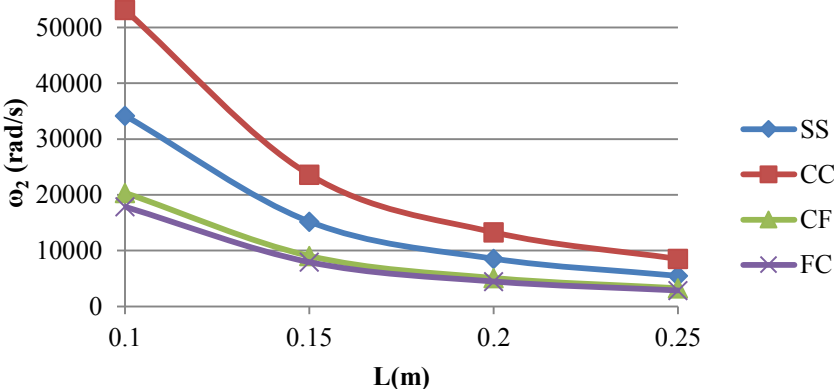


Figure 3.7 Effect of length on the second natural frequency of the width-tapered composite beam

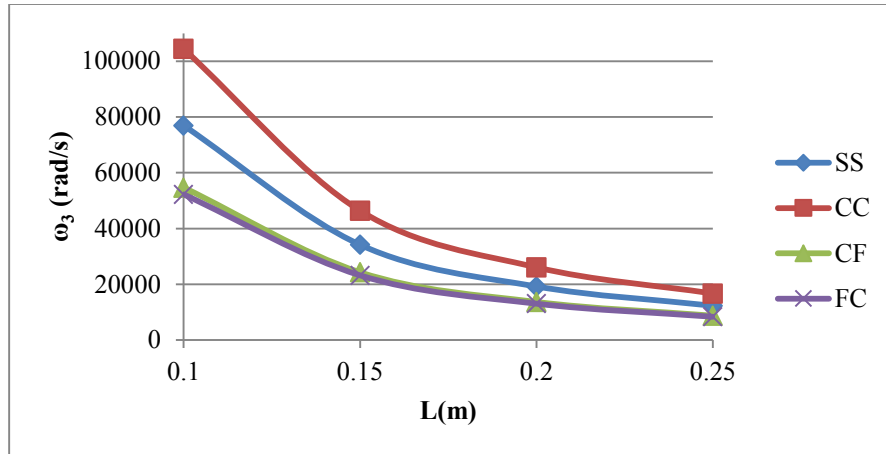


Figure 3.8 Effect of length on the third natural frequency of the width-tapered composite beam

3.2.4 Effect of laminate configuration on natural frequencies

Four different laminate configurations are being considered and labeled as LC1, LC2, LC3 and LC4 in order to study the effect of laminate configuration on natural frequencies. In this study LC1 is the laminate with $[0/90]_{9s}$ configuration, LC2 is the laminate with $[\pm 45]_{9s}$ configuration, LC3 is the laminate with $[0_4/\pm 45_7]_s$ configuration, and LC4 is the laminate with $[0/\pm 60]_{6s}$ configuration. LC1 to LC4 are illustrated in Figure 3.9. The free vibration frequency response for four boundary conditions that are simply supported (S-S), clamped-clamped (C-C), clamped-free (C-F) and free-clamped (F-C) is presented in Figures 3.10 - 3.12.

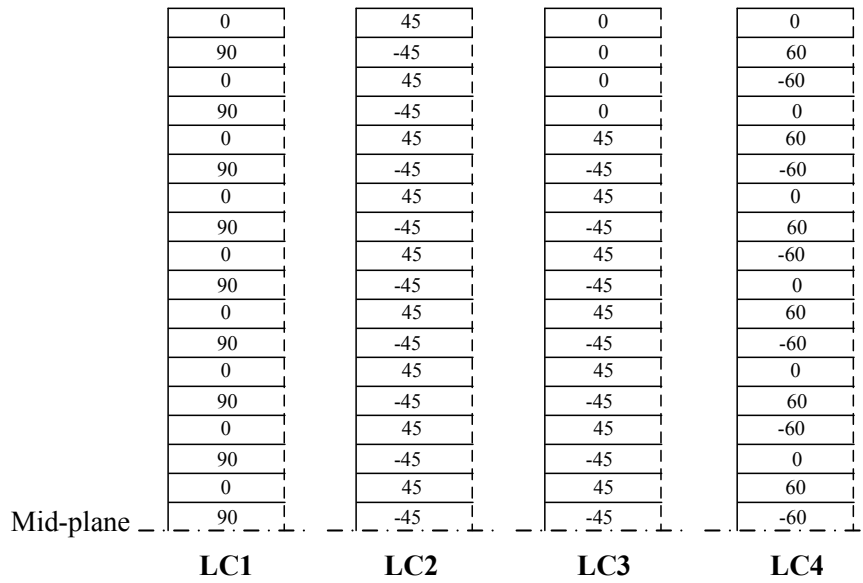


Figure 3.9 LC1, LC2, LC3 and LC4 laminate configurations

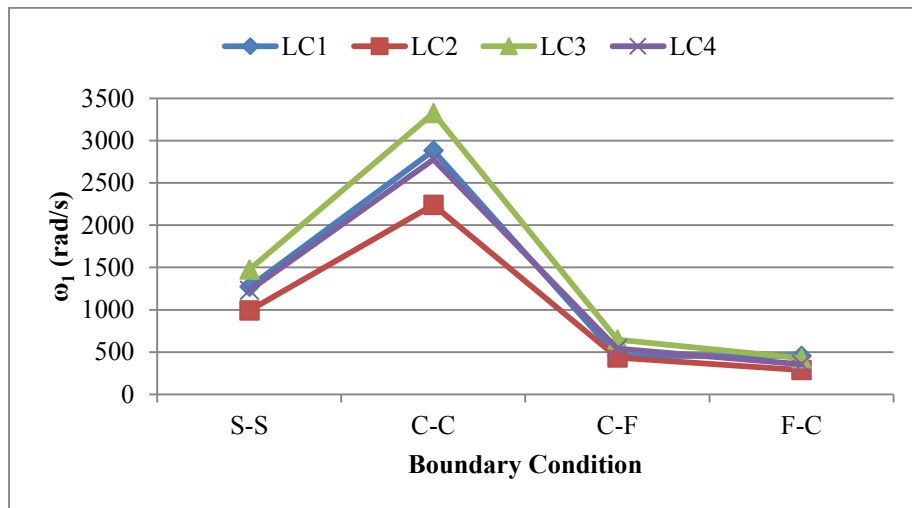


Figure 3.10 Effect of laminate configuration on the first natural frequency of the width-tapered composite beam

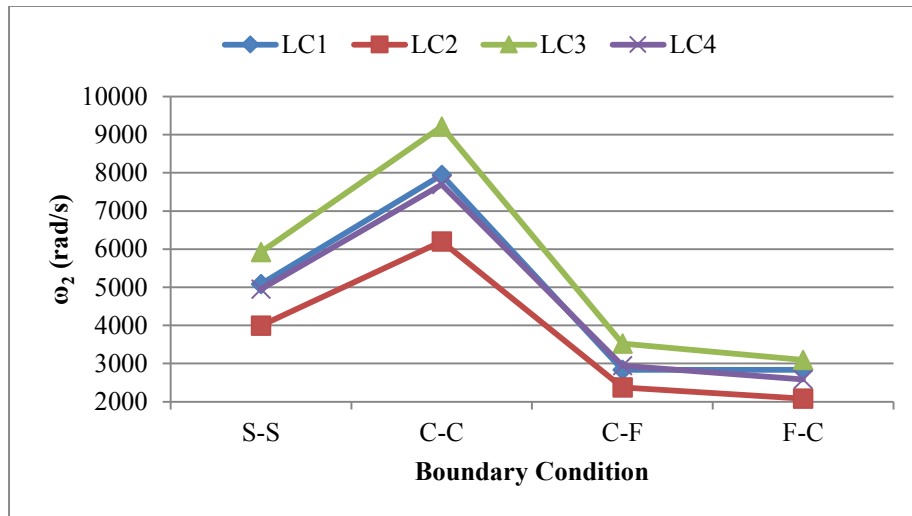


Figure 3.11 Effect of laminate configuration on the second natural frequency of the width-tapered composite beam

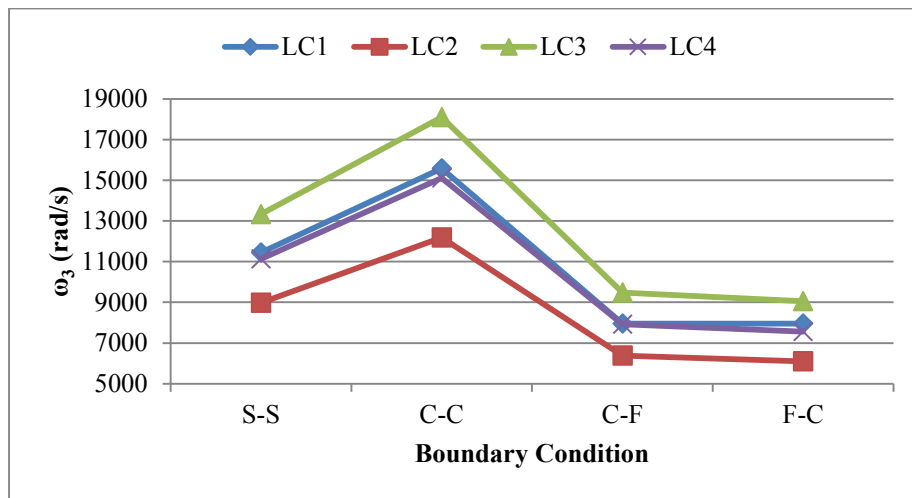


Figure 3.12 Effect of laminate configuration on the third natural frequency of the width-tapered composite beam

As it is shown in Figures 3.10 - 3.12, for all the boundary conditions LC3 has the highest frequency response while LC2 has the lowest. LC1 has higher frequency response than LC4 and lower frequency response than LC3. Also, it is evident that the clamped-clamped boundary condition has the highest frequency response for all configurations.

3.2.5 Effect of compressive axial force on natural frequencies

To consider the effect of axial force on the frequency response, first a buckling analysis is carried out on the same beam as that considered in section 3.2.1 to calculate the critical buckling load, P_{cr} . The free vibration analysis under compressive axial forces equal to 10%, 50% and 90% of P_{cr} is conducted and the first three natural frequencies are presented in Figures 3.13 - 3.15 for different boundary conditions.

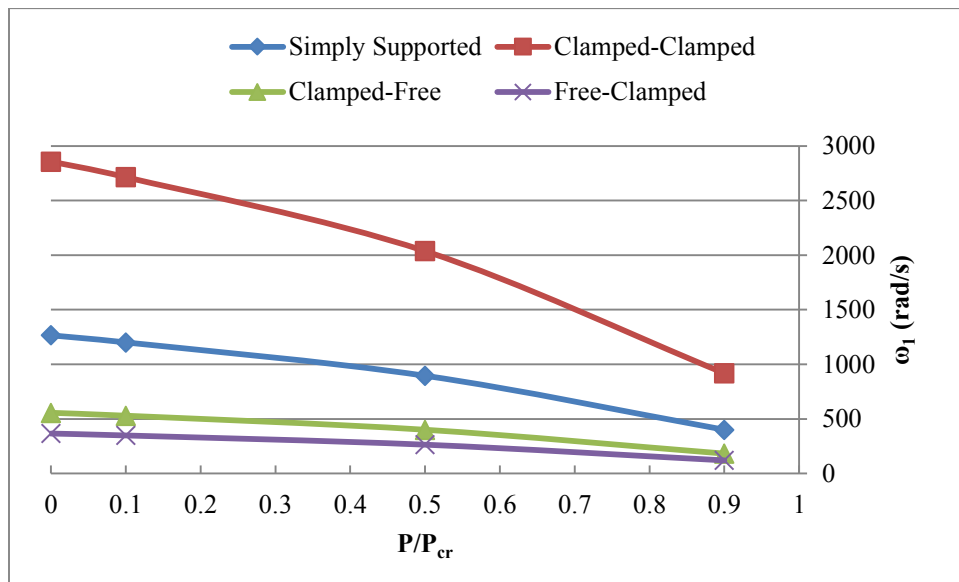


Figure 3.13 Effect of compressive axial force on the first natural frequency of the width-tapered composite beam

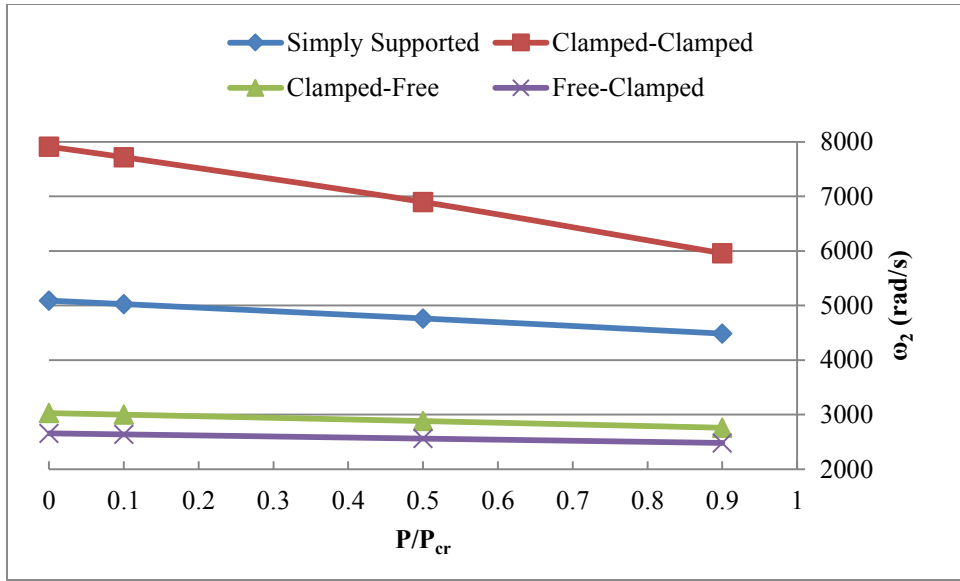


Figure 3.14 Effect of compressive axial force on the second natural frequency of the width-tapered composite beam

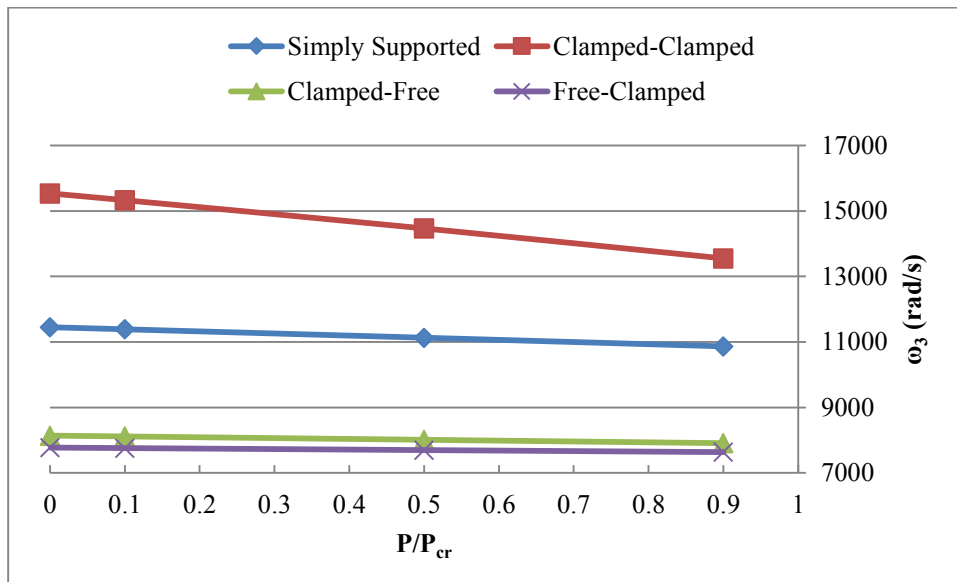


Figure 3.15 Effect of compressive axial force on the third natural frequency of the width-tapered composite beam

It can be observed from Figures 3.13 - 3.15 that by increasing the compressive axial force, the natural frequencies decrease. The rate of decrease is significant for clamped-clamped and simply supported boundary conditions, however it is negligible for clamped-free and free-clamped boundary conditions. Also, it is evident that clamped-clamped boundary condition has the highest frequency response for all the configurations.

3.3 Free vibration analysis of thickness-tapered laminated composite beams

In the present section, thickness-tapered composite beam is analyzed. Four different taper configurations are considered that are, Configurations A, B, C and D, as shown in Figure 3.16. The dark triangles are the resin pockets located in between plies. It should be mentioned that configurations A, B, C and D represent different tapered laminates in the same way that uniform laminates were represented as a combination of layers. In the following subsections, parametric studies are conducted to study the effects of boundary condition, taper angle (or equivalently length of the beam), laminate configuration, taper configuration and compressive axial force on the natural frequencies of the beam. The beam has uniform width and is assumed to be symmetric about its mid-plane and therefore only the upper-half of the beam is considered in all of the calculations.

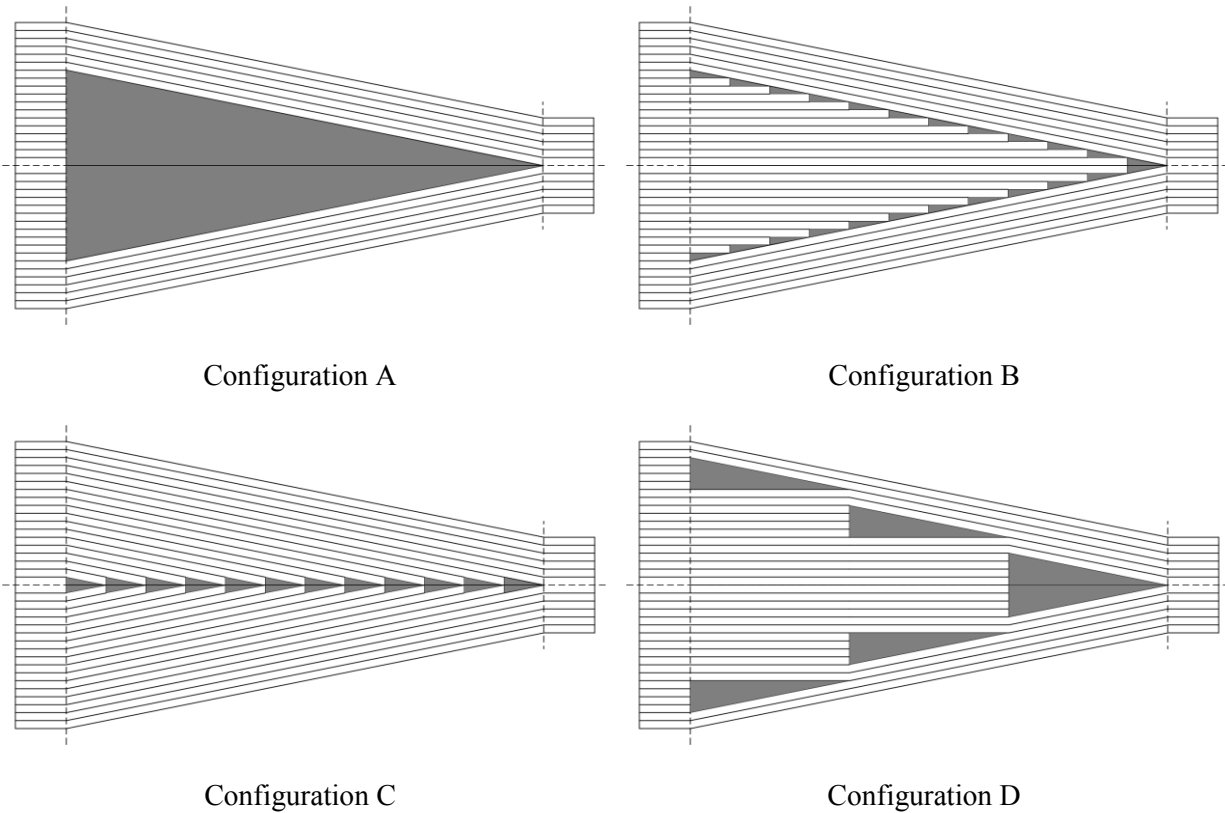


Figure 3.16 Taper Configurations

3.3.1 Effect of boundary condition on natural frequencies

A thickness-tapered composite beam composed of 36 plies at the thick (left) side and 12 plies at the thin (right) side is considered. Thickness of each ply is 0.125 mm and therefore the left side beam thickness is 4.5 mm as opposed to 1.5 mm beam thickness at the right side. The beam has a length of 25 cm, a uniform width of 15 mm and $[0/90]_{9s}$ laminate configuration. The mechanical properties of the composite material are given in Tables 2.1 and 2.2. Free vibration analysis of the beam is conducted and the first three natural frequencies are presented in Tables 3.4 - 3.6 for configurations A, B, C and D for different boundary conditions.

Table 3.2 First natural frequencies (rad/s) of thickness-tapered composite beams

	Simply Supported	Clamped-Clamped	Clamped-Free	Free-Clamped
Configuration A	784.5246	1777.5584	484.9711	142.1147
Configuration B	838.3421	1962.0792	546.5948	155.3737
Configuration C	856.3092	1995.2596	563.2578	154.5906
Configuration D	822.4534	1905.7802	508.7018	160.5938

Table 3.3 Second natural frequencies (rad/s) of thickness-tapered composite beams

	Simply Supported	Clamped-Clamped	Clamped-Free	Free-Clamped
Configuration A	3196.5868	4904.2811	2132.0842	1466.8182
Configuration B	3484.9467	5397.0563	2316.5577	1595.7555
Configuration C	3561.8175	5491.122	2379.1565	1609.9249
Configuration D	3388.9078	5290.3047	2196.2266	1617.7869

Table 3.4 Third natural frequencies (rad/s) of thickness-tapered composite beams

	Simply Supported	Clamped-Clamped	Clamped-Free	Free-Clamped
Configuration A	7140.8785	9619.3095	5310.1348	4661.7109
Configuration B	7814.0551	10574.5674	5744.3029	5119.5936
Configuration C	7977.9234	10764.3067	5890.6532	5192.5281
Configuration D	7557.4338	10289.4157	5499.2824	5114.8815

As it is shown in Tables 3.2 - 3.4, the highest values of the natural frequencies are for clamped-clamped boundary condition. The second and the third highest values of natural frequencies belong to simply supported and clamped-free boundary conditions respectively. Free-clamped beam has the lowest natural frequencies among all boundary conditions.

3.3.2 Effect of taper angle (or equivalently length of the beam) on natural frequencies

The same beam as that analyzed in section 3.3.1 is considered. Taper angles of 0.86° , 0.573° , 0.43° and 0.344° are used (corresponding lengths of tapered beam are 0.1 m, 0.15 m, 0.2 m and 0.25 m). The free vibration analysis is conducted and the frequency response is presented in Figure 3.17 and Figures A.1 and A.2.

It can be observed from Figure 3.17 that by increasing the length of the beam (or equivalently decreasing the taper angle), the first natural frequency decreases dramatically. This behavior can be interpreted by the fact that the beam becomes more rigid as its length decreases. Therefore it experiences higher natural frequencies. Also, it is evident from Figures A.1 and A.2 that the second and the third natural frequencies follow the same pattern.

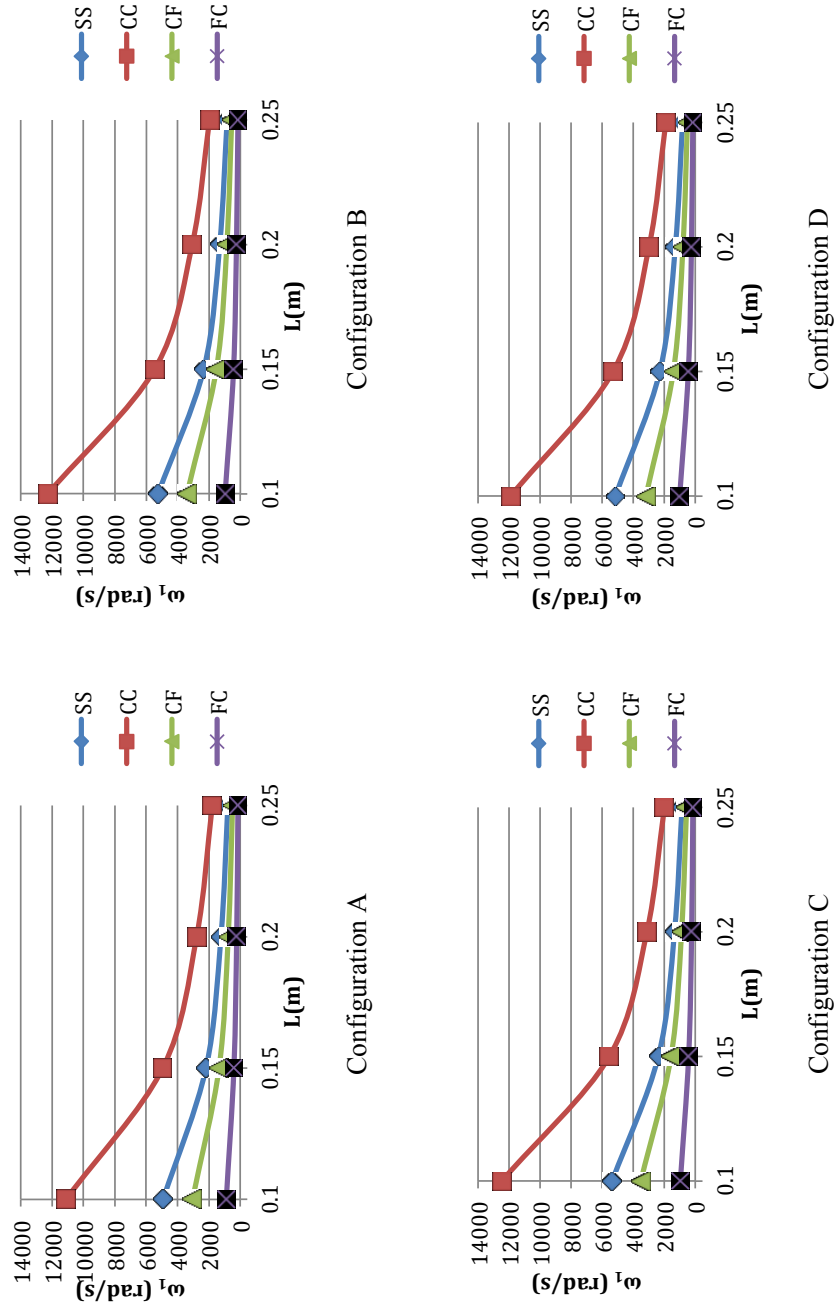


Figure 3.17 Effect of the length on the first natural frequency of the thickness-tapered composite beam

Comparing different taper configurations, it is evident that configuration C has the highest natural frequencies. Configuration B comes in second with slightly lower values than configuration C. Configuration D has lower natural frequencies than configuration B and C and the lowest natural frequencies belong to configuration A. From Figure 3.16, it can be observed that configuration A has the largest amount of resin pockets among the four configurations, which results in the lowest stiffness and therefore the lowest natural frequencies. Configuration D has bigger resin pockets compared to configuration B but they are distributed in almost the same manner as configuration B throughout the beam, which results in lower natural frequencies than configuration B. However, configuration D has lower volume of resin pockets and also they are placed farther from the center that leads to higher contribution to the stiffness, compared to configuration A. Therefore, it has higher natural frequencies than configuration A. Although Configuration B has the same volume of resin pockets as configuration C, but in configuration B they are distributed and located at much farther distance from the center and consequently they contribute more to the stiffness. However, in configuration C at the same location there is a tapered ply instead of the resin pocket that leads to higher stiffness in configuration C compared to configuration B. As a result, configuration C has slightly higher natural frequency than configuration B.

Moreover, among different boundary conditions, the highest natural frequencies are for the clamped-clamped boundary condition. Simply supported and clamped-free come in second and third respectively, and free-clamped boundary condition has the lowest natural frequencies.

3.3.3 Effect of laminate configuration on natural frequencies

In order to study the effect of laminate configuration on natural frequencies, the same beam as that analyzed in section 3.3.1 is considered. Laminate configurations LC1, LC2, LC3 and LC4 as mentioned in section 3.2.4, and as shown in Figure 3.9 are considered. The free vibration analysis of the beam for boundary conditions simply supported (S-S), clamped-clamped (C-C), clamped-free (C-F) and free-clamped (F-C) is conducted and the frequency response is presented in Figure 3.18 and Figures A.3 and A.4.

It can be observed from Figure 3.18 that LC3 configuration has the highest value of the first natural frequency for all boundary conditions. LC1 and LC4 have the second and the third highest values respectively, and LC2 has the lowest values of first natural frequency among the four configurations. It is evident in Figures A.3 and A.4 that second and third natural frequencies follow the same pattern.

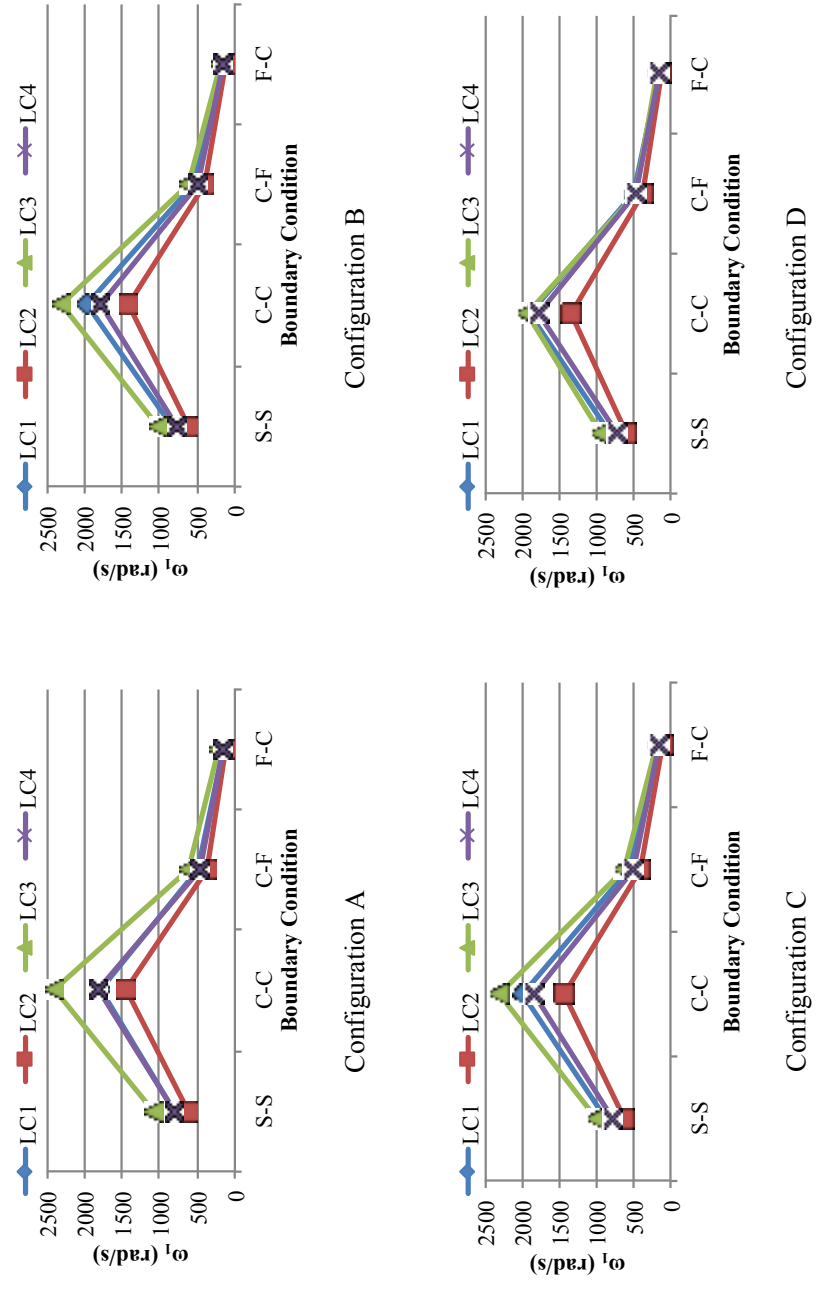


Figure 3.18 Effect of the laminate configuration on the first natural frequency of thickness-tapered composite beam

3.3.4 Effect of taper configuration on natural frequencies

The same beam as that analyzed in section 3.3.1 is considered. The free vibration analysis for taper configurations A, B, C and D that are shown in Figure 3.16 is conducted and the first three natural frequencies are presented in Figures 3.19 - 3.21.

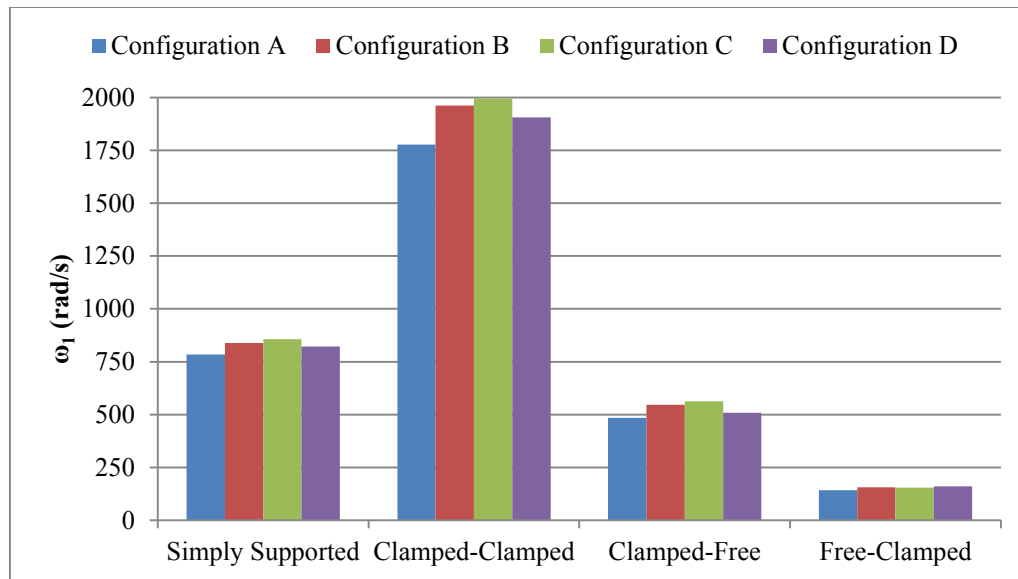


Figure 3.19 Effect of taper configuration on the first natural frequency of the thickness-tapered composite beam

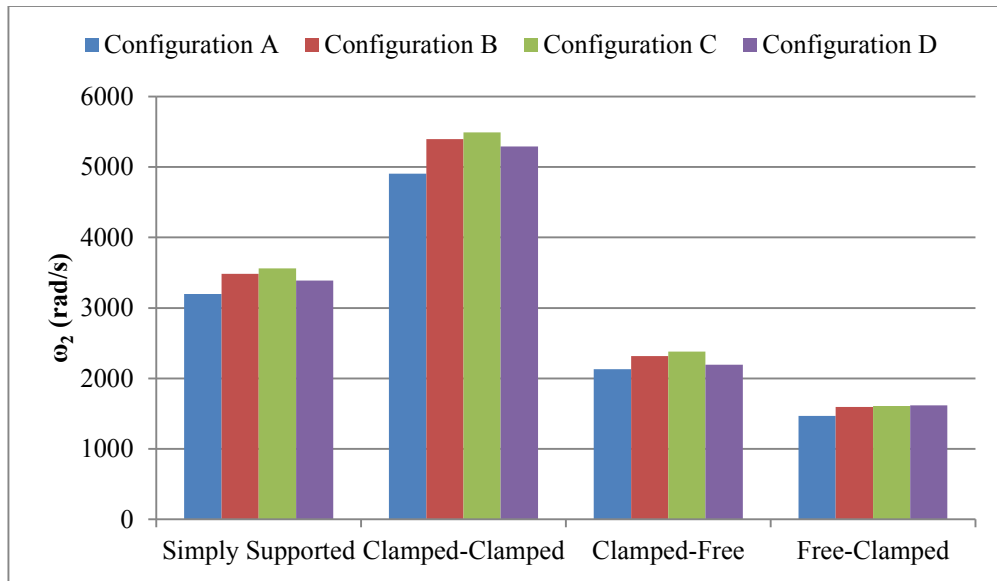


Figure 3.20 Effect of taper configuration on the second natural frequency of the thickness-composite tapered beam

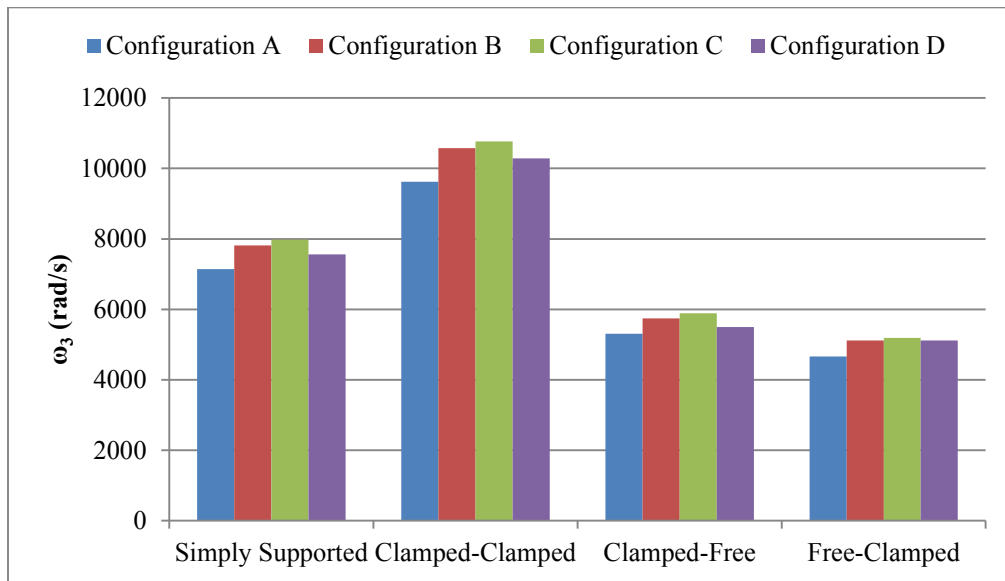


Figure 3.21 Effect of taper configuration on the third natural frequency of the thickness-tapered composite beam

As it is shown in Figures 3.19 - 3.21, for all the first three natural frequencies, configuration C has the highest values of natural frequencies. Configuration B has the second highest natural frequencies, configuration D comes in third and configuration A comes in fourth. It is reasonable because configuration A has the most volume of resin compared to other configurations and therefore it is less stiff. Same logic applies for configuration D. Configuration C has the plies at a larger distance from the mid-plane and resin pockets at a smaller distance from the mid-plane, compared to configuration B and therefore it has slightly larger D_{11} value than configuration B. Consequently it has higher natural frequencies.

3.3.5 Effect of compressive axial force on natural frequencies

To consider the effect of axial force on the natural frequencies, the same beam as that analyzed in section 3.3.1 is considered. First a buckling analysis of the beam is conducted to calculate the critical buckling load, P_{cr} . Compressive axial force is considered. Free vibration analysis under compressive axial forces equal to 10%, 50% and 90% of P_{cr} is conducted and the first three natural frequencies are shown in Figure 3.22 and Figures A.5 and A.6 for different boundary conditions and taper configurations.

It can be observed from Figure 3.22 and Figures A.5 and A.6 that by increasing the compressive axial force, the natural frequencies decrease dramatically. This is due to the fact that in the presence of compressive axial force after the initial deflection, the resultant moment pulls the beam further from its neutral position. Therefore the beam becomes more flexible and consequently the natural frequencies decrease.

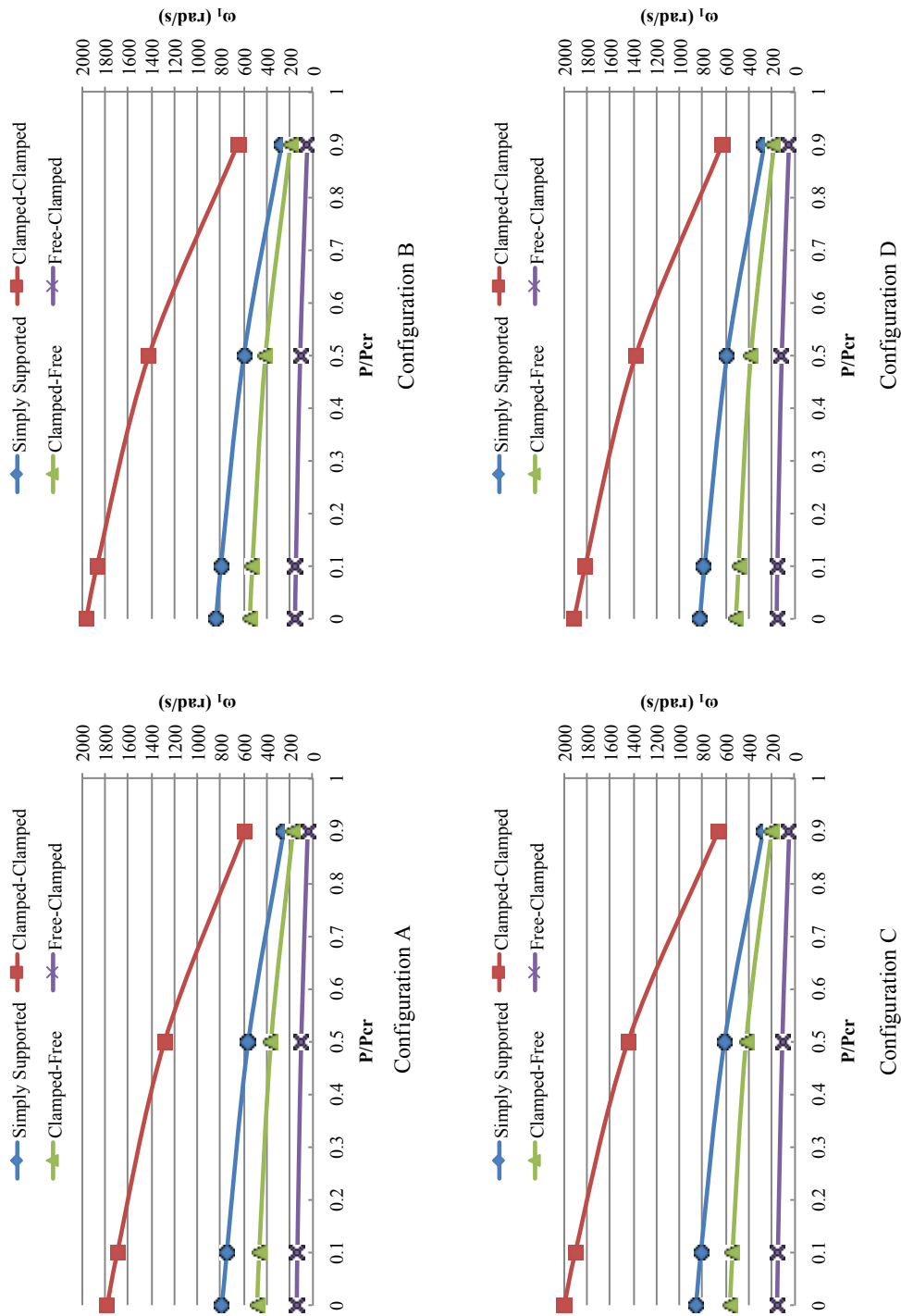


Figure 3.22 Effect of compressive axial force on the first natural frequency of the thickness-tapered composite beam

It can also be observed from Figure 3.22 and Figures A.5 and A.6 that the rate of reduction of natural frequencies is more significant for clamped-clamped boundary condition. Different taper configurations experience the same type of decrease but indeed the values of natural frequency are different as expected. Configuration A has the lowest values of natural frequency while configuration C has the highest values. Configuration B comes in second and configuration D has the third highest values of natural frequencies among the four taper configurations.

3.4 Free vibration analysis of thickness- and width-tapered laminated composite beams

In this section, the thickness- and width-tapered composite beam is analyzed. The beams that are thickness-tapered with different configurations A, B, C and D as shown in Figure 3.16, are considered. The beam is also width-tapered and has different width-ratios. In the following subsections, parametric studies are conducted to study the effects of boundary condition, taper angle (or equivalently length of the beam), laminate configuration, width-ratio, taper configuration, compressive axial force and damping on the natural frequencies of the beam. The beam is assumed to be symmetric about its mid-plane and therefore only the upper-half of the beam is considered in all of the calculations.

3.4.1 Effect of boundary condition on natural frequencies

A thickness- and width-tapered composite beam composed of 36 plies on the thick (left) side and 12 plies on the thin (right) side, is considered. Thickness of each ply is 0.125 mm and therefore the thick side beam thickness is 4.5 mm as opposed to 1.5 mm beam thickness at the thin side. The beam has a width of 15 mm at the wide section (b_L) and 7.5 mm at the narrow section

(b_R), which leads to a width-ratio (b_R/b_L) of 0.5. The beam has a length of 25 cm and $[0/90]_{9s}$ laminate configuration. The mechanical properties of the composite material are given in Tables 2.1 and 2.2. Free vibration analysis of the beam is conducted and the first three natural frequencies are presented in Tables 3.5 - 3.7 for taper configurations A, B, C and D and for different boundary conditions.

Table 3.5 First natural frequency (rad/s) of the thickness- and width-tapered composite beams for different boundary conditions ($b_R/b_L = 0.5$)

	Simply Supported	Clamped-Clamped	Clamped-Free	Free-Clamped
Configuration A	759.7928	1808.167	584.1598	111.4681
Configuration B	810.6909	1994.2656	656.9071	122.1972
Configuration C	827.8537	2031.0045	676.6413	121.364
Configuration D	795.5791	1926.6602	613.2257	126.8407

Table 3.6 Second natural frequency (rad/s) of the thickness- and width-tapered composite beams for different boundary conditions ($b_R/b_L = 0.5$)

	Simply Supported	Clamped-Clamped	Clamped-Free	Free-Clamped
Configuration A	3220.7583	4947.4488	2274.0021	1369.3277
Configuration B	3513.4503	5441.8962	2472.9561	1487.6723
Configuration C	3590.3567	5539.979	2540.0671	1501.2869
Configuration D	3418.7143	5324.4812	2342.4926	1507.6234

Table 3.7 Third natural frequency (rad/s) of the thickness- and width-tapered composite beams for different boundary conditions ($b_R/b_L=0.5$)

	Simply Supported	Clamped-Clamped	Clamped-Free	Free-Clamped
Configuration A	7178.7787	9668.0845	5462.9339	4598.3232
Configuration B	7857.2848	10623.9842	5913.0091	5049.08
Configuration C	8021.9524	10818.8145	6063.7484	5122.81
Configuration D	7604.2207	10326.0708	5656.5905	5039.1064

As it is shown in Tables 3.5 - 3.7, the highest values of the natural frequencies are for clamped-clamped boundary condition. The second and the third highest values of natural frequencies are for simply supported and clamped-free boundary conditions respectively. Free-clamped boundary condition has the lowest natural frequencies among all boundary conditions.

3.4.2 Effect of taper angle (or equivalently length of the beam) on natural frequencies

The same beam as that analyzed in section 3.4.1 is considered. Taper angles of 0.86° , 0.573° , 0.43° and 0.344° are used (corresponding lengths of the tapered beam are 0.1 m, 0.15 m, 0.2 m and 0.25 m). The free vibration analysis is conducted and the first three natural frequencies are presented in Figure 3.23 and Figures A.7 and A.8.

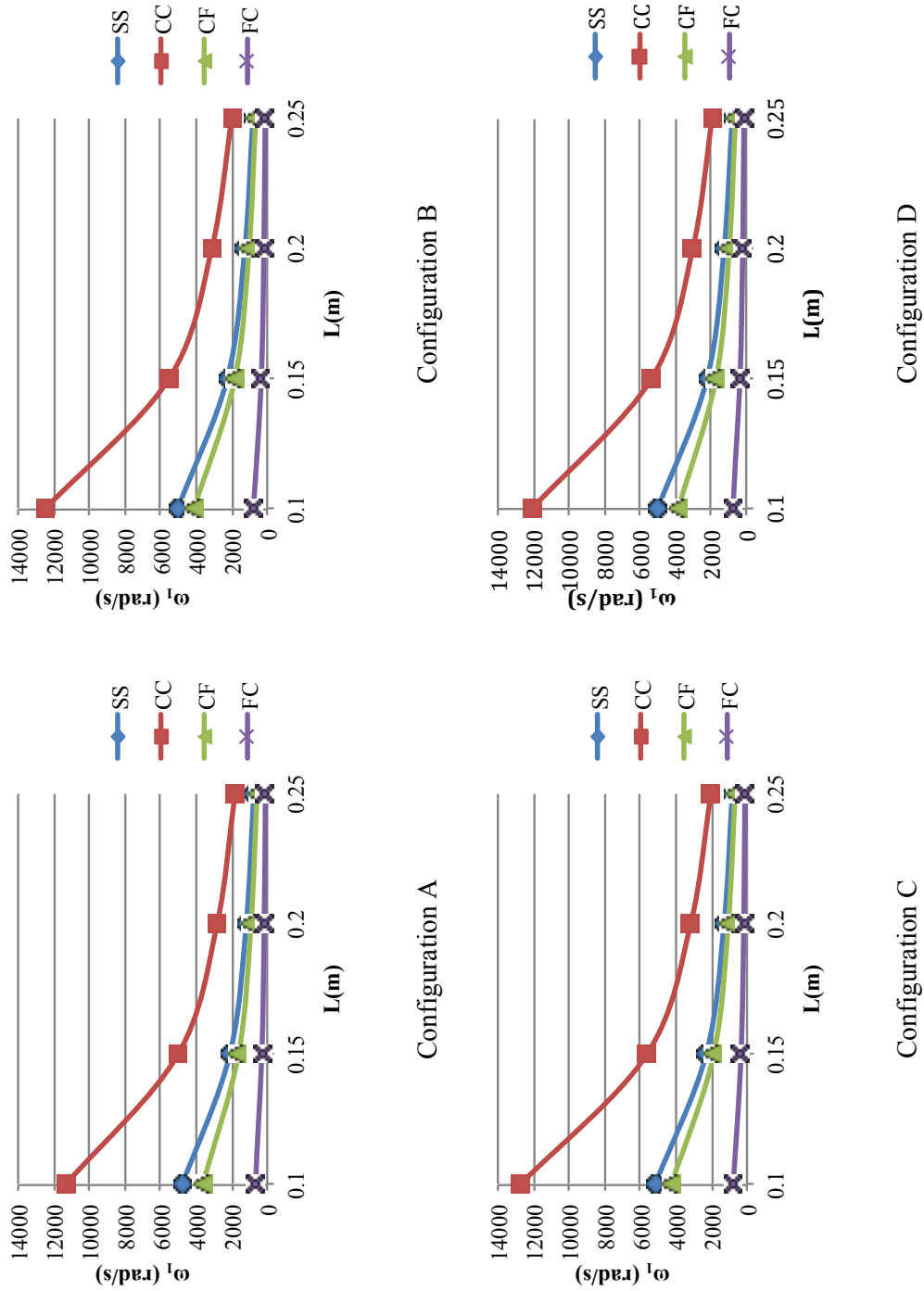


Figure 3.23 Effect of the length on the first natural frequency of the thickness- and width-tapered composite beams ($b_R/b_L=0.5$)

It can be observed from Figure 3.23 that by increasing the length of the beam (or equivalently decreasing the taper angle), the first natural frequency decreases dramatically. This behavior can be interpreted by the fact that the beam becomes more rigid as its length decreases and therefore it has higher natural frequencies. Also, it is evident from Figures A.7 and A.8 that the second and the third natural frequencies follow the same pattern.

3.4.3 Effect of laminate configuration on natural frequencies

In order to study the effect of laminate configuration on natural frequencies, the same beam as that analyzed in section 3.4.1 is considered. Laminate configurations LC1, LC2, LC3 and LC4 that are mentioned in section 3.2.4 and are shown in Figure 3.9 are considered. The free vibration analysis for boundary conditions simply supported (S-S), clamped-clamped (C-C), clamped-free (C-F) and free-clamped (F-C) is conducted and the first three natural frequencies are presented in Figure 3.24 and Figures A.9 and A.10.

As it is shown in Figure 3.24, laminate configuration LC3 has the highest values of the first natural frequency in all of the taper configurations and boundary conditions. LC1 and LC4 have the second and the third highest first natural frequencies respectively. LC2 has the lowest first natural frequency among all laminate configurations. It is also evident from Figures A.9 and A.10 that the second and the third natural frequencies follow the same pattern.

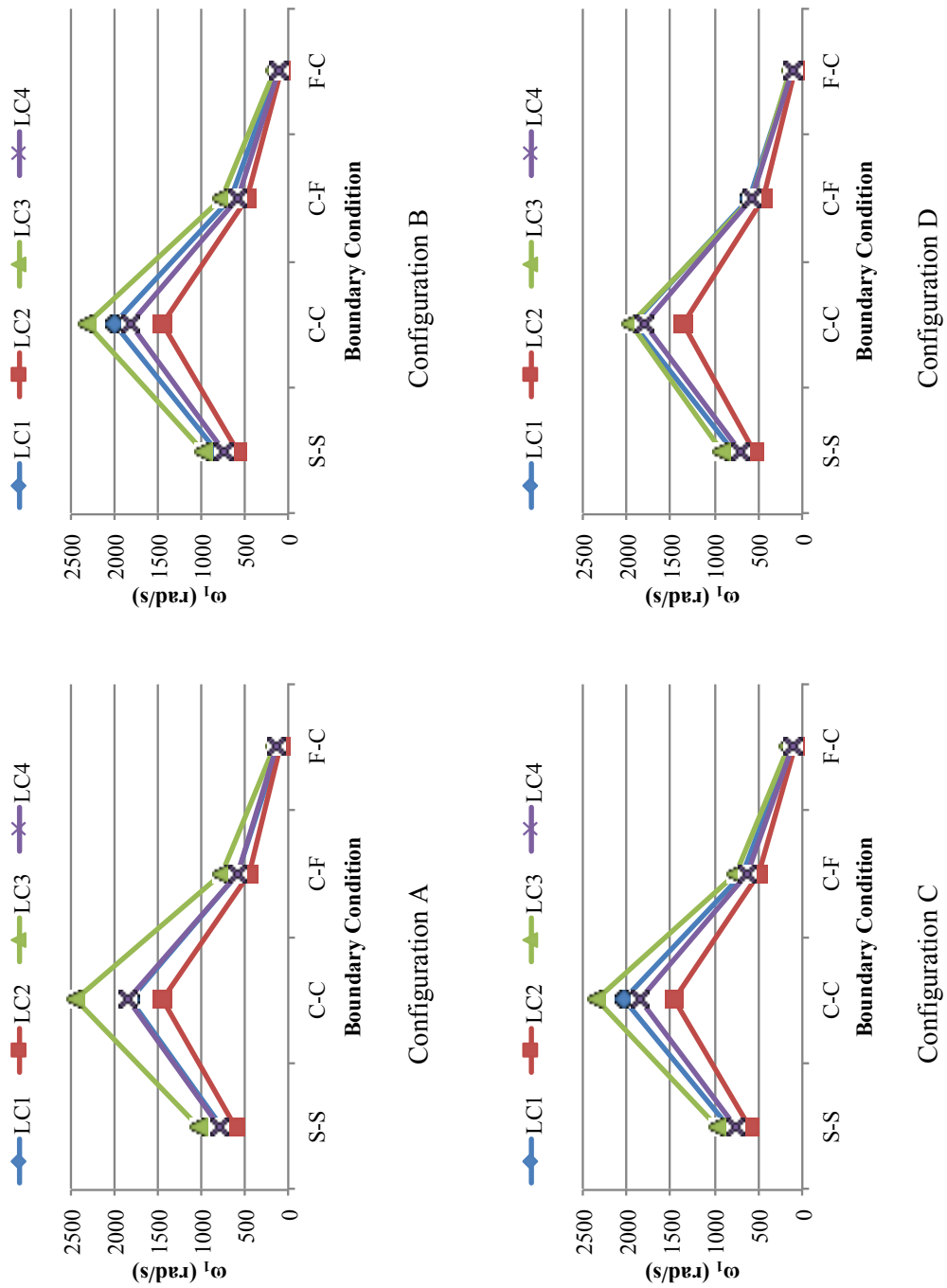


Figure 3.24 Effect of laminate configuration on the first natural frequency of the thickness- and width-tapered composite beam ($b_R/b_L=0.5$)

3.4.4 Effect of width-ratio on natural frequencies

The same beam as that analyzed in section 3.4.1 is considered. The beam has width-ratios of 0.01, 0.02, 0.05, 0.1, 0.2, 0.4, 0.6, 0.8 and 1.0. The free vibration analysis is conducted and the first three natural frequencies for taper configurations A, B, C and D are presented in Figure 3.25 and Figures A.11 and A.12.

As it is shown in Figure 3.25 by increasing the width-ratio, the first natural frequencies increase for the simply supported, the clamped-clamped and the free-clamped boundary conditions but they decrease for the clamped-free boundary condition. The reason is that in the clamped-free boundary condition by increasing the width-ratio, the material on the free side is being added up and therefore the beam becomes more resistant to vibration and that leads to reduction of natural frequencies. Also, it is evident that the highest natural frequency is for the clamped-clamped boundary condition, while the lowest is for the free-clamped boundary condition.

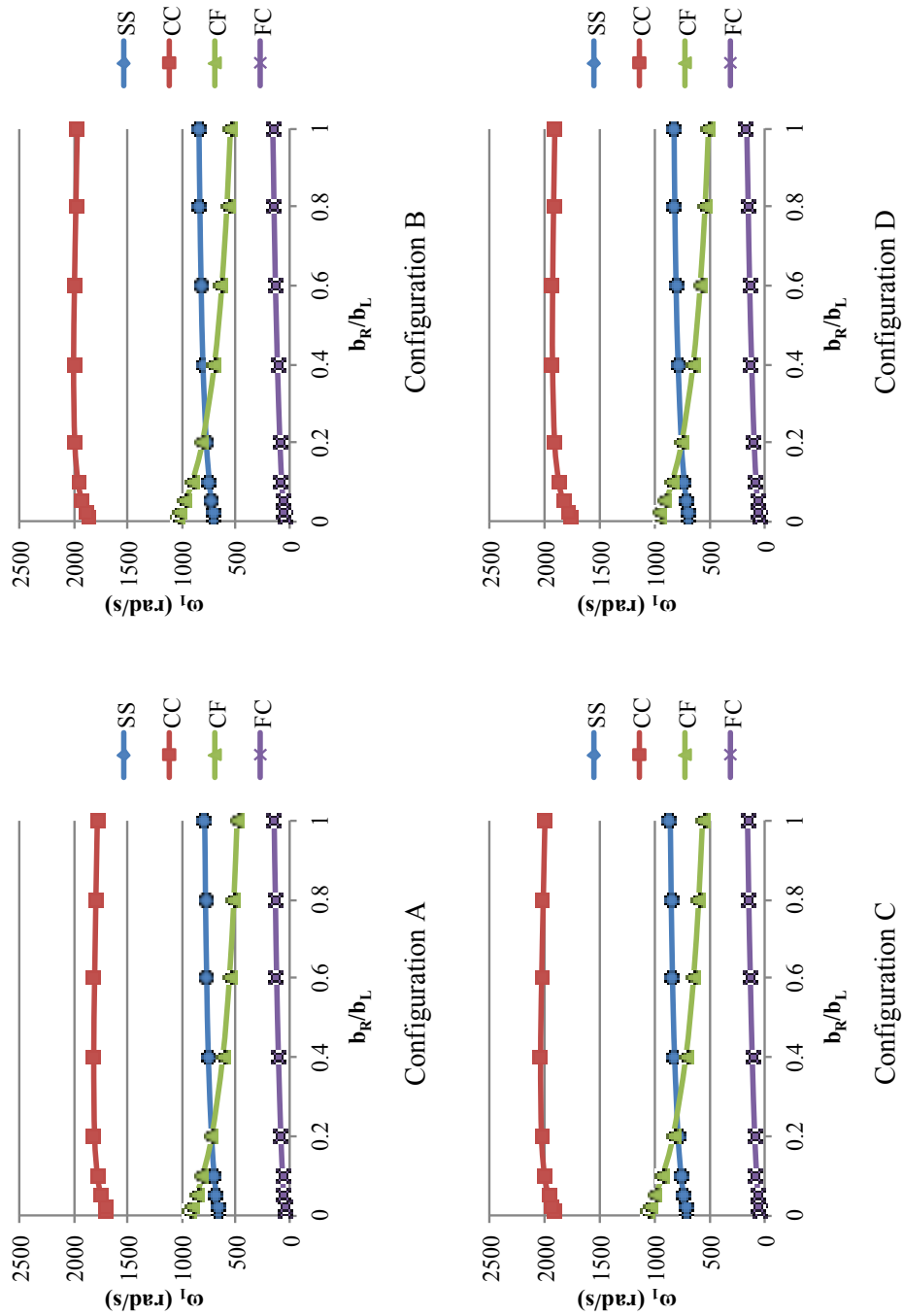


Figure 3.25 Effect of width-ratio on the first natural frequency of the thickness- and width-tapered composite beam

3.4.5 Effect of taper configuration on natural frequencies

The same beam as that analyzed in section 3.4.4 with the width-ratio of 0.5 and length of 25 cm is considered. The free vibration analysis is conducted and the first three natural frequencies for taper configurations A, B, C and D are presented in Figures 3.26 - 3.28.

As it is shown in Figures 3.26 - 3.28, for all three natural frequencies configuration A has the lowest natural frequencies. The highest natural frequencies are for configuration C. Configuration B has slightly lower values of natural frequencies than configuration C and has the second highest natural frequencies. Configuration D has the third highest natural frequencies among all configurations. An interpretation of this behavior was presented in section 3.3.4.

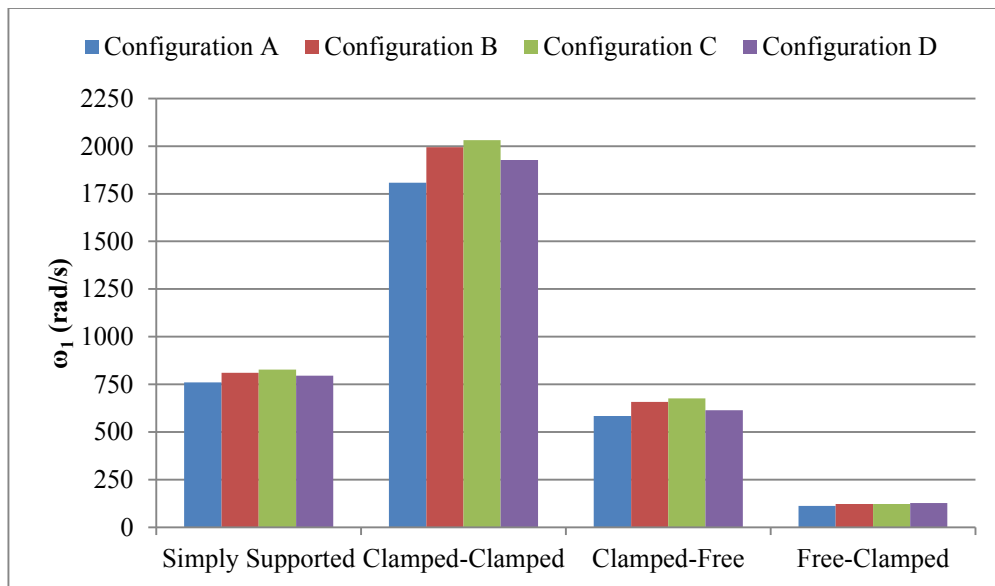


Figure 3.26 Effect of taper configuration on the first natural frequency of the thickness- and width-tapered composite beam ($b_R/b_L=0.5$)

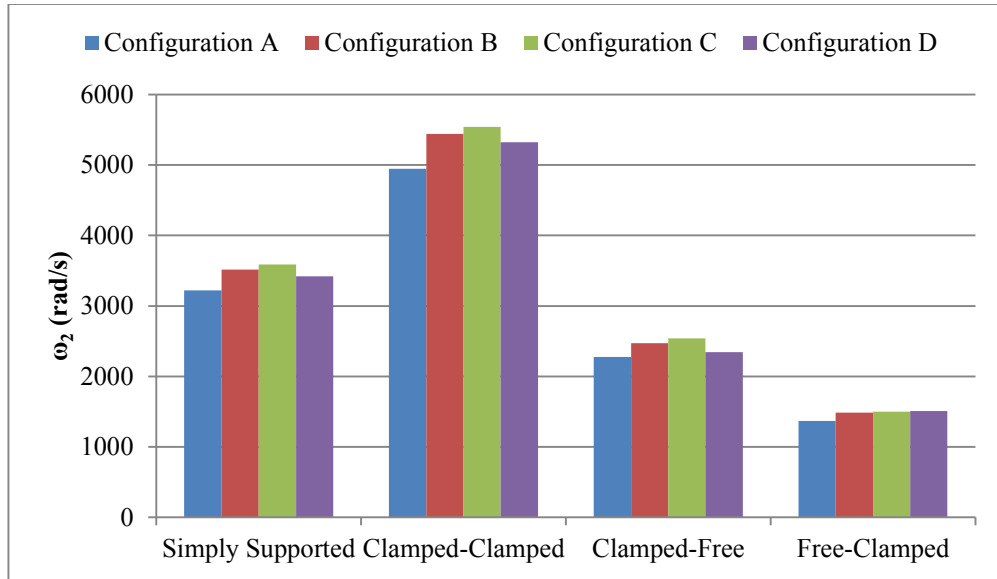


Figure 3.27 Effect of taper configuration on the second natural frequency of the thickness- and width-tapered composite beam ($b_R/b_L=0.5$)

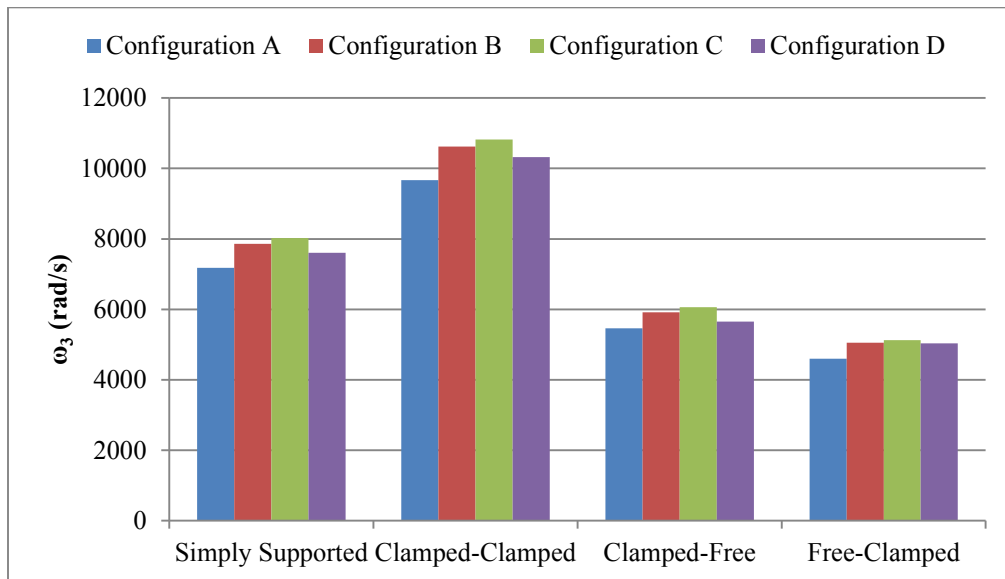


Figure 3.28 Effect of taper configuration on the third natural frequency of the thickness- and width-tapered composite beam ($b_R/b_L=0.5$)

3.4.6 Effect of compressive axial force on natural frequencies

The same beam as that analyzed in section 3.4.5 is considered. First a buckling analysis is conducted to calculate the critical buckling load, P_{cr} . The free vibration analysis under compressive axial forces equal to 10%, 50% and 90% of P_{cr} is conducted and the first three natural frequencies are shown in Figure 3.29 and Figures A.13 and A.14 for different boundary conditions and taper configurations.

As it is shown in Figure 3.29, the first natural frequency for all the taper configurations and also all the boundary conditions decreases by increasing the compressive axial force. It is also evident from Figures A.13 and A.14 that the second and the third natural frequencies follow the same pattern. This is due to the fact that in the presence of compressive axial force after the initial deflection, the resultant moment pulls the beam further from its neutral position. Therefore the beam becomes more flexible and consequently the natural frequencies decrease.

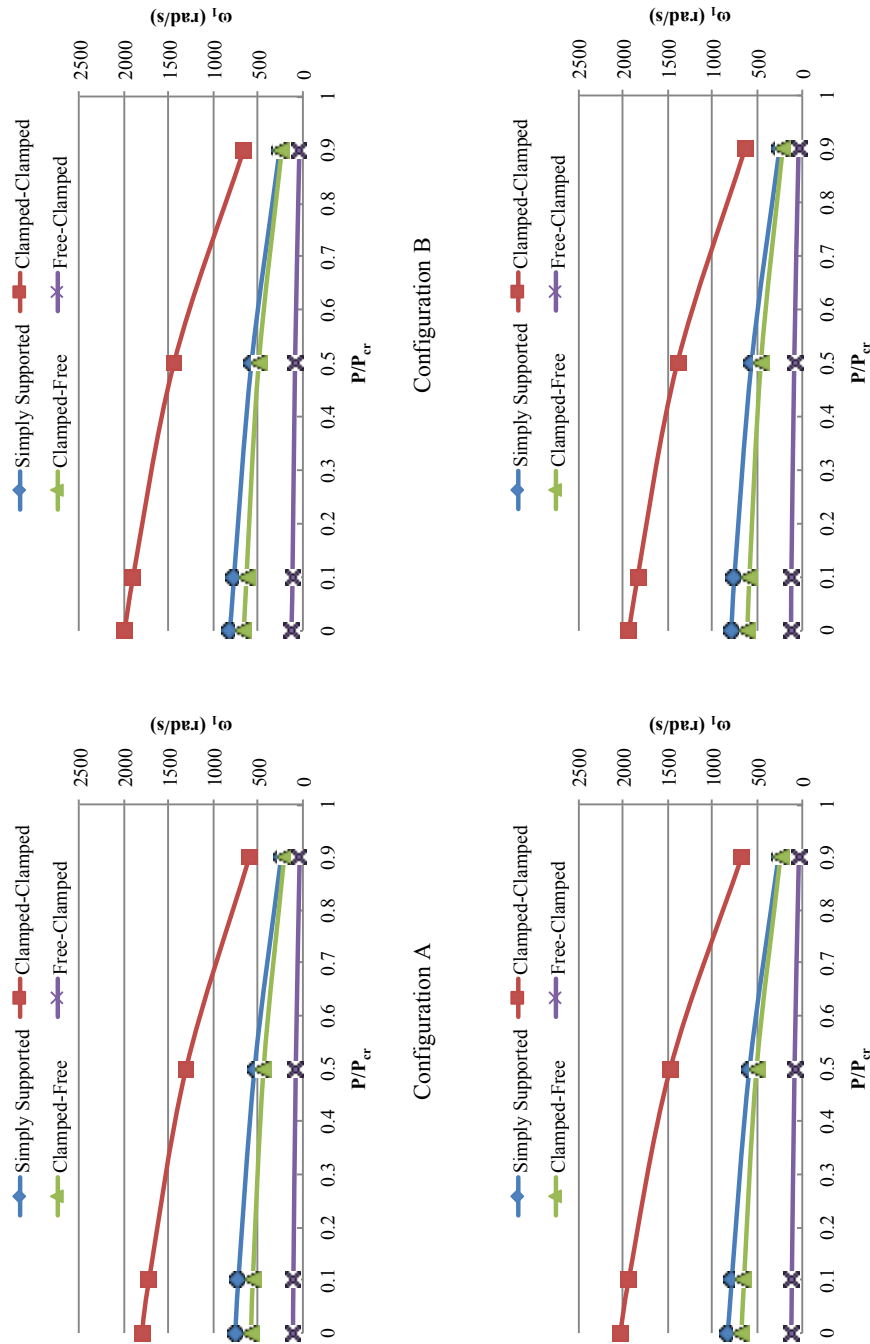


Figure 3.29 Effect of compressive axial force on the first natural frequency of the thickness- and width-tapered composite beam ($b_R/b_L=0.5$)

3.4.7 Effect of damping on natural frequencies

In order to take into account the effect of damping on natural frequencies of the thickness- and width-tapered laminated composite beam, Rayleigh damping method is used to model the viscous damping of the beam. Classical Rayleigh damping model uses a system damping matrix $[C]$ defined as:

$$[C] = \alpha[M] + \beta[K] \quad (3.1)$$

in which α denotes the mass proportional Rayleigh damping constant and β is the stiffness proportional Rayleigh damping constant, and $[M]$ and $[K]$ are the mass and stiffness matrices respectively.

The same beam as that analyzed in section 3.4.5 is considered. The beam is assumed to have Rayleigh damping with:

$$\alpha = 3.752 \quad (3.2)$$

$$\beta = 4.83 \times 10^{-5} \quad (3.3)$$

that were determined by experiment [22].

Damped free vibration analysis is conducted and the first three natural frequencies for taper configurations A, B, C and D are given in Tables 3.8 - 3.11 for different boundary conditions.

It is evident from Tables 3.8 - 3.11 that the addition of damping results in the reduction of the natural frequencies for all taper configurations and boundary conditions. The percentage of reduction varies between 0.01 % (Configuration A, Clamped-Free) to 3.48 % (Configuration C, Clamped-Clamped) depending on the taper configuration and boundary condition. It can be seen that the reduction in natural frequencies caused by damping is directly correlated with the damping ratio (ξ) of the beam. As damping ratio increases, the percentage of difference between undamped

and damped natural frequencies also increases. It can be seen from Tables 3.8-3.11 that damping ratio (ξ) for the first natural frequency is much smaller than that for the second and the third natural frequencies. Therefore the effect of damping on first natural frequency is higher than the second and the third natural frequencies. Moreover, it can be observed that the effect of damping on natural frequencies is higher for clamped-clamped beams than simply supported and clamped-free beams.

Table 3.8 Effect of damping on natural frequencies of thickness- and width-tapered composite beam with the taper configuration A ($b_R/b_L=0.5$)

Boundary Condition		ω_1 (rad/s)	ω_2 (rad/s)	ω_3 (rad/s)
Simply Supported	Undamped	784.52	3196.59	7140.88
	Damped	784.35	3186.90	7033.56
	Difference (%)	0.02	0.30	1.50
	ξ	0.021	0.078	0.173
Clamped - Clamped	Undamped	1777.56	4904.28	9619.31
	Damped	1775.84	4869.54	9355.70
	Difference (%)	0.10	0.71	2.74
	ξ	0.044	0.119	0.233
Clamped - Free	Undamped	484.97	2132.08	5310.13
	Damped	484.91	2129.16	5266.05
	Difference (%)	0.01	0.14	0.83
	ξ	0.016	0.052	0.129

Table 3.9 Effect of damping on natural frequencies of thickness- and width-tapered composite beam with the taper configuration B ($b_R/b_L=0.5$)

Boundary Condition		ω_1 (rad/s)	ω_2 (rad/s)	ω_3 (rad/s)
Simply Supported	Undamped	810.69	3513.45	7857.28
	Damped	810.50	3500.62	7714.17
	Difference (%)	0.02	0.37	1.82
	ξ	0.022	0.085	0.190
Clamped - Clamped	Undamped	1994.27	5441.90	10623.98
	Damped	1976.88	5435.33	10267.86
	Difference (%)	0.87	0.12	3.35
	ξ	0.132	0.049	0.257
Clamped - Free	Undamped	656.91	2472.96	5913.01
	Damped	656.79	2468.43	5852.14
	Difference (%)	0.02	0.18	1.03
	ξ	0.019	0.060	0.143

Table 3.10 Effect of damping on natural frequencies of thickness- and width-tapered composite beam with the taper configuration C ($b_R/b_L=0.5$)

Boundary Condition		ω_1 (rad/s)	ω_2 (rad/s)	ω_3 (rad/s)
Simply Supported	Undamped	827.85	3590.36	8021.95
	Damped	827.65	3576.67	7869.60
	Difference (%)	0.02	0.38	1.90
	ξ	0.022	0.087	0.194
Clamped - Clamped	Undamped	2031.00	5539.98	10818.81
	Damped	2012.65	5533.06	10442.51
	Difference (%)	0.90	0.12	3.48
	ξ	0.134	0.050	0.261
Clamped - Free	Undamped	676.64	2540.07	6063.75
	Damped	676.52	2535.17	5998.10
	Difference (%)	0.02	0.19	1.08
	ξ	0.019	0.062	0.147

Table 3.11 Effect of damping on natural frequencies of thickness- and width-tapered composite beam with the taper configuration D ($b_R/b_L=0.5$)

Boundary Condition		ω_1 (rad/s)	ω_2 (rad/s)	ω_3 (rad/s)
Simply Supported	Undamped	795.58	3418.71	7604.22
	Damped	795.39	3406.89	7474.55
	Difference (%)	0.02	0.35	1.71
	ξ	0.022	0.083	0.184
Clamped - Clamped	Undamped	1926.66	5324.48	10326.07
	Damped	1924.49	5280.04	9999.36
	Difference (%)	0.11	0.83	3.16
	ξ	0.048	0.129	0.250
Clamped - Free	Undamped	613.23	2342.49	5656.59
	Damped	613.13	2338.63	5603.30
	Difference (%)	0.02	0.16	0.94
	ξ	0.018	0.057	0.137

3.5 Summary

In this chapter a parametric study was carried out to study the free vibration of tapered composite beams. Three types of tapering were considered as width-tapered, thickness-tapered and thickness- and width-tapered. For each type of tapering, the effects of main parameters (boundary condition, width-ratio, length (or taper angle), laminate configuration, taper configuration and compressive axial force) on the natural frequencies were studied. A summary of observations is given below:

- Among all boundary conditions, for the width-tapered beam, the clamped-clamped boundary condition has the highest values of natural frequencies. With a rather large difference, the simply supported boundary condition has the second highest natural frequencies. Clamped-free and free-clamped boundary conditions have the third and fourth highest natural frequencies respectively, but the difference is not as significant. For the thickness-tapered beam, there is an overall decrease in all the natural frequencies (compared to width-tapered beam). However, the difference between the natural frequencies that correspond to clamped-free and free-clamped boundary conditions is much more significant. For the thickness- and width-tapered beam, the difference (compared to thickness-tapered beam) is not significant but the order of the effect of boundary condition is the same.

- By decreasing the length of the tapered beam (or equivalently increasing the taper angle while preserving the thicknesses at both sides of the beam), the natural frequencies increase dramatically for all boundary conditions and tapering types. For the width-tapered beam, as the length decreases, the clamped-free and free-clamped boundary conditions show the same rate of

increase. Simply supported boundary condition has a higher rate of increase compared to the clamped-free and the free-clamped boundary conditions. The clamped-clamped beam has the highest rate of increase in natural frequencies. For the other two tapering types, the clamped-free boundary condition has a much higher rate of increase compared to the free-clamped boundary condition but the other two boundary conditions follow the same pattern as that for the width-tapered beam.

- For all the tapering types, boundary conditions and taper configurations, the laminate configuration LC3 has the highest natural frequencies, LC2 has the lowest natural frequencies and LC1 and LC4 have the second and third highest natural frequencies respectively.

- For all the tapering types, boundary conditions and taper configurations, increasing the compressive axial force results in decreasing the natural frequencies. This is due to the fact that in the presence of compressive axial force after the initial deflection, the resultant moment pulls the beam further from its neutral position. Therefore the beam becomes more flexible and consequently the natural frequencies decrease. This decrease is more significant in the first natural frequency (compared to the second and the third natural frequencies).

- For the width-tapered beam by increasing the width-ratio the natural frequencies increase for simply supported, clamped-clamped and free-clamped boundary conditions but they decrease for the clamped-free boundary condition. The reason is that by increasing the width-ratio, the additional material on the free side of the beam results in the corresponding changes in the stiffness and mass of the beam and consequently, decrease in natural frequencies. The thickness- and width-tapered beam shows a total decrease in natural frequencies (compared to width-tapered beam) but follows the same pattern.

- For the thickness-tapered beam, configuration C has the highest values of natural frequencies for all the boundary conditions. Configuration B has the second highest natural frequencies. Configuration D and configuration A come in third and fourth respectively. Because configuration A has the largest volume of resin compared to other configurations, it is less stiff and consequently has the lowest natural frequencies. Configuration D has less volume of resin than configuration A but much more than configurations B and C. Configuration C has the plies at a larger distance from the mid-plane and resin pockets at a smaller distance from the mid-plane, compared to configuration B and therefore has a slightly larger D_{11} value than configuration B and higher natural frequencies. Thickness- and width-tapered beam has slightly higher values of natural frequencies compared to the other two tapering types, but the effect of taper configuration on natural frequencies is the same.

- Addition of damping results in reduction of natural frequencies. The amount of reduction highly depends on the damping ratio (ξ) and therefore, the amount of reduction is higher for the second and the third natural frequencies (compared to the amount of reduction for the first natural frequency).

- Overall, thickness-tapering has much more significant effect on natural frequencies than width-tapering. This comes from the fact that the difference between the natural frequencies of the thickness-tapered and the thickness- and width-tapered beams is not that significant. However, this difference is much more significant between the thickness-tapered and the width-tapered beams. The reason is that the thickness of the beam has cubic impact on the $D_{11}(x)$ [13] and consequently the stiffness of the beam while the width of the beam $b(x)$ has a linear impact on the stiffness of the beam as shown in Equation 2.20.

4. Forced vibration analysis of tapered composite beams

4.1 Introduction

In the previous chapter, free vibration analysis of tapered laminated composite beams was conducted and the effects of main parameters on natural frequencies were presented. Three types of tapered laminated composite beams (width-tapered, thickness-tapered and thickness- and width-tapered beams) were considered. In this chapter, forced vibration analysis of uniform and thickness- and width-tapered laminated composite beams is carried out using modal analysis and the effects of different parameters such as taper configuration, width-ratio and boundary condition on the response in terms of deflection (w) and rotation (θ), are determined in section 4.2. In section 4.3 the effect of damping on the natural frequencies and the forced vibration response of uniform and thickness- and width-tapered laminated composite beams is presented. The cylindrical bending theory and Hierarchical Finite Element Method (HFEM) are used in all formulations. The NCT-301 graphite-epoxy composite material is considered and the mechanical properties of the ply and the resin are given in Tables 2.1 and 2.2. Symmetric laminated beams are considered in all problems. At the end of the chapter a summary of observations and results are presented.

4.2 Undamped Forced vibration analysis

4.2.1 Formulation

The equation of motion of an n -DOF (n-degrees of freedom) undamped composite beam is given by:

$$[M]\{\ddot{w}\} + [K]\{w\} = \{F\} \quad (4.1)$$

in which $[M]$ and $[K]$ are the mass and stiffness matrices and $\{w\}$ and $\{F\}$ represent displacement and force vectors respectively. The homogenous solution to equation (4.1) is obtained by solving the eigenvalue problem:

$$|[K] - \lambda[M]|\{\phi\} = 0 \quad (4.2)$$

in which λ is the eigenvalue and ϕ is the corresponding eigenvector. Stiffness and mass matrices for the beam can be obtained using hierarchical or conventional finite element formulations as it has been explained in previous chapters. The forced vibration of the composite laminated beams is determined using mode superposition method [37]. Having the stiffness and the mass matrices for a laminated composite beam and solving the eigenvalue problem as in equation (4.2) using MATLAB[®] software, one can find the eigenvalues and the orthonormal eigenvector matrix $[\tilde{P}]$ of the beam. Eigenvalues are equal to the square of natural frequencies and the orthonormal eigenvector matrix $[\tilde{P}]$ can be used to decouple the equations of motion.

One can decouple the equations of motion by transforming the coordinates using orthonormal eigenvector matrix as:

$$\{w\} = [\tilde{P}]\{y\} \quad (4.3)$$

Substituting equation (4.3) into equation (4.1) and pre-multiplying by $[\tilde{P}]$ leads to:

$$[\tilde{P}]^T [M] [\tilde{P}] \{\ddot{y}\} + [\tilde{P}]^T [K] [\tilde{P}] \{y\} = [\tilde{P}]^T \{F\} \quad (4.4)$$

In the equation (4.3) $\{y\}$ is the vector of nodal displacements in the transformed coordinates. $\{F\}$ is the force vector applied to the beam which represents the nodal forces applied to the beam. It can be easily seen [37] then that:

$$[\tilde{P}]^T [M] [\tilde{P}] = [I] \quad (4.5)$$

$$[\tilde{P}]^T [K] [\tilde{P}] = [\Lambda] \quad (4.6)$$

where $[I]$ is the $n \times n$ unity matrix and $[\Lambda]$ is the diagonal matrix of the eigenvalues.

$$[\Lambda] = \begin{bmatrix} \lambda_1 & 0 & \cdots & 0 \\ 0 & \lambda_2 & \cdots & 0 \\ \vdots & \vdots & \ddots & \vdots \\ 0 & 0 & \cdots & \lambda_n \end{bmatrix} \quad (4.7)$$

$$\omega_i = \sqrt{\lambda_i} \quad (4.8)$$

Because the products $[\tilde{P}]^T [M] [\tilde{P}]$ and $[\tilde{P}]^T [K] [\tilde{P}]$ are diagonal matrices, the new equations in terms of transformed coordinates are uncoupled. Substituting Equations (4.5) and (4.6) into Equation (4.4) results in n decoupled second-order differential equations that are:

$$\{\ddot{y}\}_i + \lambda_i \{y\}_i = \{f\}_i, \quad i = 1, 2, \dots, n \quad (4.9)$$

in which

$$\{f\} = [\tilde{P}]^T \{F\} \quad (4.10)$$

Then solving each differential equation in equation (4.9) results in:

$$y_i = y_i(0) \cos \omega_i t + \frac{\dot{y}_i(0) \sin \omega_i t}{\omega_i} + \frac{f_i \sin \omega t}{\omega_i^2 - \omega^2} \quad (4.11)$$

in which ω_i is the i -th natural frequency, ω is the frequency of excitation, and $y_i(0)$ and $\dot{y}_i(0)$ are the initial conditions.

Having the nodal displacement vector in transformed coordinates $\{y\}$ and using equation (4.3), one can find the forced vibration response in terms of nodal displacement matrix $\{w\}$.

4.2.2 Forced vibration response of uniform composite beams

A uniform-thickness uniform-width laminated composite beam made of NCT-301 graphite-epoxy composite material with the mechanical properties given in Tables 2.1 and 2.2 is considered. The beam has $[0/90]_{9s}$ laminate configuration and a length (L) of 25 cm. The beam is composed of 36 plies. Individual ply thickness (t_i) is 0.125 mm and the beam thickness (H) is 4.5 mm. The beam has a width of 15 mm. The beam is assumed to be symmetric about its mid-plane and therefore only the upper-half of the beam is considered in all the calculations.

As it is shown in Figures 4.1 and 4.2, the beam is divided into 6 elements. Each element has 2 nodes and each node has two degrees of freedom that are deflection (w) and rotation (θ).

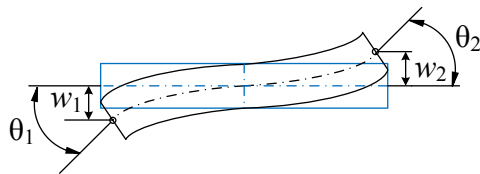


Figure 4.1 Element's nodal degrees of freedom

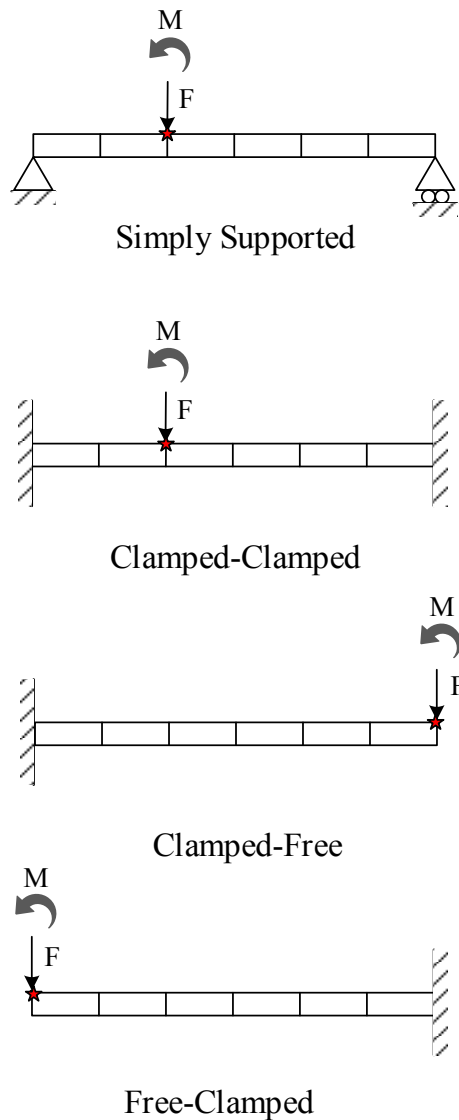


Figure 4.2 Location of the forces and the moments and the response points for different boundary conditions for uniform laminated composite beam; the red star represents the point of response

Moreover, as it was discussed in previous chapters, in Hierarchical Finite Element Method (HFEM) additional virtual degrees-of-freedom are added to the system that correspond to the number of elements. In this study the beam is divided into 6 elements with each element having 4

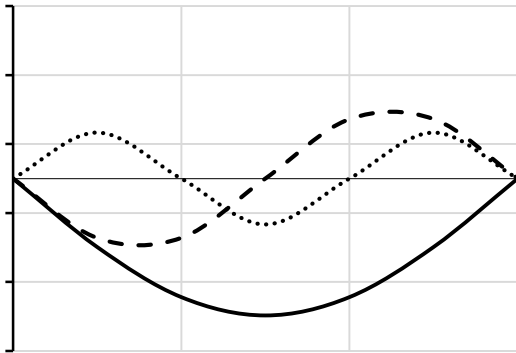
degrees-of-freedom at the nodes and one hierarchical degree-of-freedom. This results in a 20 degrees-of-freedom system and consequently the nodal displacement matrix $\{w\}$ is in the form of:

$$\{w\} = \begin{bmatrix} w_1 \\ \theta_1 \\ w_2 \\ \theta_2 \\ \vdots \\ w_7 \\ \theta_7 \\ A_1 \\ \vdots \\ A_6 \end{bmatrix} \quad (4.12)$$

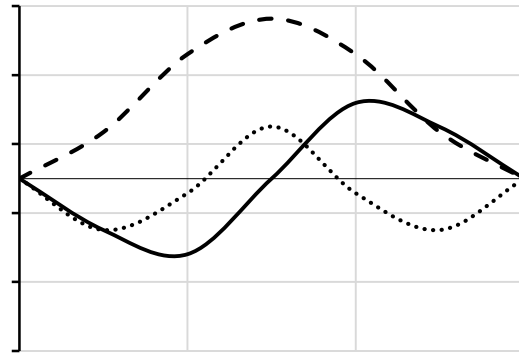
The corresponding force matrix $\{F\}$ is in the form of:

$$\{F\} = \begin{bmatrix} F_1 \\ M_1 \\ F_2 \\ M_2 \\ \vdots \\ F_7 \\ M_7 \\ B_1 \\ \vdots \\ B_6 \end{bmatrix} \quad (4.13)$$

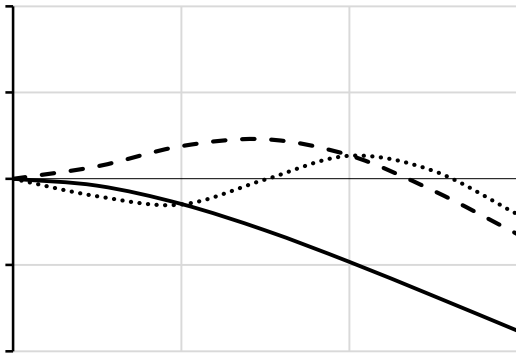
A sinusoidal force (F) with the magnitude of 2 N and a sinusoidal moment (M) with the magnitude of 2 N-m both with the excitation frequency of ω are applied close to the center of the beam for simply supported and clamped-clamped boundary conditions, and at the free-end of the beam for clamped-free and free-clamped boundary conditions as shown in Figure 4.2. The points of response (red stars) are chosen according to mode shapes of free vibration of the laminated composite beam with different boundary conditions as shown in Figure 4.3. In order to avoid applying the force to the nodal points of the second mode shape of the uniform beams, the force is not applied exactly at the middle of the clamped-clamped and simply supported beams as is shown in Figure 4.2.



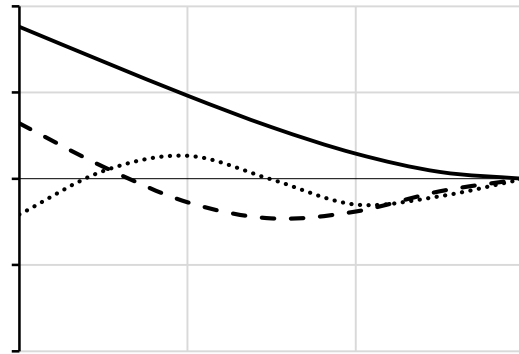
Simply Supported



Clamped-Clamped



Clamped-Free



Free-Clamped

Figure 4.3 First three mode shapes of uniform laminated composite beams with different boundary conditions; solid line represents the 1st mode, dashed line represents the 2nd mode and dotted line represents the 3rd mode

The forced vibration response of the uniform laminated composite beam are shown in Figures 4.4 and 4.5 for simply supported, clamped-clamped, clamped-free and free-clamped boundary conditions using hierarchical finite element method.

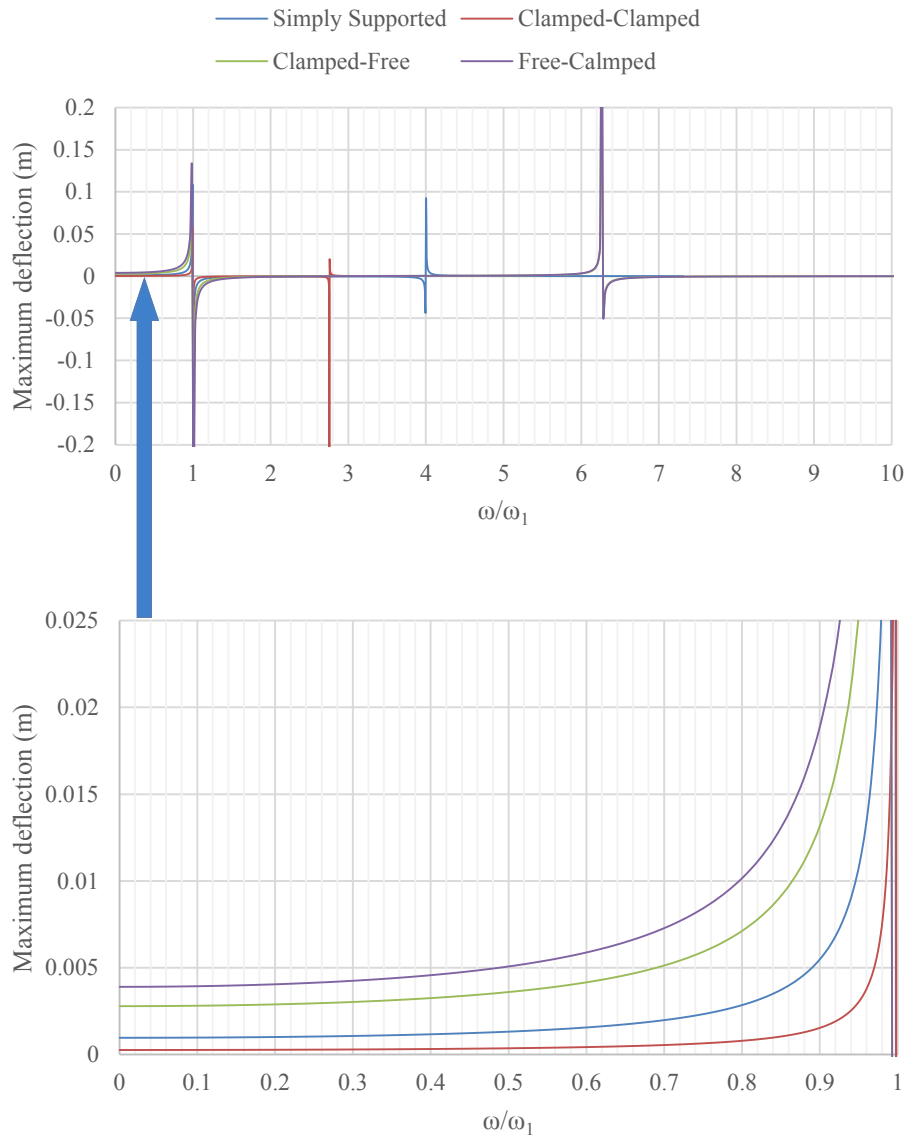


Figure 4.4 Forced vibration response (maximum deflection) of the uniform composite beams for different boundary conditions; bottom figure represents the magnified area of the top figure

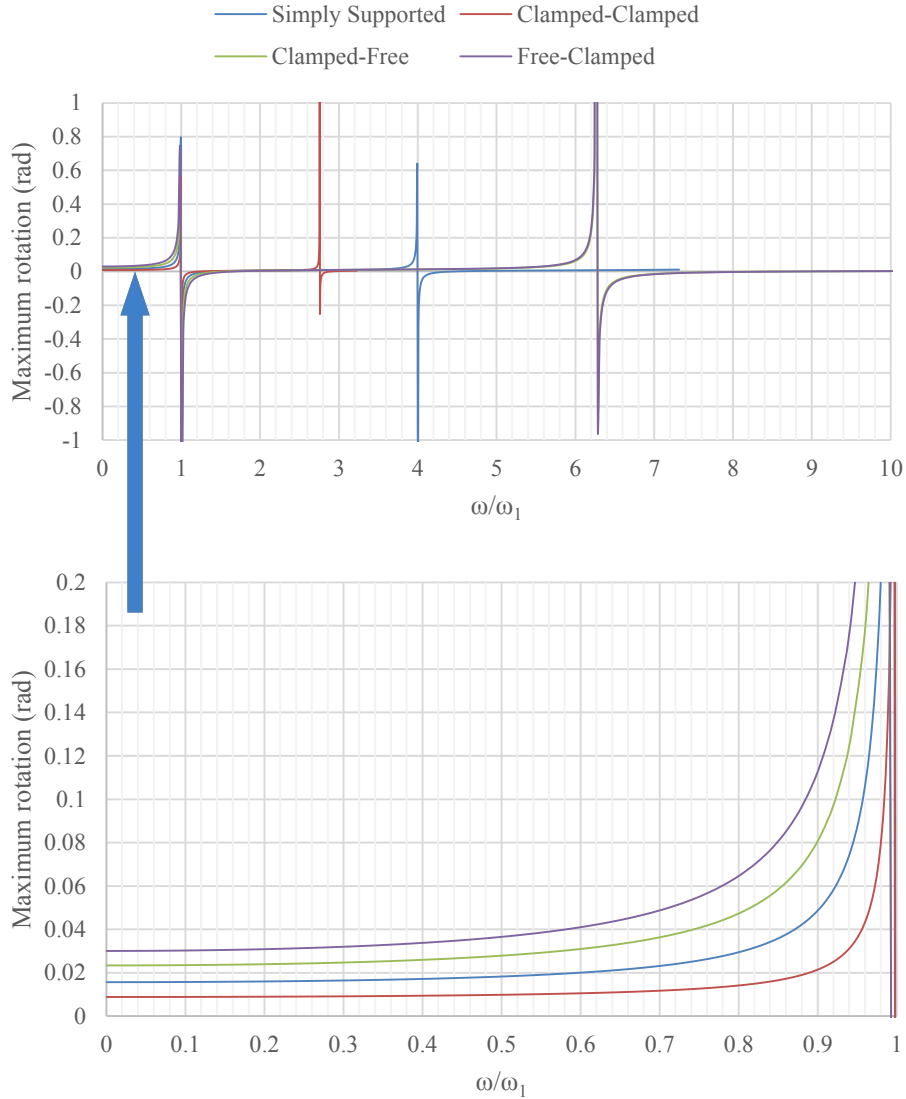


Figure 4.5 Forced vibration response (maximum rotation) of the uniform composite beams for different boundary conditions; bottom figure represents the magnified area of the top figure

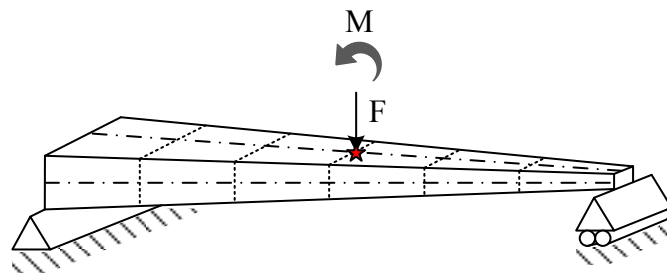
It can be observed that as excitation frequency (ω) nears the natural frequencies, due to resonance the response approaches infinity and becomes unstable. Therefore, only a stable part of the response ($0 < \frac{\omega}{\omega_1} < 1$) is used for comparison. It should be noted that in Figures 4.4 and 4.5 (ω_1) is the first natural frequency of the laminated composite beam with the corresponding

boundary condition. Therefore as excitation frequency (ω) reaches the second or the third natural frequencies, the value of $(\frac{\omega}{\omega_1})$ would be different for different boundary conditions or taper configurations.

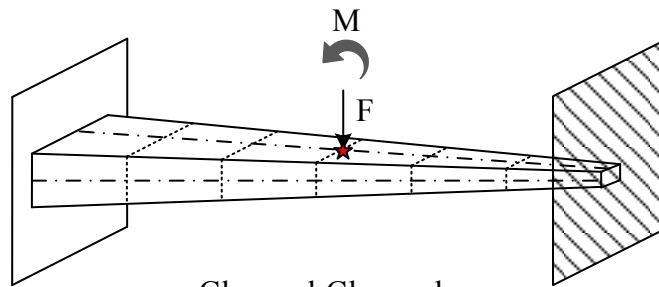
It is evident from Figures 4.4 and 4.5 that clamped-clamped beam has the lowest amplitude of the response (in terms of maximum deflection and maximum rotation). It is due to the fact that clamped-clamped beam has the highest stiffness among all boundary conditions. Simply supported beam has a lower stiffness than clamped-clamped beam, however it has a higher stiffness than clamped-free and free-clamped beams. Free-clamped has the lowest stiffness among all the boundary conditions. As a result, simply supported, clamped-free and free-clamped boundary conditions have the second, the third and the fourth highest amplitudes of the response respectively.

4.2.3 Forced vibration response of thickness- and width-tapered composite beams

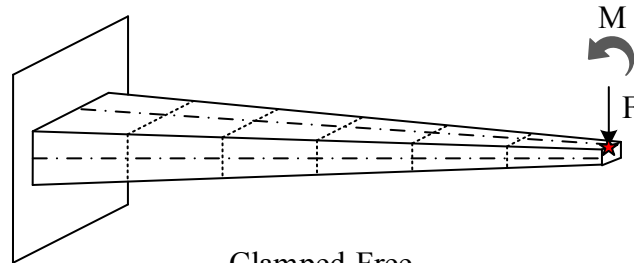
A thickness- and width-tapered laminated composite beam made of NCT-301 graphite-epoxy composite material with the mechanical properties given in Tables 2.1 and 2.2 is considered. The beam has a width of 15 mm at the wide (left) section with the width-ratio of 0.5. The beam is composed of 36 plies at the thick (left) side and 12 plies at the thin (right) side. Thickness of each ply is 0.125 mm and therefore the left side beam thickness is 4.5 mm as opposed to 1.5 mm beam thickness at the right side. The beam has a length of 25 cm and $[0/90]_{9s}$ laminate configuration. The beam is assumed to be symmetric about its mid-plane and therefore only the upper-half of the beam is considered in all the calculations. As it is shown in Figure 4.3, the beam is divided into 6 elements. Each element has 2 nodes and each node has two degrees of freedom that are deflection (w) and rotation (θ) as shown in Figure 4.1.



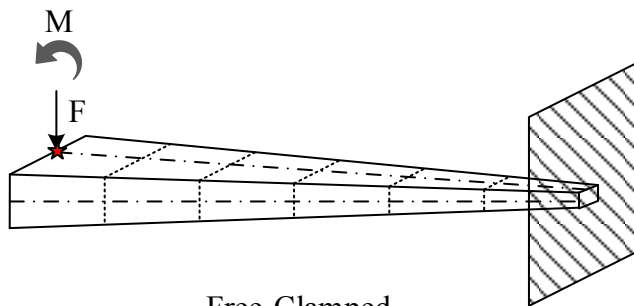
Simply Supported



Clamped-Clamped



Clamped-Free



Free-Clamped

Figure 4.6 Location of the forces and the moments and the response points for different boundary conditions; red stars represent the points of response

A sinusoidal force (F) with the magnitude of 2 N and a sinusoidal moment (M) with the magnitude of 2 N-m both with the excitation frequency of ω are applied at the center of the beam for simply supported and clamped-clamped boundary conditions, and at the free-end of the beam for clamped-free and free-clamped boundary conditions. The points of excitation and the points of response are chosen according to mode shapes of free vibration of the laminated composite beam with different boundary conditions as shown in Figure 4.6.

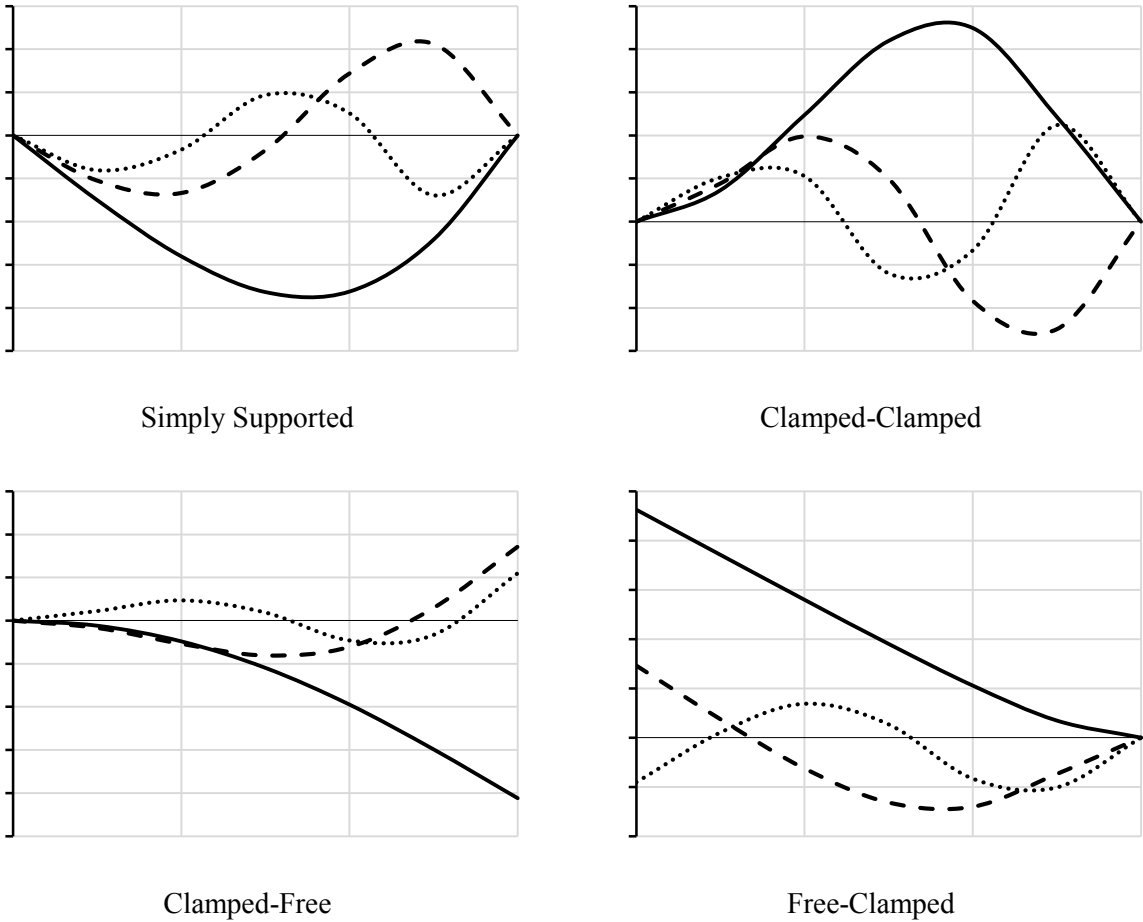


Figure 4.7 First three mode shapes of thickness- and width-tapered laminated composite beams with different boundary conditions; solid line represents the 1st mode, dashed line represents the 2nd mode and dotted line represents the 3rd mode

As it is shown in Figure 4.7 in mode shapes of thickness- and width tapered composite beams the nodal points are shifted towards the thin side of the beam compared to that of uniform composite beams as shown in Figure 4.3.

4.2.3.1 Effect of taper configuration on forced vibration response

Forced vibration analysis is conducted for four different boundary conditions that are simply supported, clamped-clamped, clamped-free and free-clamped. It is assumed that $y_i(0) = \dot{y}_i(0) = 0$. The forced vibration response in terms of maximum deflection and maximum rotation at the response point is presented in Figures 4.8 - 4.11 for different boundary conditions. It can be observed that as excitation frequency (ω) nears the natural frequencies, due to resonance the response approaches infinity and becomes unstable. Therefore, only a stable part of the response ($0 < \frac{\omega}{\omega_1} < 1$) is used for comparison. It should be noted that in Figures 4.8 - 4.11 (ω_1) is the first natural frequency of the laminated composite beam with the corresponding boundary condition. Therefore as excitation frequency (ω) reaches the second or the third natural frequencies, the value of $(\frac{\omega}{\omega_1})$ would be different for different boundary conditions or taper configurations.

As it is shown in Figures 4.8 - 4.11 for all boundary conditions, configuration A has the highest amplitude of the response (maximum deflection and maximum rotation). Configuration D, B and C have the second, the third and the fourth highest amplitudes of the response respectively. It is evident that configuration A has the lowest stiffness among all configurations and therefore it experiences larger displacement and also larger rotation than other configurations. Configuration D has a higher stiffness than configuration A, but lower stiffness than configurations B and C and

therefore it has the second highest amplitude of the response. Configuration C has a slightly higher stiffness than configuration B and therefore has the lowest amplitude of the response.

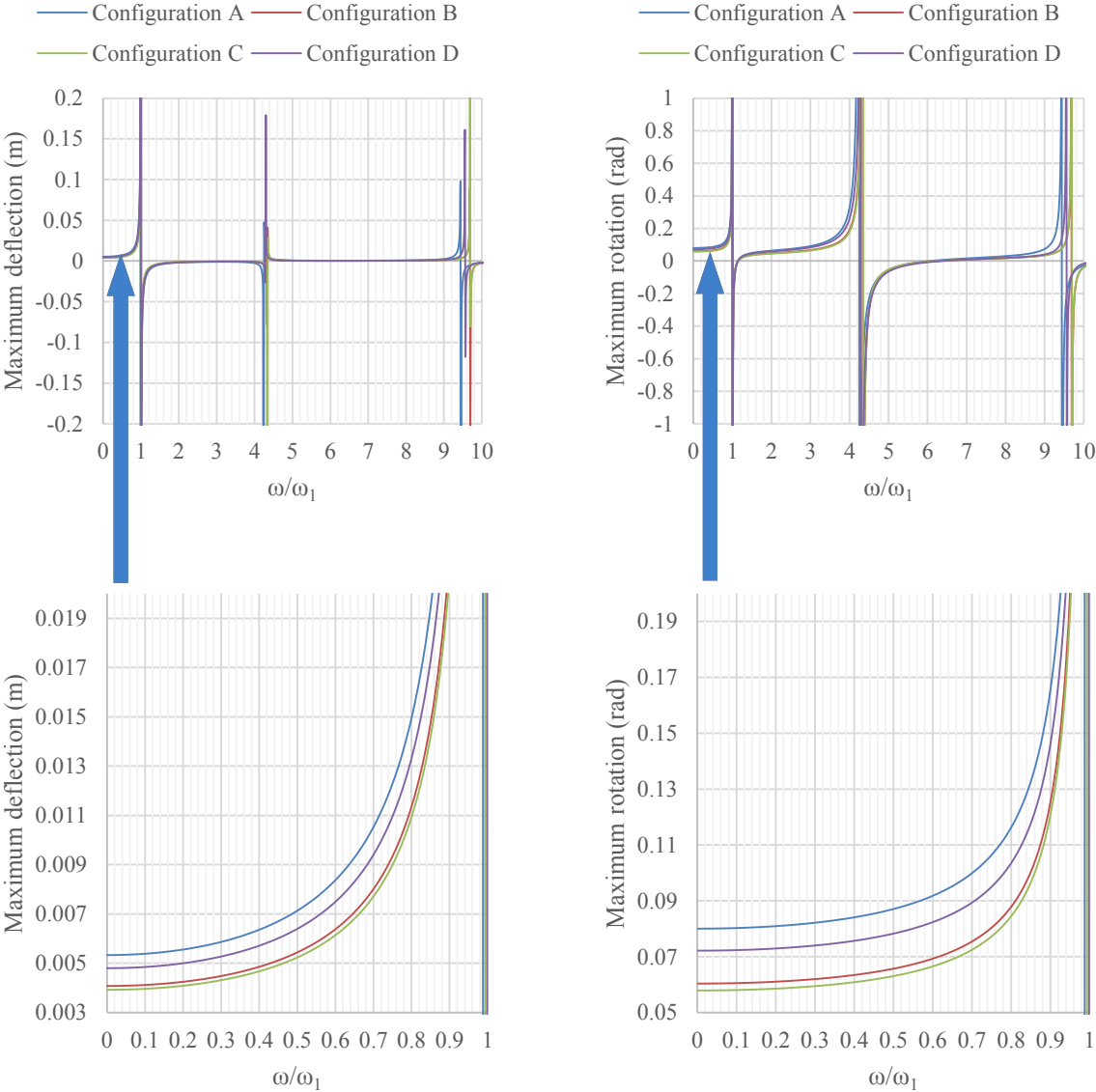


Figure 4.8 Forced vibration response of the thickness- and width-tapered simply supported composite beams with different taper configurations; bottom figures represent the magnified area of the top figures

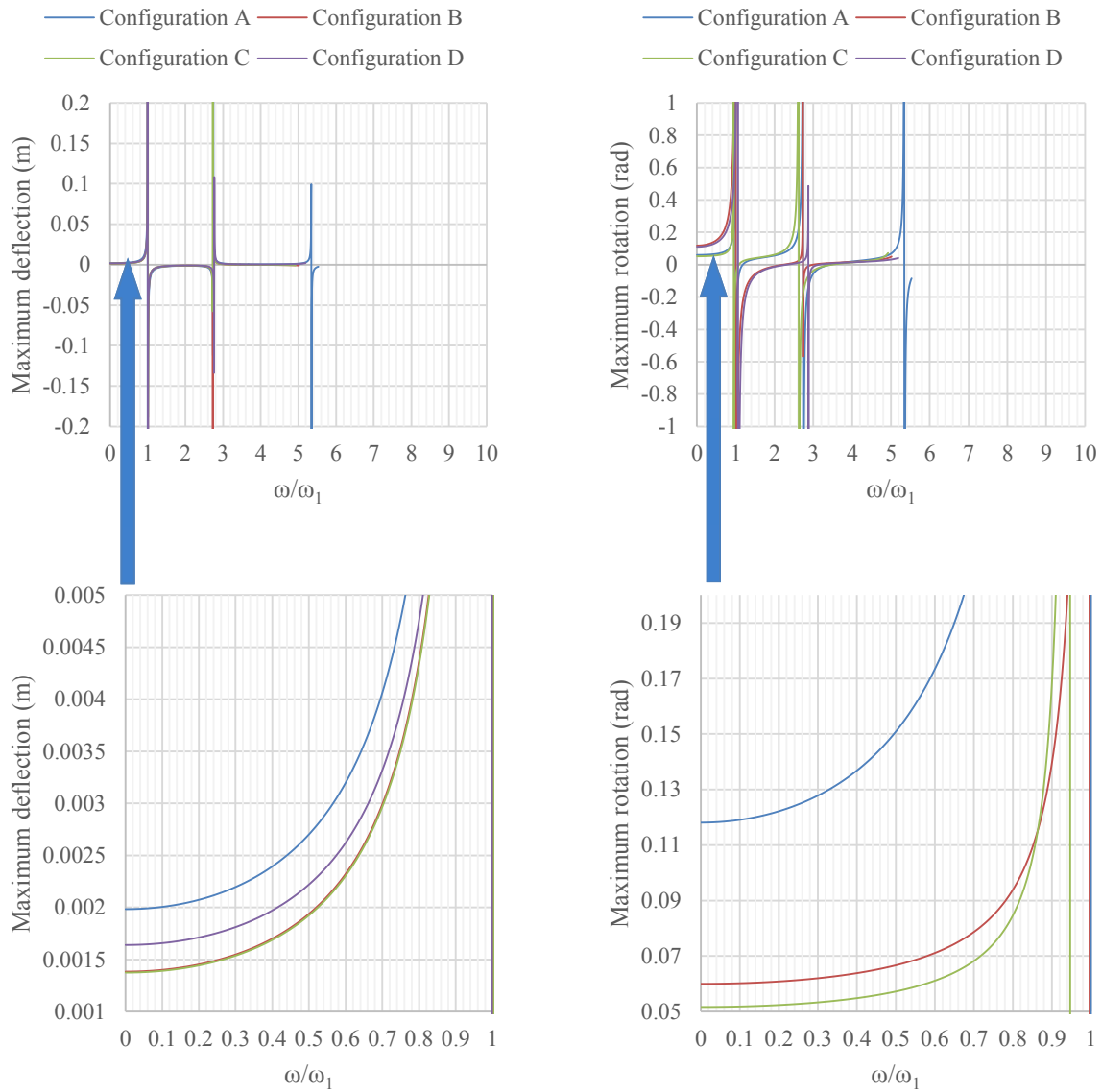


Figure 4.9 Forced vibration response of the thickness- and width-tapered clamped-clamped composite beams with different taper configurations; bottom figures represent the magnified area of the top figures

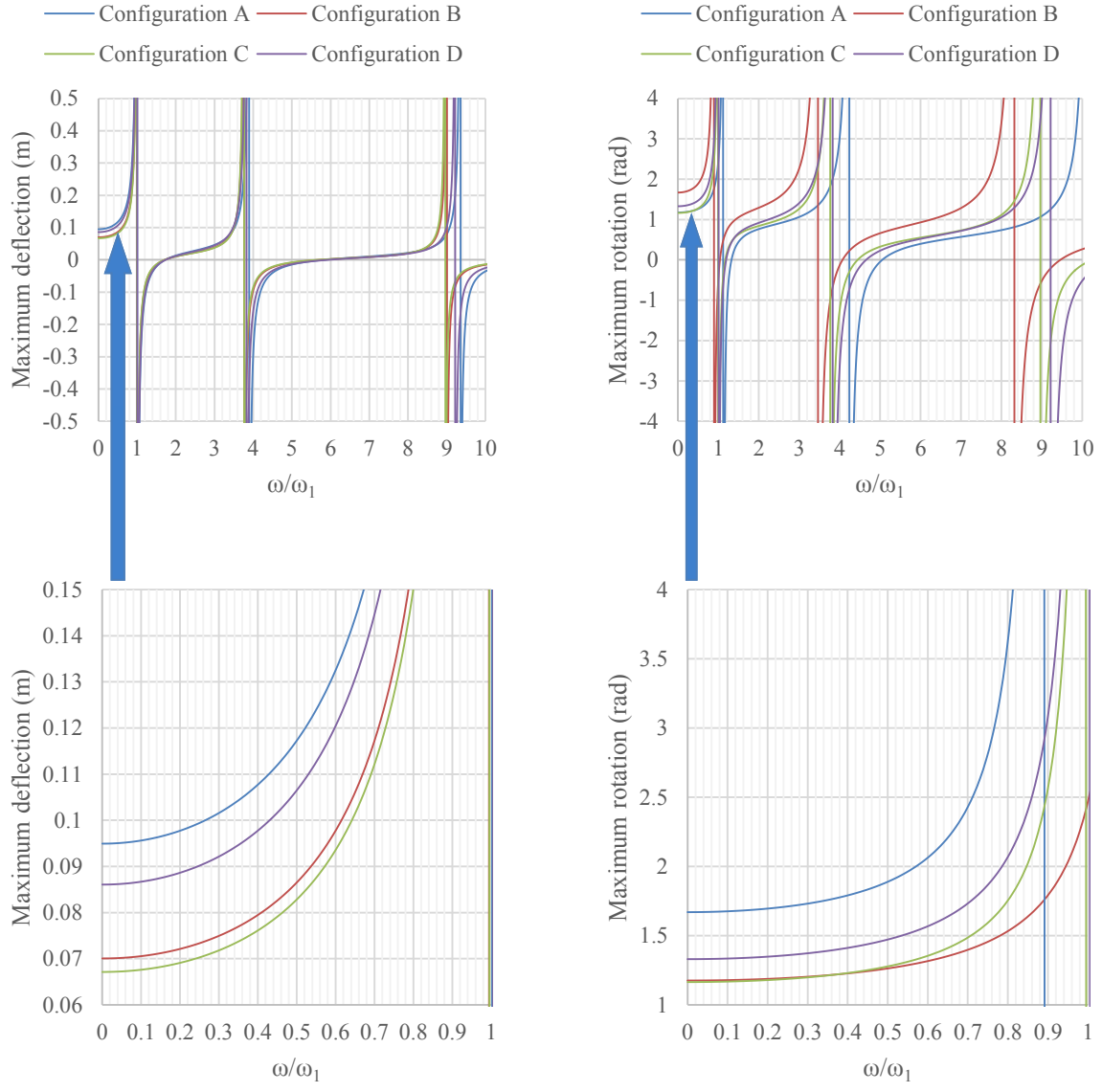


Figure 4.10 Forced vibration response of the thickness- and width-tapered clamped-free composite beams with different taper configurations; bottom figures represent the magnified area of the top figures

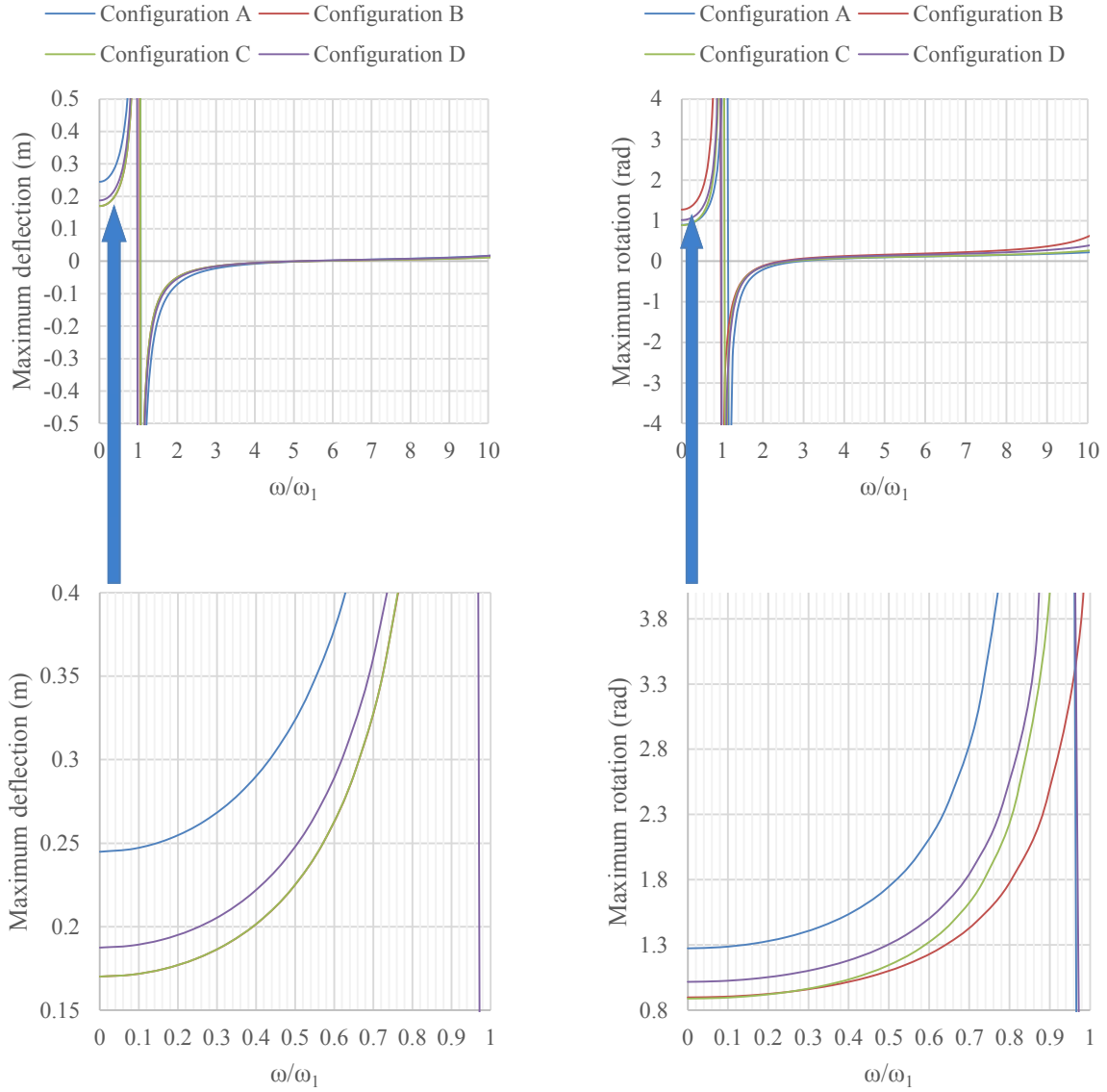


Figure 4.11 Forced vibration response of the thickness- and width-tapered free-clamped composite beams with different taper configurations; bottom figures represent the magnified area of the top figures

It is evident from Figures 4.8 - 4.11 that for all the taper configurations, clamped-clamped beam has the lowest amplitude of the response (in terms of maximum deflection and maximum rotation). It is due to the fact that clamped-clamped beam has the highest stiffness among all boundary conditions. Simply supported beam has a lower stiffness than clamped-clamped beam, however it has a higher stiffness than clamped-free and free-clamped beams. Free-clamped has the lowest stiffness among all the boundary conditions. As a result, simply supported, clamped-free and free-clamped boundary conditions have the second, the third and the fourth highest amplitudes of the response respectively.

4.2.3.2 Effect of width-ratio on forced vibration response

The same beam as that analyzed in section 4.2.3.1 is considered. The beam is considered to have width-ratios (b_R/b_L) of 0.2, 0.5 and 1. A sinusoidal force (F) with the magnitude of 2 N and a sinusoidal moment (M) with the magnitude of 2 N-m both with the excitation frequency of ω are applied at the center of the beam for simply supported and clamped-clamped boundary conditions, and at the free-end of the beam for clamped-free and free-clamped boundary conditions as shown in Figure 4.6.

Forced vibration analysis is conducted for simply supported, clamped-clamped, clamped-free and free-clamped boundary conditions and it is assumed that $y_i(0) = \dot{y}_i(0) = 0$. Forced vibration response in terms of maximum deflection and maximum rotation at the points of response is presented in Figures 4.12 - 4.15 for different taper configurations.

It should be noted that in Figures 4.12 - 4.15 due to instability of the forced vibration response when the excitation frequency approaches natural frequencies, only the stable part of the response ($0 < \frac{\omega}{\omega_1} < 1$) is used for comparison.

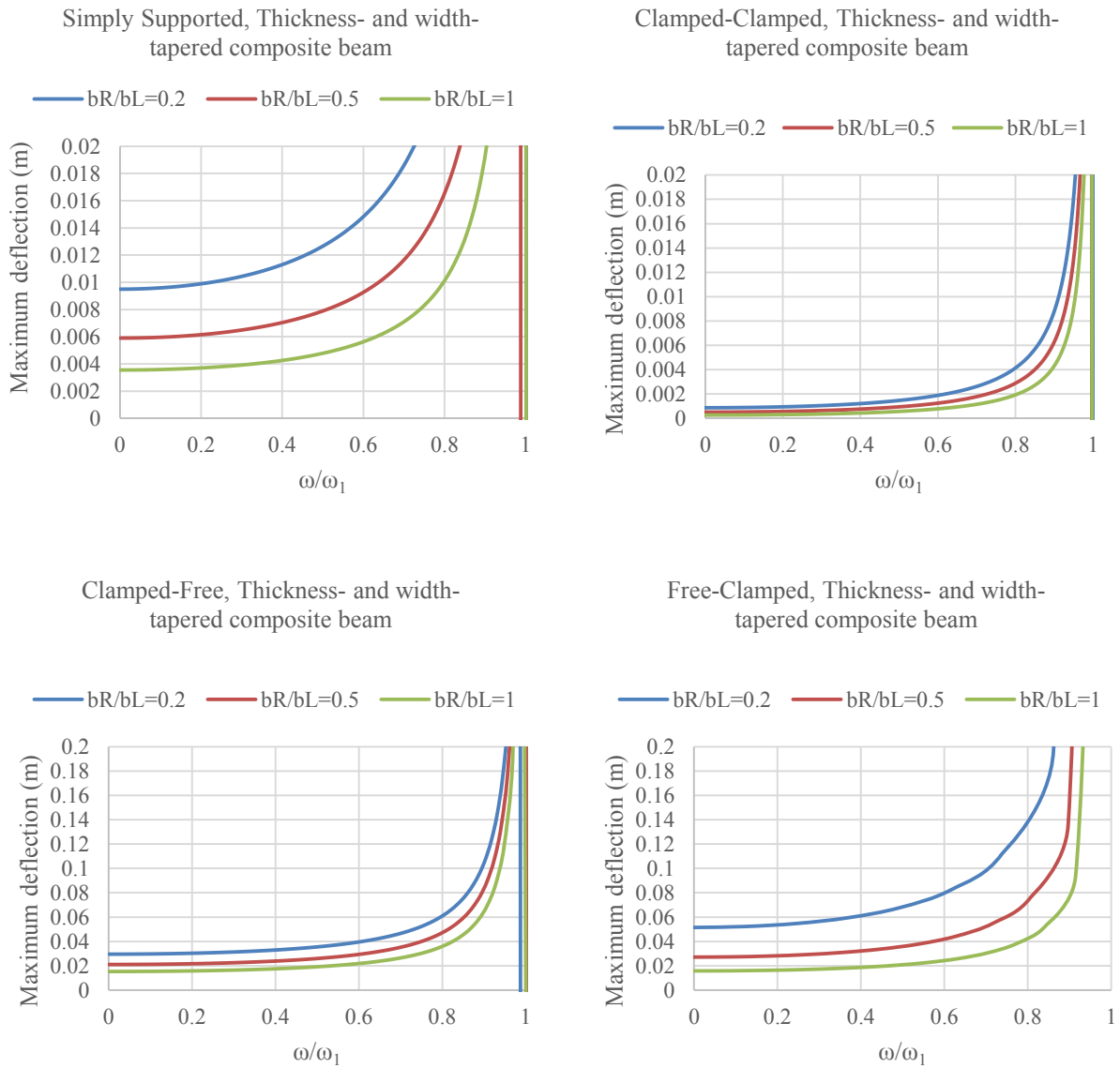


Figure 4.12 Effect of width-ratio (b_R/b_L) on forced vibration response in terms of maximum deflection of the thickness- and width-tapered composite beam with taper configuration A

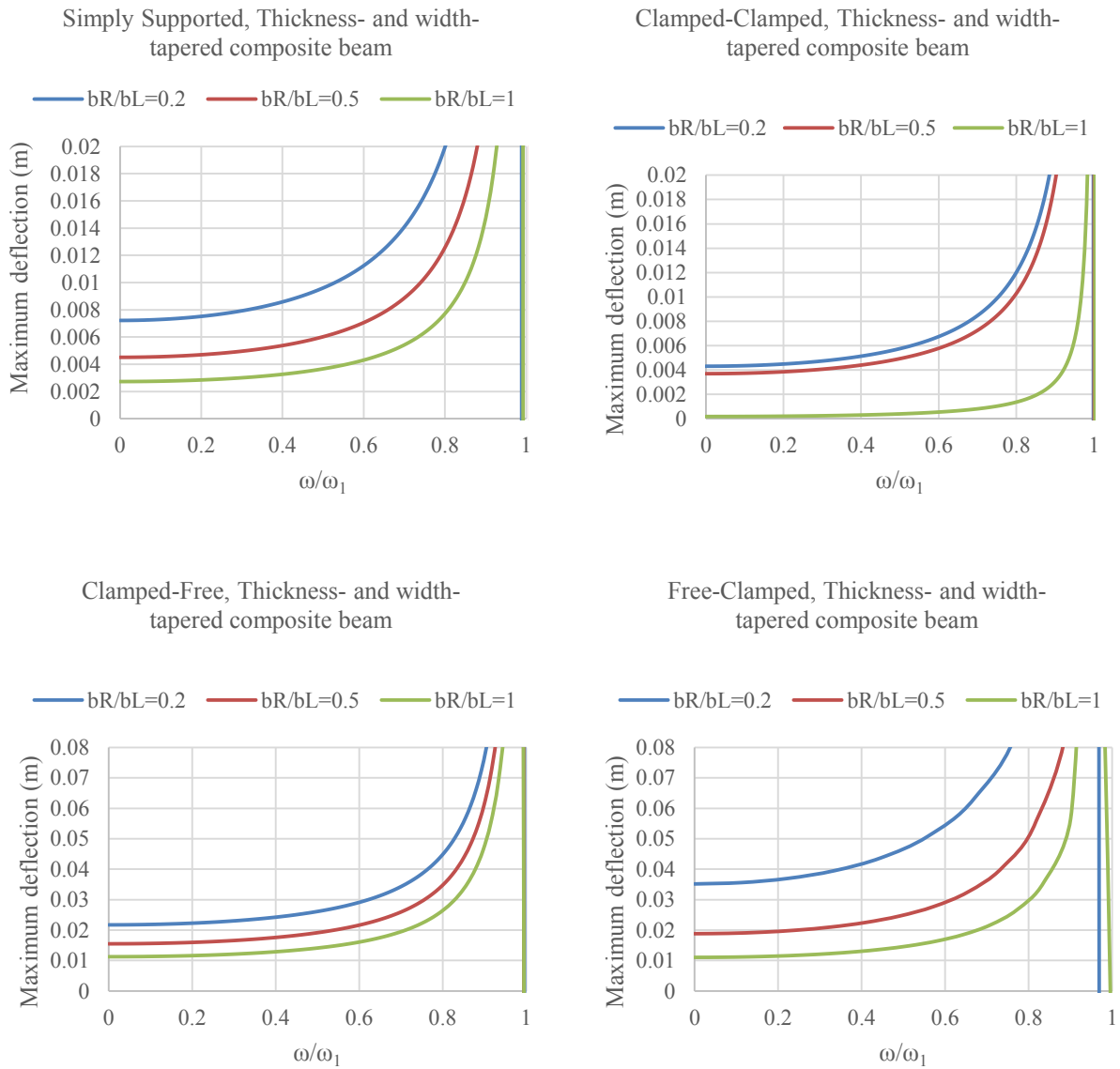


Figure 4.13 Effect of width-ratio (b_R/b_L) on forced vibration response in terms of maximum deflection of the thickness- and width-tapered composite beam with taper configuration B

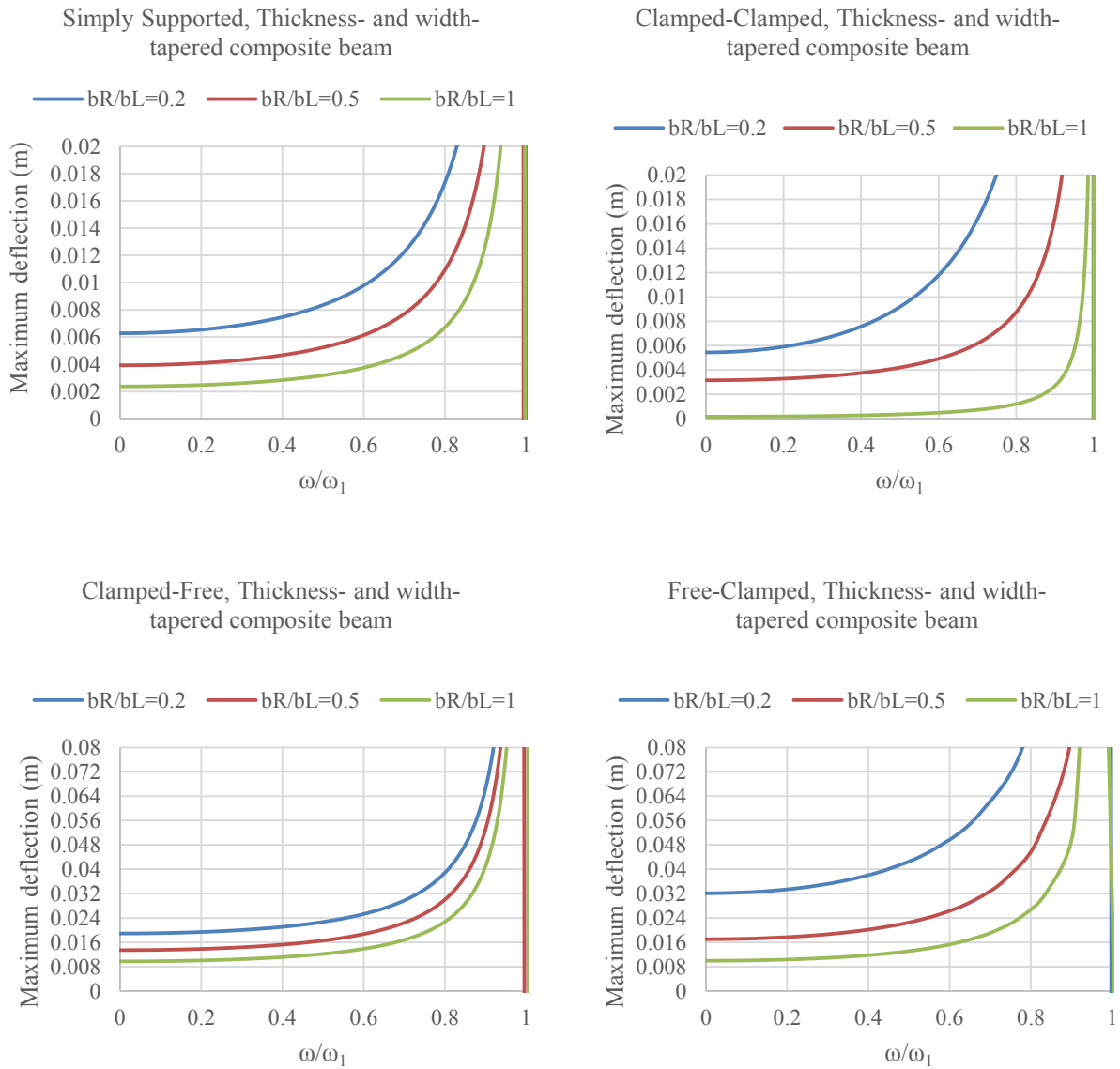


Figure 4.14 Effect of width-ratio (b_R/b_L) on forced vibration response in terms of maximum deflection of the thickness- and width-tapered composite beam with taper configuration C

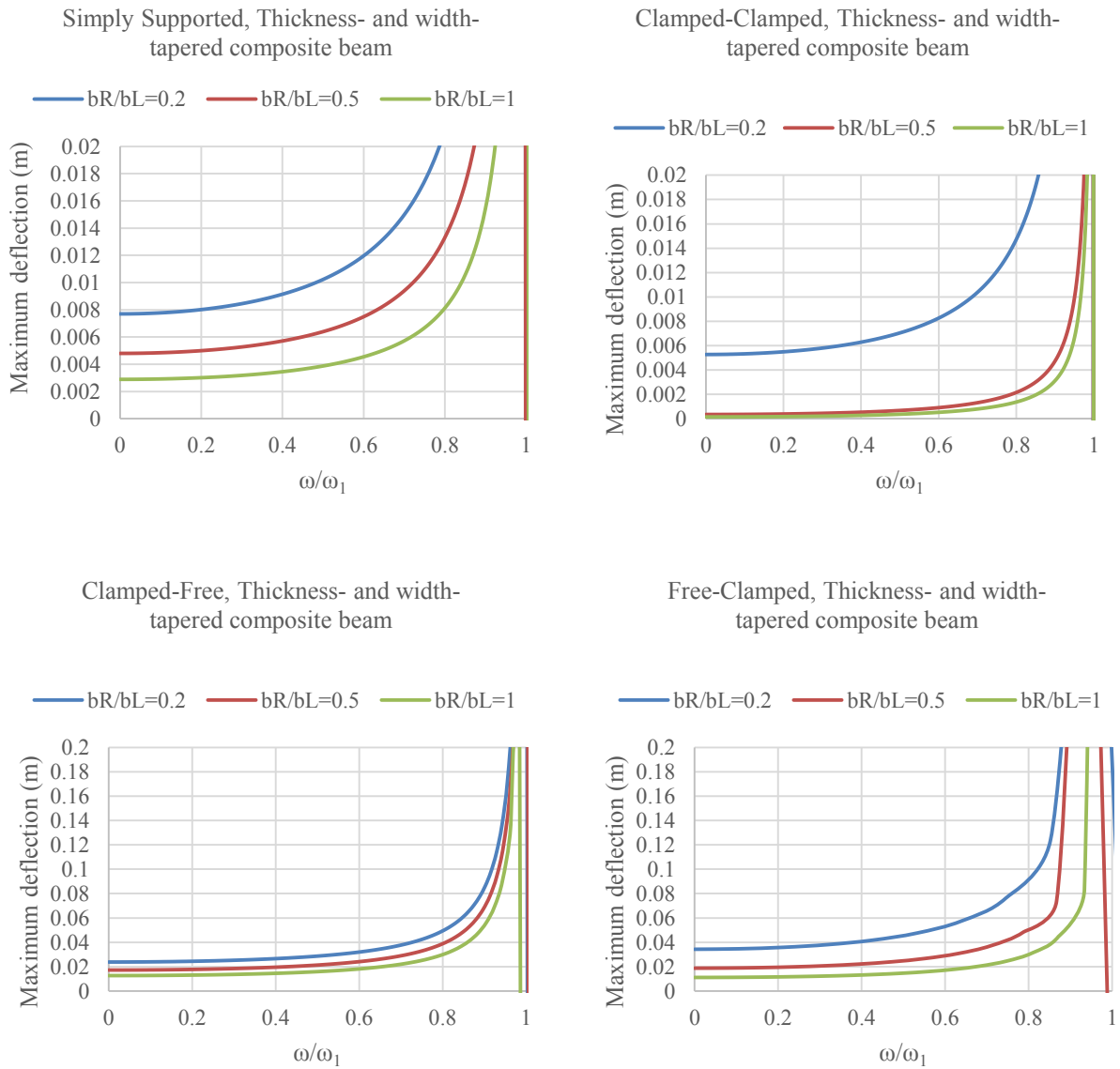


Figure 4.15 Effect of width-ratio (b_R/b_L) on forced vibration response in terms of maximum deflection of the thickness- and width-tapered composite beam with taper configuration D

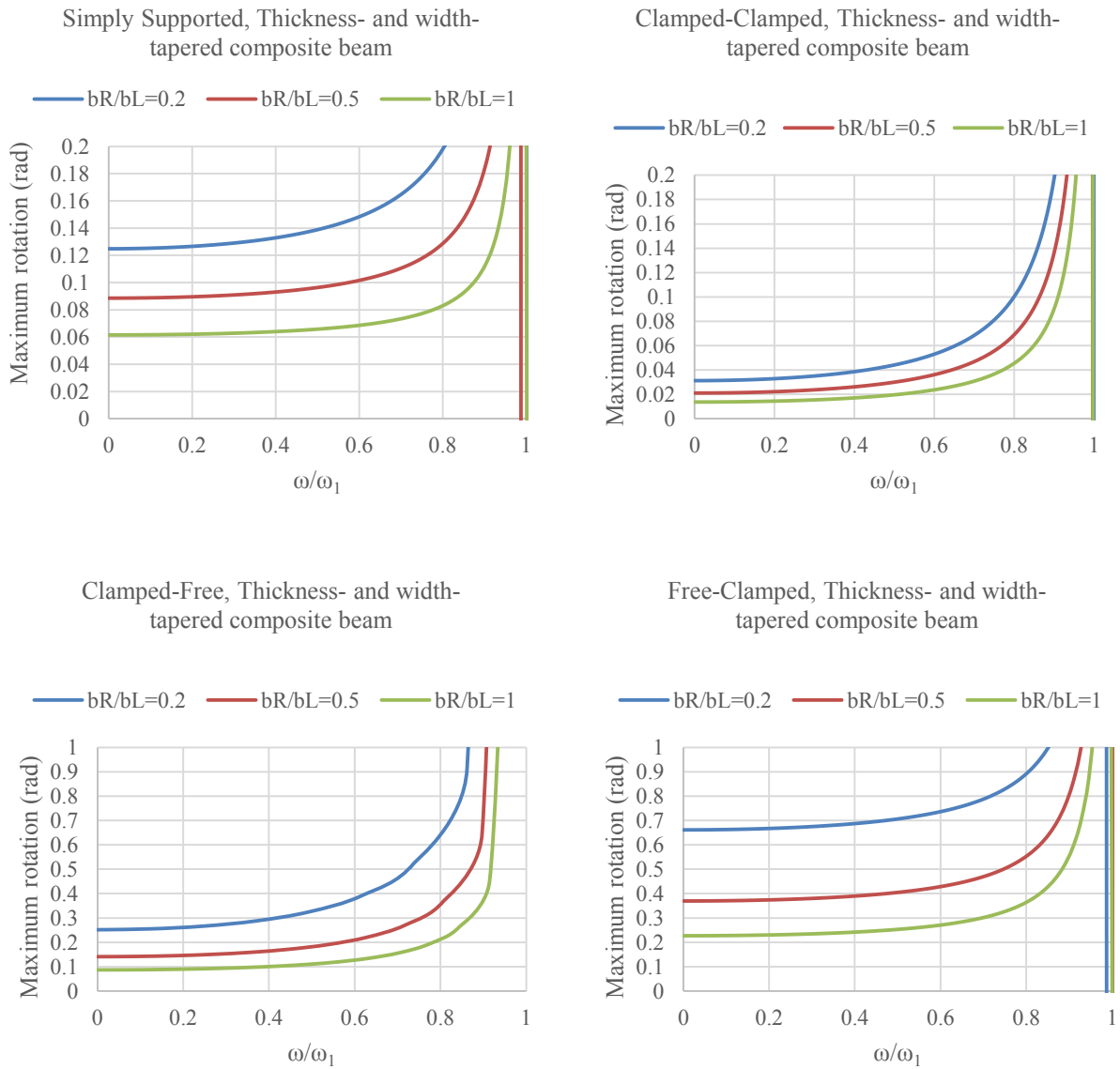


Figure 4.16 Effect of width-ratio (b_R/b_L) on forced vibration response in terms of maximum rotation of the thickness- and width-tapered composite beam with taper configuration A

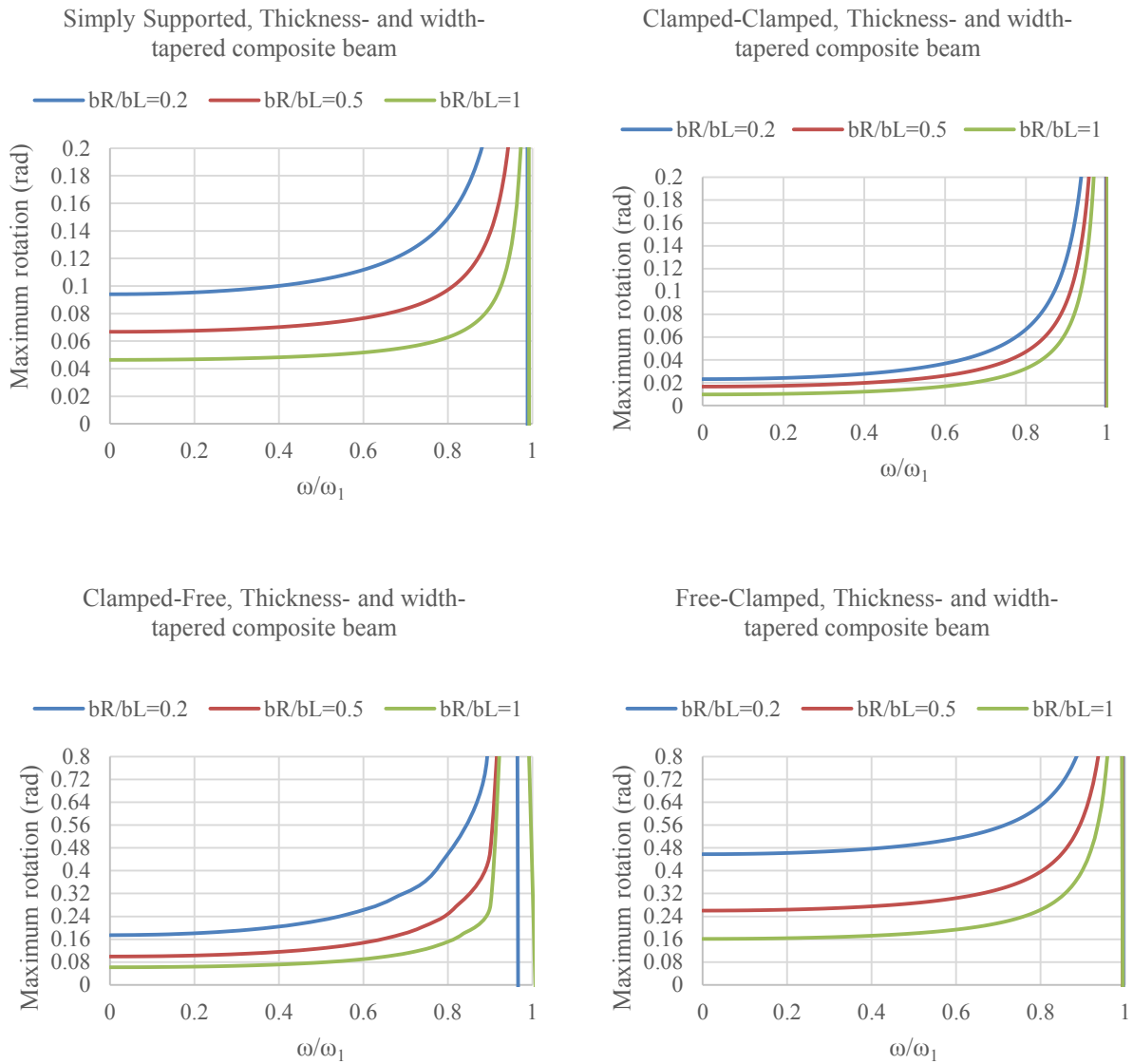


Figure 4.17 Effect of width-ratio (b_R/b_L) on forced vibration response in terms of maximum rotation of the thickness- and width-tapered composite beam with taper configuration B

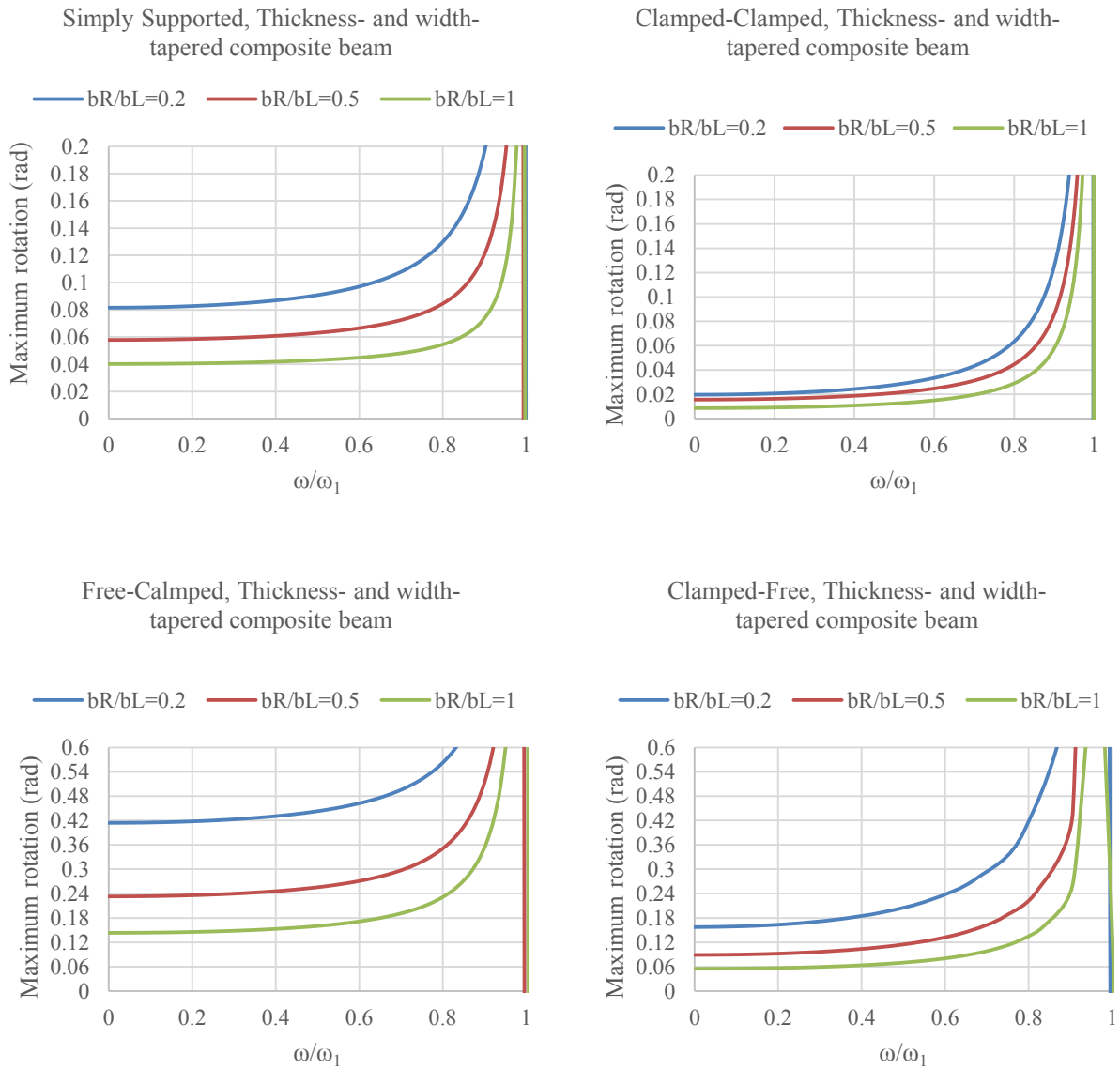


Figure 4.18 Effect of width-ratio (b_R/b_L) on forced vibration response in terms of maximum rotation of the thickness- and width-tapered composite beam with taper configuration C

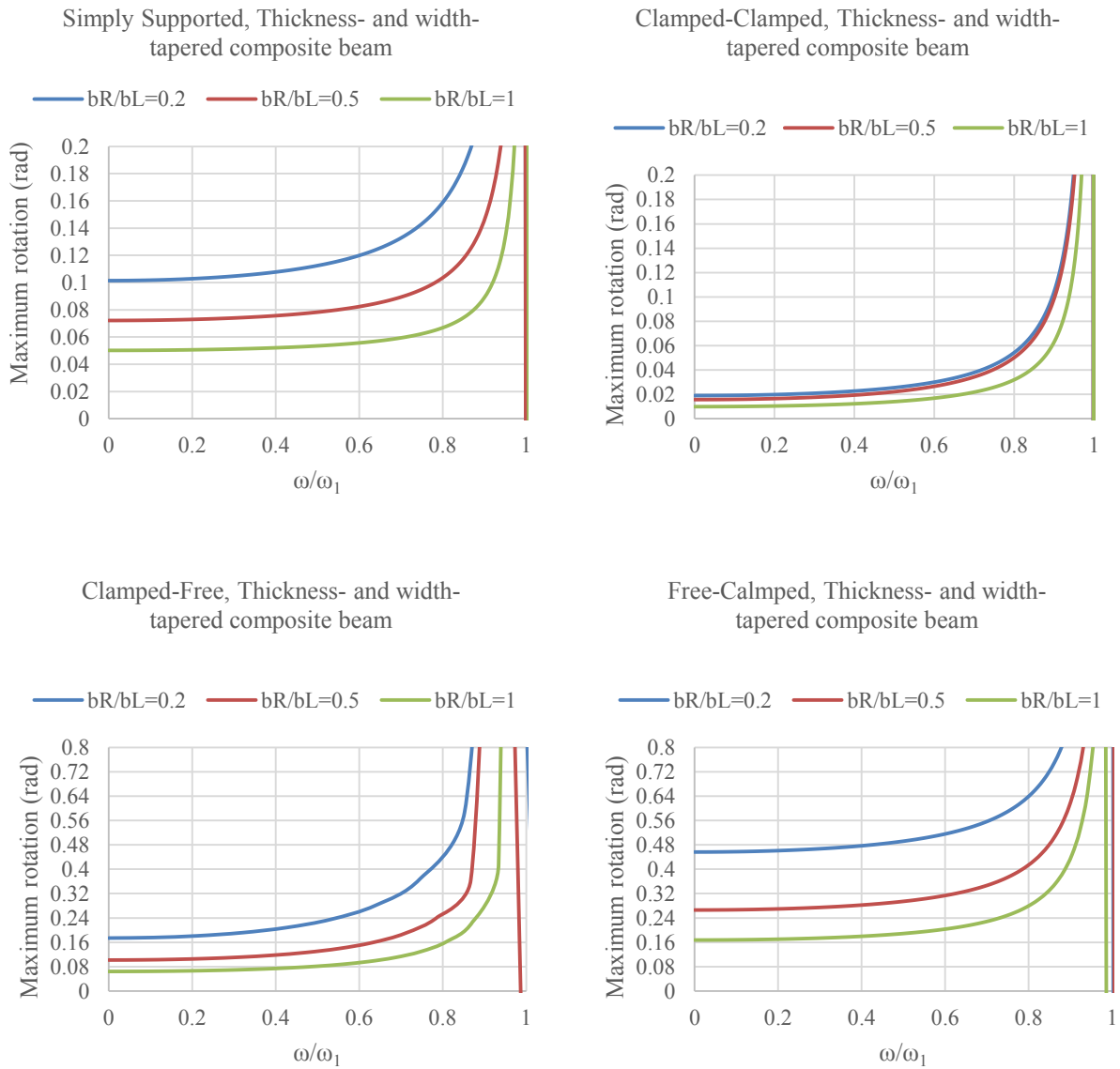


Figure 4.19 Effect of width-ratio (b_R/b_L) on forced vibration response in terms of maximum rotation of the thickness- and width-tapered composite beam with taper configuration D

As it is shown in Figures 4.12 – 4.19, by increasing the width-ratio the amplitudes of the response in terms of both maximum deflection and maximum rotation decreases for all taper configurations and boundary conditions.

4.3 Damped forced vibration analysis

4.3.1 Formulation

The equation of motion of an n -DOF damped laminated composite beam with an arbitrary excitation force is given by:

$$[M]\{\ddot{w}\} + [C]\{\dot{w}\} + [K]\{w\} = \{F\} \quad (4.14)$$

in which $[M]$, $[K]$ and $[C]$ are the mass, stiffness and damping matrices and $\{w\}$ and $\{F\}$ represent displacement and force vectors respectively.

By assuming $\{w\} = [\tilde{P}]\{y\}$ and pre-multiplying both sides of the Equation (4.14) by $[\tilde{P}]^T$, the equation transforms into:

$$[\tilde{P}]^T[M][\tilde{P}]\{\ddot{y}\} + [\tilde{P}]^T[C][\tilde{P}]\{\dot{y}\} + [\tilde{P}]^T[K][\tilde{P}]\{y\} = [\tilde{P}]^T\{F\} \quad (4.15)$$

It was shown in section 4.2.1 that the matrices $[\tilde{P}]^T[M][\tilde{P}]$ and $[\tilde{P}]^T[K][\tilde{P}]$ are diagonal matrices. In general, $[\tilde{P}]^T[C][\tilde{P}]$ is not a diagonal matrix and therefore Equation (4.15), is coupled by the damping matrix. However it can be shown [37] that if $[C]$ is proportional to $[K]$ and $[M]$, $[\tilde{P}]^T[C][\tilde{P}]$ becomes diagonal, which results in n uncoupled equations. Using Rayleigh proportional damping theory as discussed in section 3.4.7 and substituting Equation (3.1) into Equation (4.15) results in:

$$\{\ddot{y}\} + (\alpha[I] + \beta[A])\{\dot{y}\} + [A]\{y\} = \{f\} \quad (4.16)$$

Equation (4.16) is a set of n uncoupled equations that are:

$$\{\ddot{y}\}_i + 2\xi_i\omega_i\{\dot{y}\}_i + \omega_i^2\{y\}_i = \{f\}_i, \quad i = 1, 2, \dots, n \quad (4.17)$$

in which,

$$\xi_i = \frac{1}{2} \left(\frac{\alpha}{\omega_i} + \beta\omega_i \right) \quad (4.18)$$

ξ_i is the damping ratio corresponding to the i -th mode.

It can be shown that the solution to Equation (4.17) is in the form of:

$$y_i = e^{-\xi_i\omega_i t} \left[y_i(0) \cos \omega_{di} t + \frac{\dot{y}_i(0) + y_i(0)\xi_i\omega_i}{\omega_{di}} \sin \omega_{di} t \right] + \frac{f_i}{\sqrt{(\omega_i^2 - \omega^2)^2 + (2\xi_i\omega_i\omega)^2}} \sin(\omega t - \tan^{-1} \frac{2\xi_i\omega_i\omega}{\omega_i^2 - \omega^2}) \quad (4.19)$$

$$\omega_{di} = \omega_i \sqrt{1 - \xi_i^2} \quad (4.20)$$

In equations (4.19) and (4.20), ω_i is the i -th natural frequency, ω_{di} is the i -th damped frequency and ω is the frequency of the excitation. Having the nodal displacement vector in transformed coordinates $\{y\}$ and using equation (4.3), one can find the damped forced vibration response in terms of nodal displacement matrix $\{w\}$.

4.3.2 Damped forced vibration response of uniform composite beams

The same beam as that analyzed in section 4.2.2 is considered. The beam is assumed to have Rayleigh damping with mass and stiffness proportional Rayleigh damping constants that are $\alpha = 3.752$ and $\beta = 4.83 \times 10^{-5}$ respectively. A sinusoidal force (F) with the magnitude of 2 N and a sinusoidal moment (M) with the magnitude of 2 N-m both with the excitation frequency of ω

are applied close to the center of the beam for simply supported and clamped-clamped boundary conditions, and at the free-end of the beam for clamped-free and free-clamped boundary conditions as shown in Figure 4.2. It is assumed that $y_i(0) = \dot{y}_i(0) = 0$.

Damped forced vibration analysis is conducted and the damped response alongside the undamped response in terms of maximum deflection and maximum rotation at the point of response is presented in Figures 4.20 and 4.21 for different boundary conditions.

It can be observed from Figures 4.20 - 4.21 that by considering damping, the amplitude of the response decreases, especially as the frequency of excitation nears natural frequencies (resonance). The reduction of amplitude is much more significant near the second and the third natural frequencies compared to that near the first natural frequency. The reason is that the damping ratio is very small for the first natural frequency (compared to the second and the third natural frequencies).

Moreover, it is evident that the effect of damping on the response is most significant for the clamped-clamped boundary condition. Simply supported, clamped-free and free-clamped boundary conditions have the second, the third and the fourth largest amount of amplitude reductions of the forced vibration response respectively. (This is illustrated in Figure 4.20).

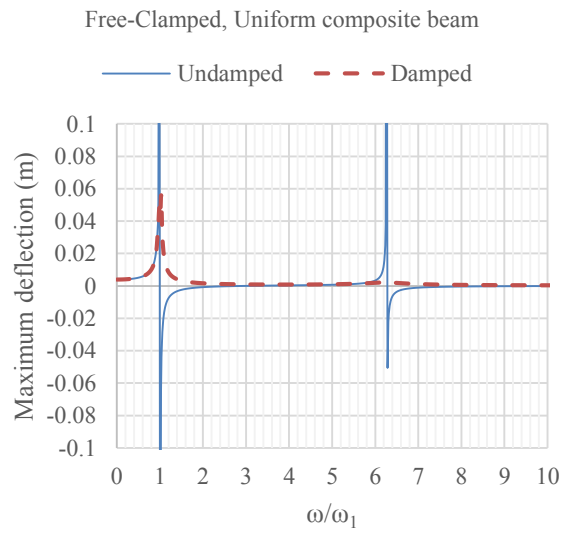
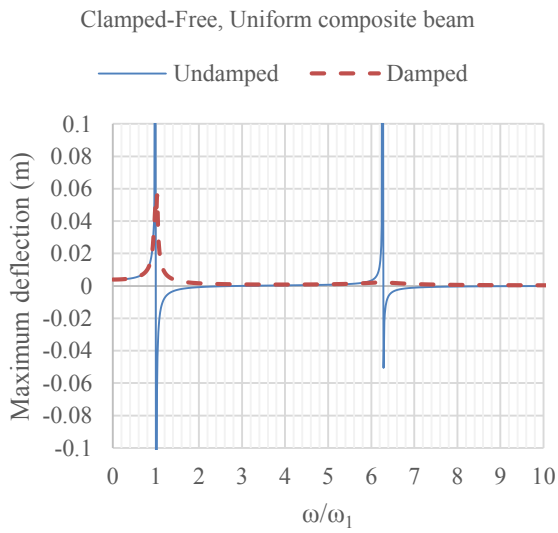
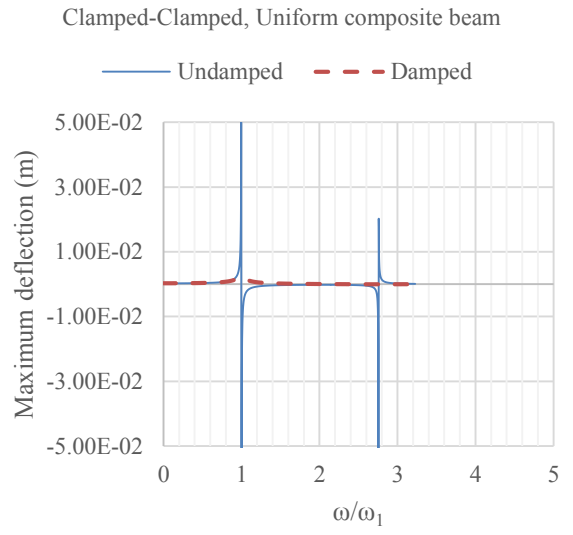
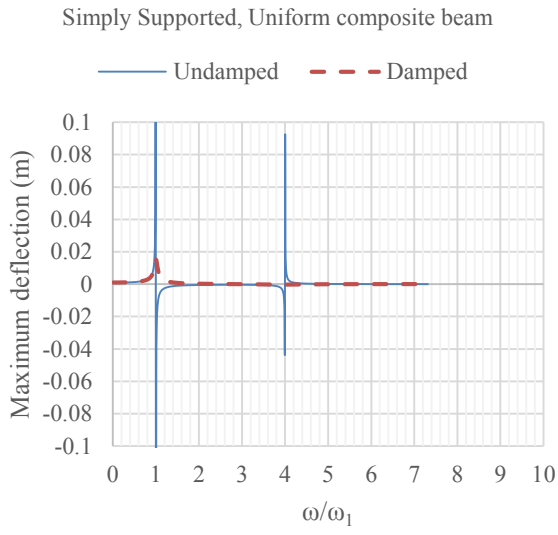


Figure 4.20 Undamped (solid line) vs. damped (dashed line) forced response in terms of maximum deflection for the uniform composite beam with different boundary conditions

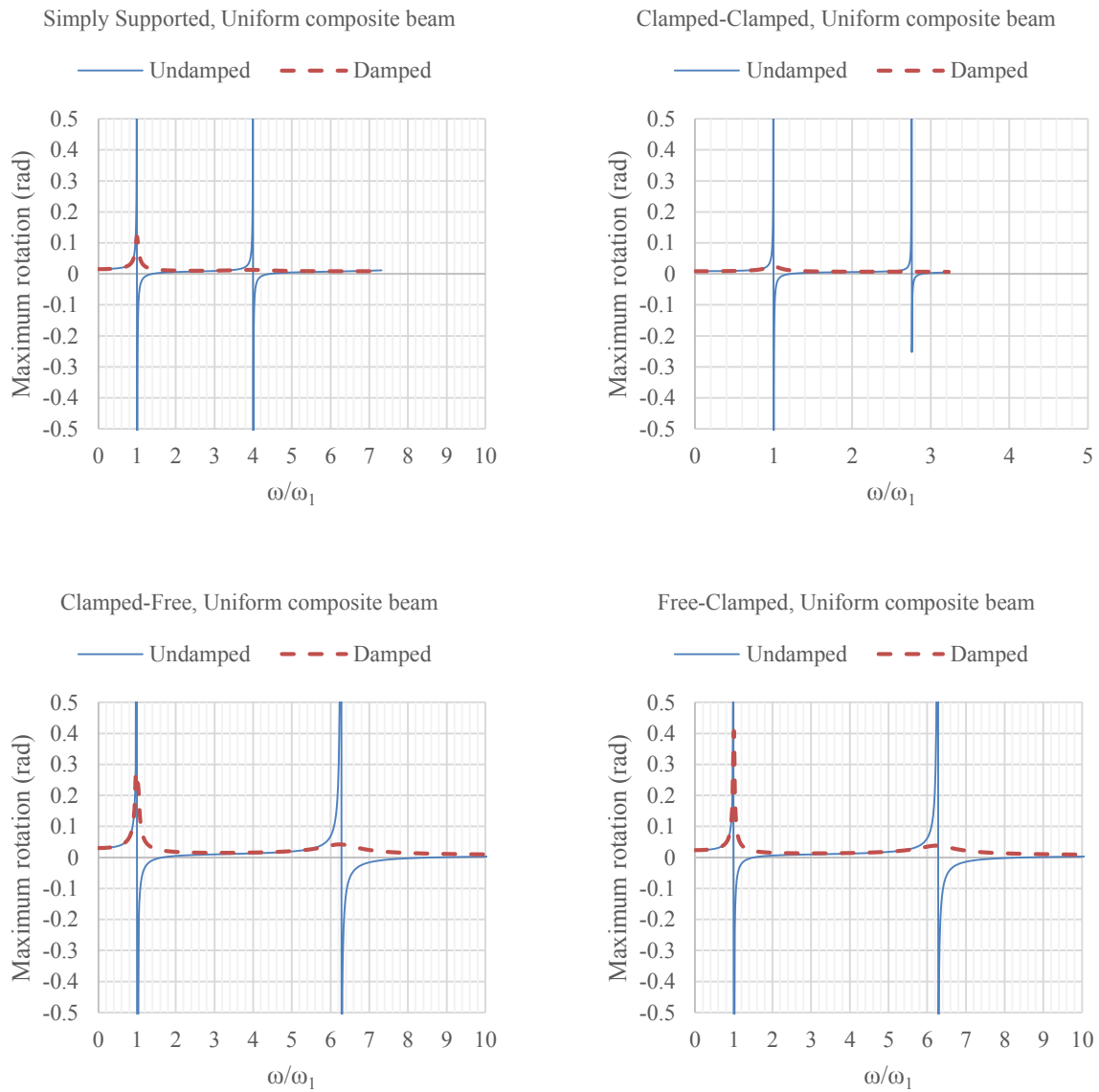


Figure 4.21 Undamped (solid line) vs. damped (dashed line) forced response in terms of maximum rotation for the uniform composite beam with different boundary conditions

4.3.3 Damped forced vibration response of thickness- and width-tapered composite beams

The same beam as that analyzed in section 4.2.3.1 is considered. The beam is assumed to have Rayleigh damping with mass and stiffness proportional Rayleigh damping constants that are $\alpha = 3.752$ and $\beta = 4.83 \times 10^{-5}$ respectively. A sinusoidal force (F) with the magnitude of 2 N and a sinusoidal moment (M) with the magnitude of 2 N-m both with the excitation frequency of ω are applied at the center of the beam for simply supported and clamped-clamped boundary conditions, and at the free-end of the beam for clamped-free and free-clamped boundary conditions as shown in Figure 4.6. It is assumed that $y_i(0) = \dot{y}_i(0) = 0$.

Damped forced vibration analysis is conducted and the damped response alongside the undamped response in terms of maximum deflection at the point of response is presented in Figures 4.22a - 4.25a for different boundary conditions. . It can be observed that as excitation frequency (ω) nears the natural frequencies, due to resonance the undamped response approaches infinity and becomes unstable. Therefore, a stable part of the response ($0 < \frac{\omega}{\omega_1} < 1$) is presented in Figures 4.22b - 4.25b for comparison.

It can be observed from Figures 4.22a - 4.25a that by considering damping, the amplitude of the response decreases, especially as the frequency of excitation nears natural frequencies (resonance). The reduction of amplitude is much more significant near the second and the third natural frequencies compared to that near the first natural frequency. The reason is that the damping ratio is very small for the first natural frequency (compared to the second and the third natural frequencies), as it was discussed in section 3.4.7. Moreover, it is evident that the effect of damping on the response is most significant for the clamped-clamped boundary condition. Simply

supported, clamped-free and free clamped boundary conditions have the second, the third and the fourth largest amount of amplitude reductions of the forced vibration response respectively.

It can also be seen from Figures 4.22b - 4.25b that for all boundary conditions, configuration A has the highest damped response among all taper configurations. Configurations D and B have the second and the third highest amplitudes of the damped response, respectively. Configuration C has the lowest amplitude of the damped response among all taper configurations.

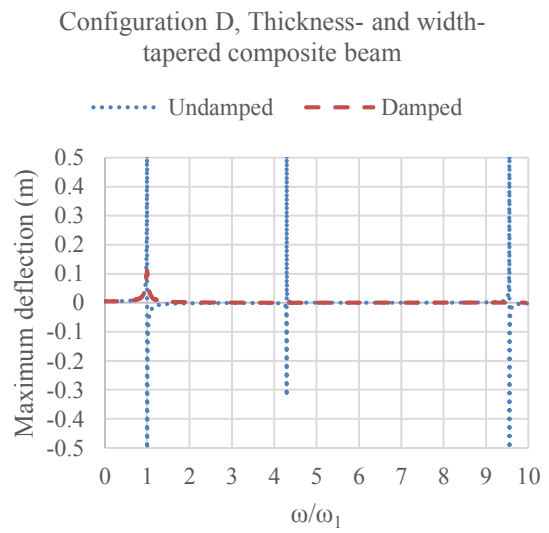
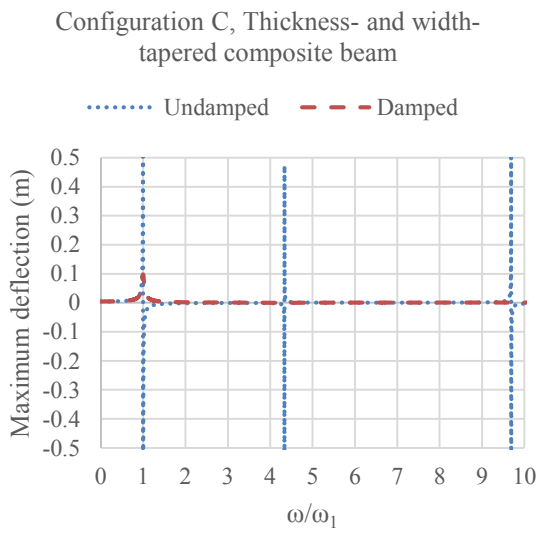
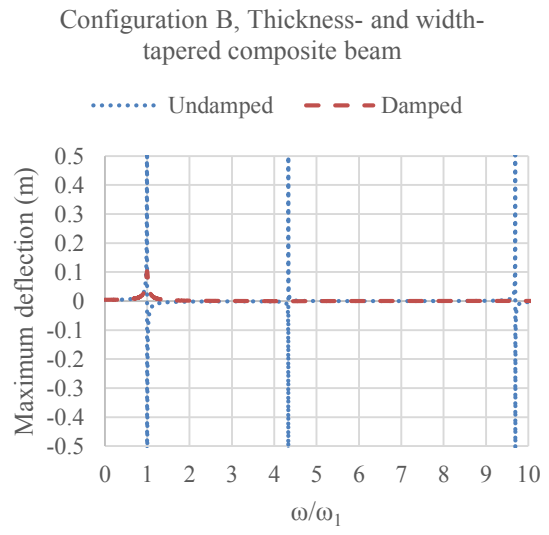
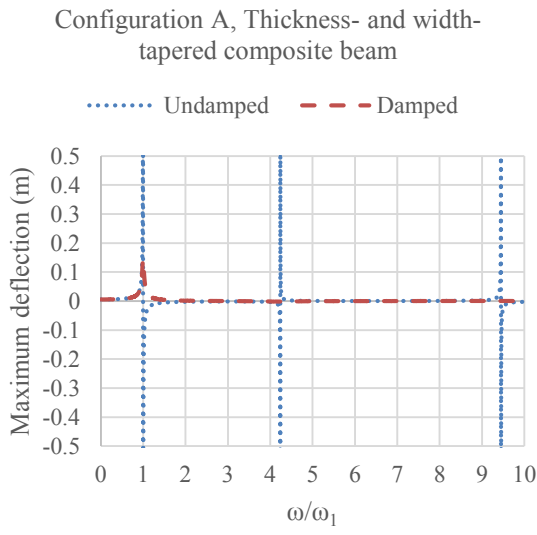


Figure 4.22a Effect of damping on forced vibration response in terms of maximum deflection of the simply supported composite beams with different taper configurations

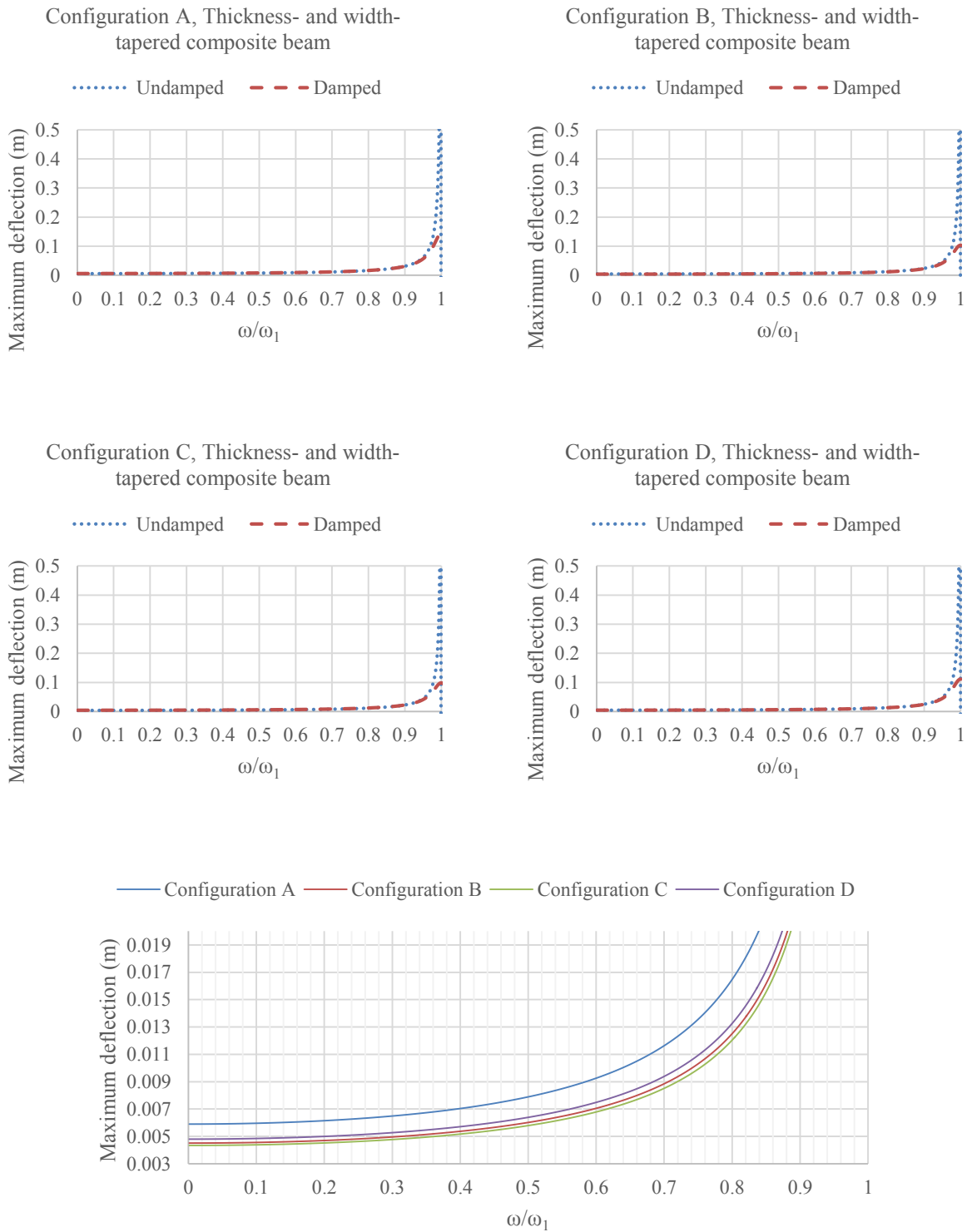


Figure 4.22b Magnified views of plots given in Figure 4.22a near 1st resonance

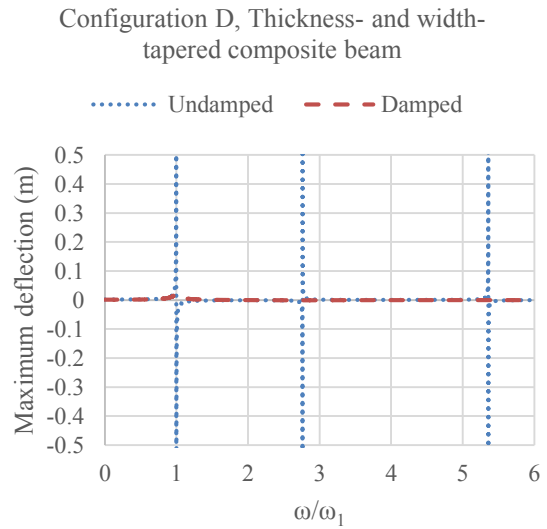
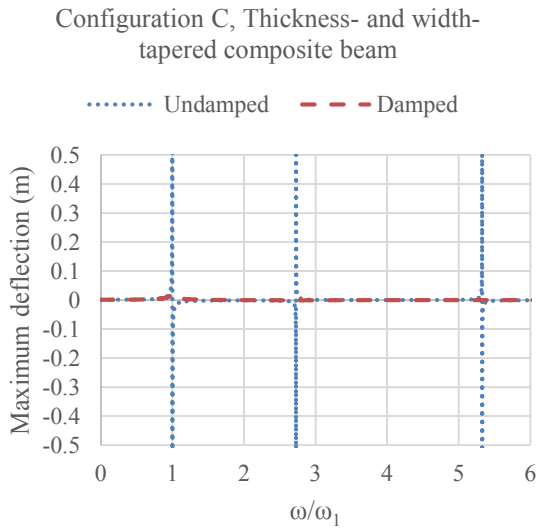
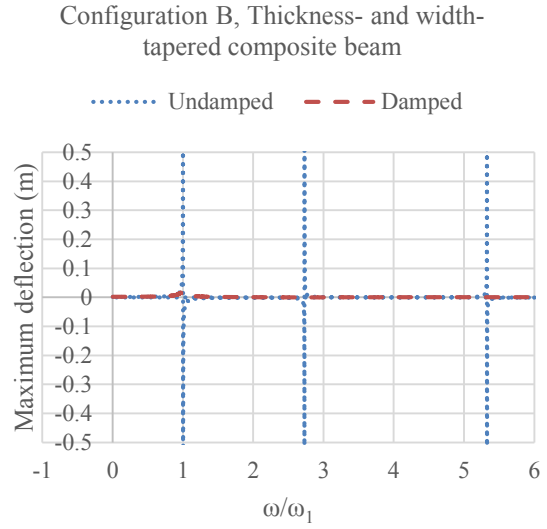
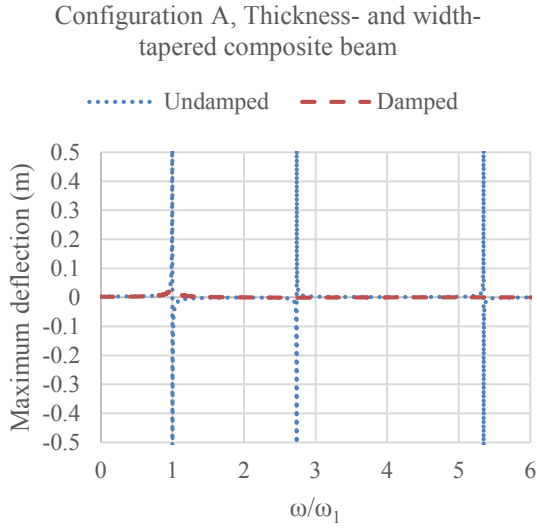


Figure 4.23a Effect of damping on forced vibration response in terms of maximum deflection of the clamped-clamped composite beams with different taper configurations

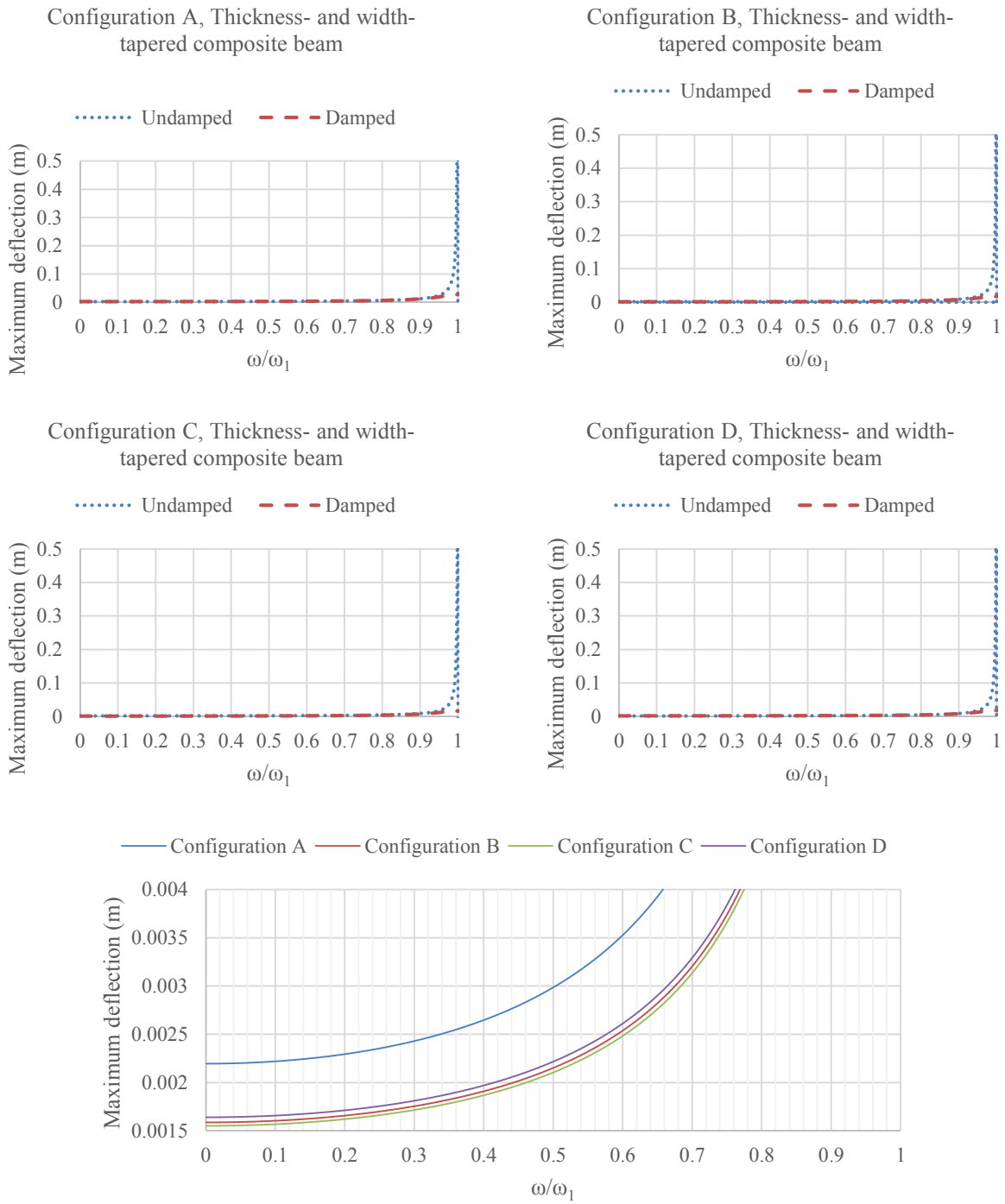


Figure 4.23b Magnified views of plots given in Figure 4.23a near 1st resonance

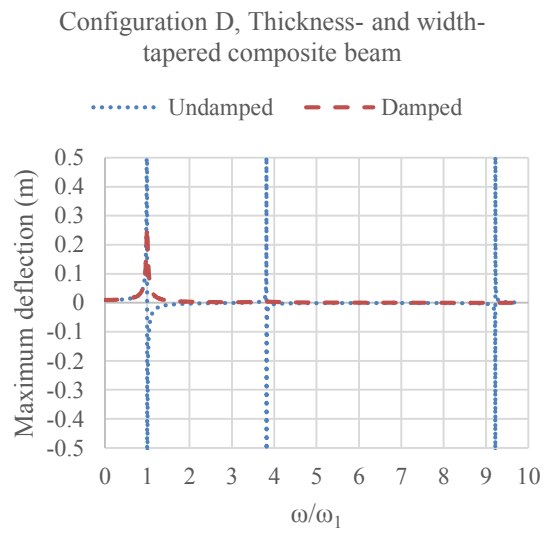
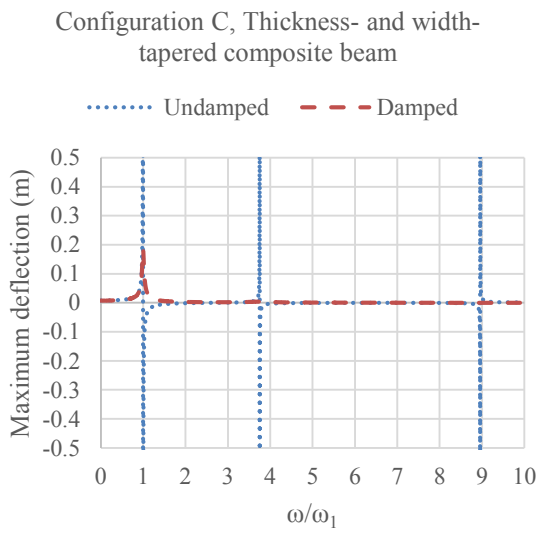
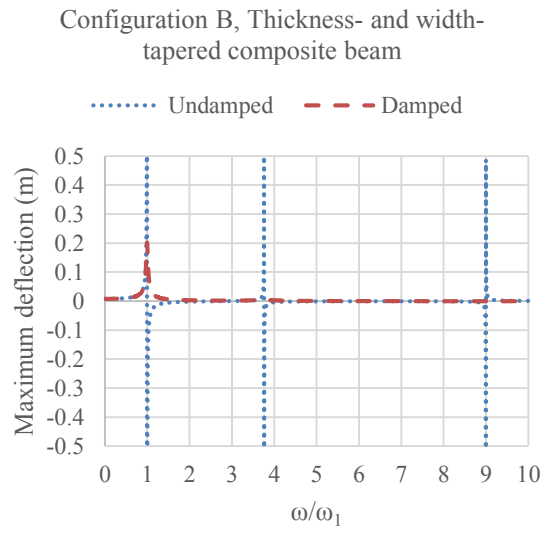
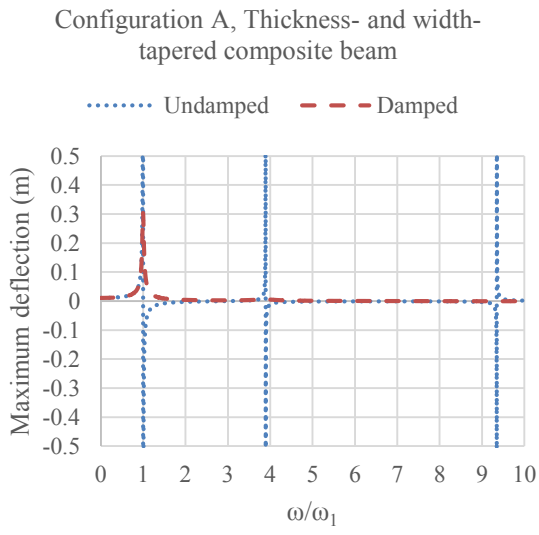


Figure 4.24a Effect of damping on forced vibration response in terms of maximum deflection of the clamped-free composite beams with different taper configurations

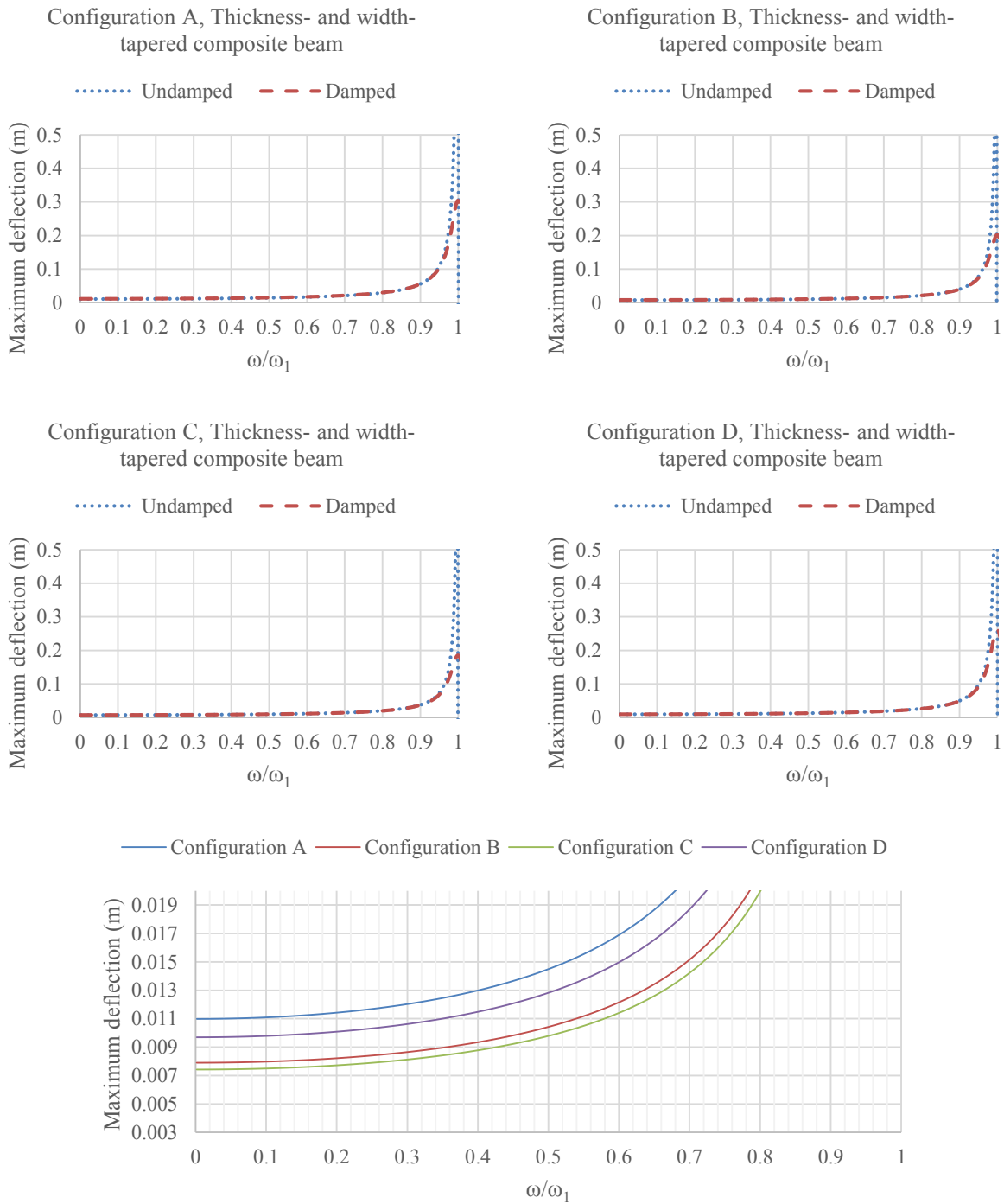


Figure 4.24b Magnified views of plots given in Figure 4.24a near 1st resonance

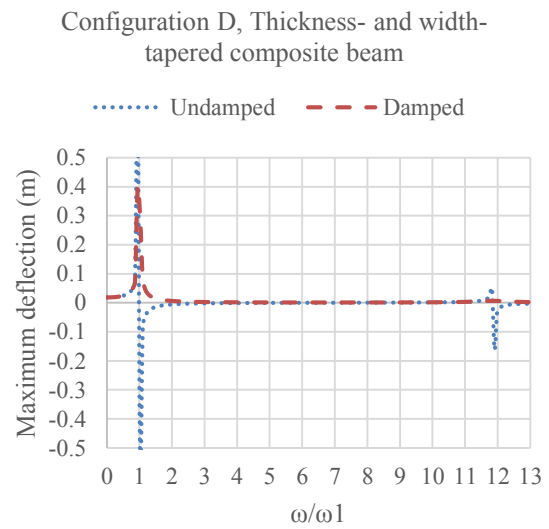
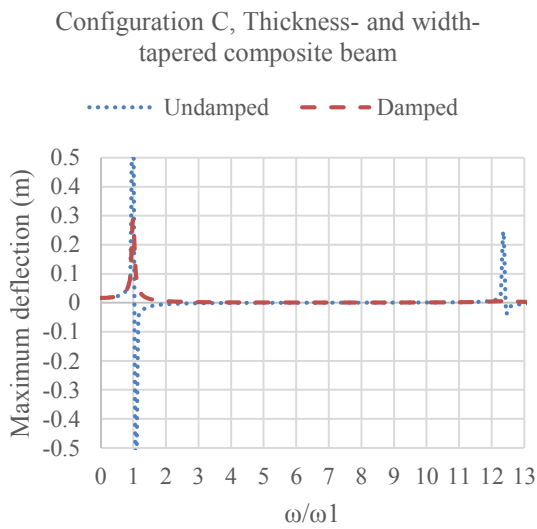
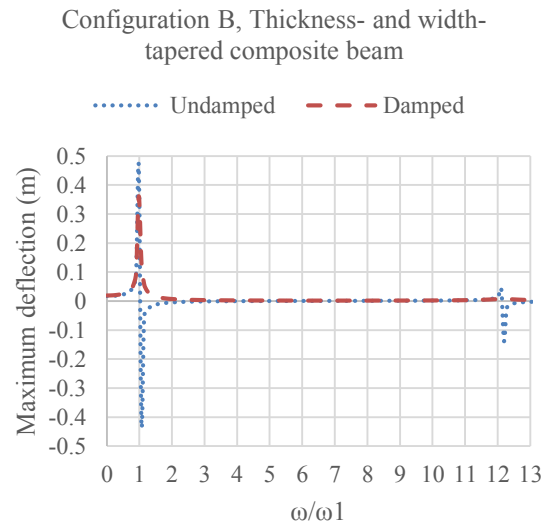
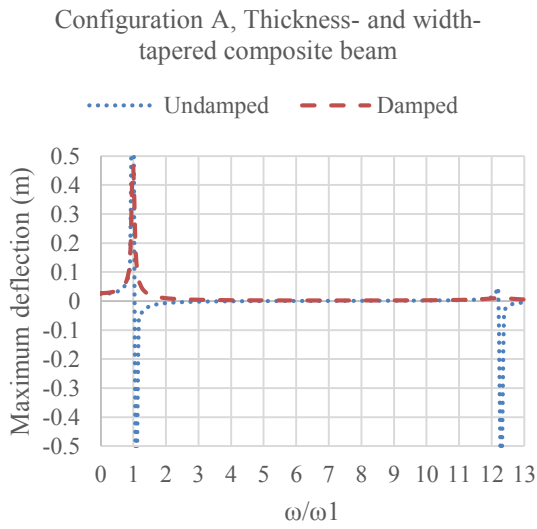


Figure 4.25a Effect of damping on forced vibration response in terms of maximum deflection of the free-clamped composite beams with different taper configurations

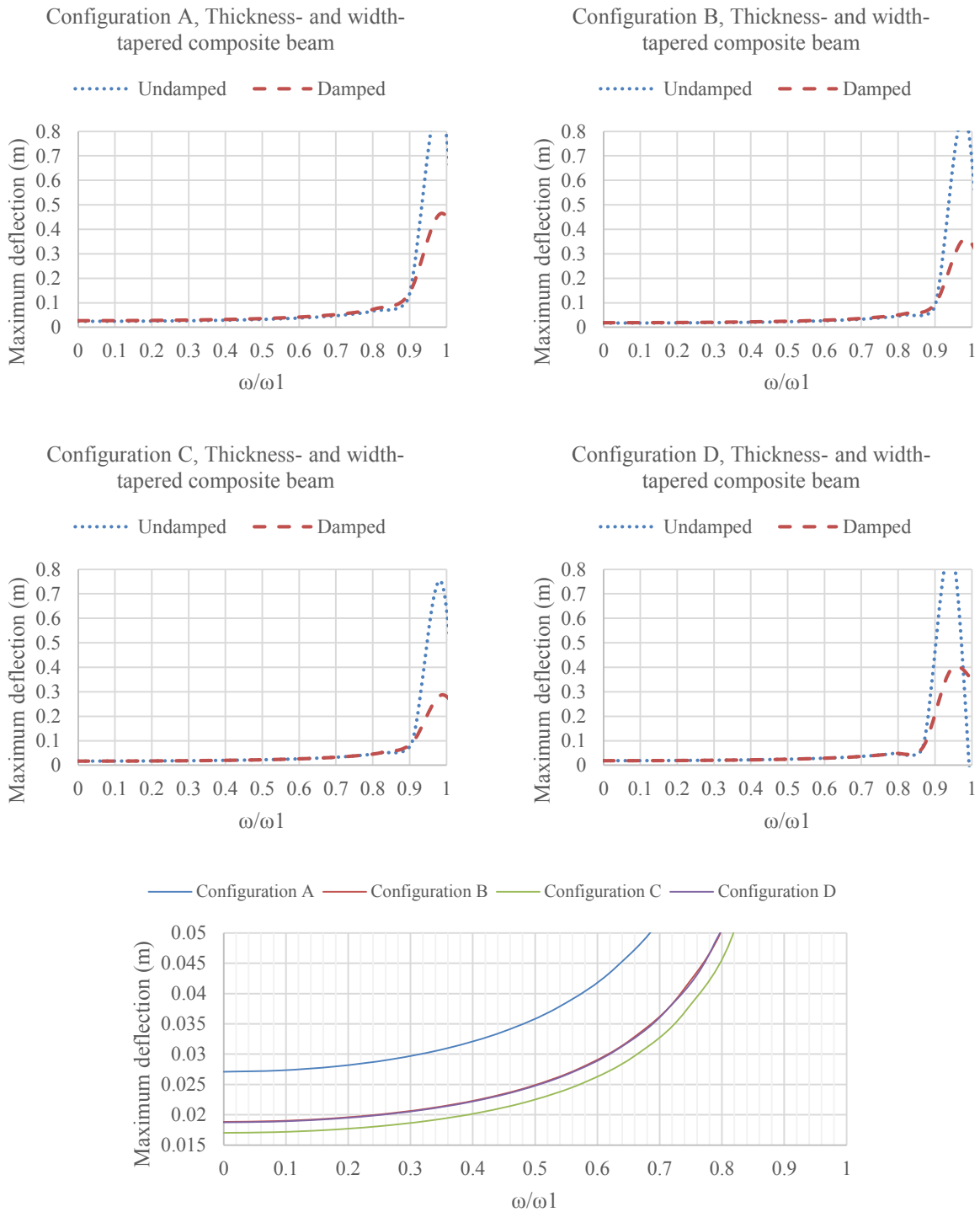


Figure 4.25b Magnified views of plots given in Figure 4.25a near 1st resonance

4.4 Summary

In this chapter forced vibration analysis was carried out on uniform and thickness- and width-tapered composite beams. The effects of main parameters (boundary condition, width-ratio and taper configuration) on the response were studied. Moreover, damped forced vibration analysis was carried out and the effects of damping on forced vibration response were presented. A summary of observations is given below:

- For the undamped beam, as the excitation frequency approaches the natural frequencies, the amplitude of the response reaches infinity. This causes instability of the response near the natural frequencies and therefore in this study, only a stable part of the response ($0 < \frac{\omega}{\omega_1} < 1$) is used for comparison.
- For the uniform composite beam, clamped-free boundary condition has the largest amplitude of response. Simply supported boundary condition has the second largest amplitude of response and clamped-clamped boundary condition has the smallest amplitude of response.
- For the thickness- and width-tapered composite beam (for all the taper configurations and width-ratios) free-clamped boundary condition has the largest amplitude of response. Clamped-free and simply supported boundary conditions have the second and the third largest amplitudes of response respectively. Clamped-clamped boundary condition has the smallest amplitude of response.
- For the thickness- and width-tapered composite beam, for all the boundary conditions taper configuration A has the largest amplitude of response. Configurations D and B have the second and the third largest amplitudes of responses and configuration C has the smallest amplitude of response.

- For the thickness- and width-tapered composite beam, for all the boundary conditions and taper configurations, by increasing the width-ratio, the amplitude of response decreases. The percentage of reduction is more significant for simply supported boundary condition compared to clamped-clamped and clamped-free boundary conditions.
- Addition of damping results in reduction of the amplitude of the response, especially near natural frequencies. The amount of reduction highly depends on the damping ratio (ξ) and therefore, the amount of reduction is larger for the second and the third natural frequencies (compared to the amount of reduction for the first natural frequency).
- Also, clamped-clamped boundary condition has the largest damping ratio (ξ) among all boundary conditions. Simply supported, clamped-free and free-clamped boundary conditions have the second, the third and the fourth largest damping ratios respectively. Therefore the amount of reduction for the clamped-clamped boundary condition is the largest for all the taper configurations. Simply supported and clamped-free boundary conditions have the second and the third highest amounts of reduction of the amplitudes of the response. Free-clamped boundary condition has the smallest amount of reduction of the amplitude of the response.

5. Conclusion and future work

5.1 Major contributions

In the present study, free and forced vibration analyses of tapered laminated composite beams were conducted using Hierarchical Finite Element Method (HFEM). The HFEM formulation of a laminated composite beam was carried out based on cylindrical bending theory. In the HFEM formulation two degrees of freedom (deflection and rotation) per node, two nodes per element and one trigonometric hierarchical term were considered. A comprehensive parametric study was conducted to study the effects of main parameters (boundary condition, width-ratio, thickness-taper angle, laminate configuration, thickness-taper configuration and compressive axial force) on free vibration frequency response of width-tapered, thickness-tapered and thickness- and width tapered composite beams.

Moreover, the effects of boundary condition, width-ratio, thickness-taper configuration and damping on the forced vibration response of the uniform and thickness- and width-tapered composite beams in terms of maximum deflection and maximum rotation were studied. The viscous damping of the beams was modeled using Rayleigh damping method.

5.2 Conclusions

The most important and principal conclusions of the present study are given below:

- HFEM gives more accurate results with the same number of elements compared to CFEM. Also, the natural frequencies reach the exact values with much less number of elements compared to CFEM.
- Adding the second hierarchical trigonometric term does not make a significant improvement in the accuracy nor the number of elements required to reach the exact values. As a result, in this study HFEM with one trigonometric hierarchical term is considered.
- For the width-tapered beam, the clamped-clamped boundary condition has the highest values of natural frequencies. With a rather large difference, the simply supported boundary condition has the second highest natural frequencies. Clamped-free and free-clamped boundary conditions have the third and fourth highest natural frequencies respectively, but the difference is not as significant. For the thickness-tapered beam, there is an overall decrease in all the natural frequencies (compared to width-tapered beam). However, the difference between the natural frequencies that correspond to clamped-free and free-clamped boundary conditions is much more significant. For the thickness- and width-tapered beam, the difference (compared to thickness-tapered beam) is not significant but the order of the effect of boundary condition is the same.
- By decreasing the length of the tapered beam (or equivalently increasing the thickness-taper angle while preserving the thicknesses at both sides of the beam), the natural frequencies increase dramatically for all boundary conditions and tapering types. For the width-tapered beam, as the length decreases, the clamped-free and free-clamped boundary conditions show the same rate of increase. Simply supported boundary condition has a higher rate of increase compared to

the clamped-free and the free-clamped boundary conditions. The clamped-clamped beam has the highest rate of increase in natural frequencies. For the other two tapering types, the clamped-free boundary condition has a much higher rate of increase compared to the free-clamped boundary condition but the other two boundary conditions follow the same pattern as that for the width-tapered beam.

- For all the tapering types, boundary conditions and taper configurations, the laminate configuration LC3 has the highest natural frequencies, LC2 has the lowest natural frequencies and LC1 and LC4 have the second and third highest natural frequencies respectively.
- For all the tapering types, boundary conditions and taper configurations, increasing the compressive axial force results in decreasing the natural frequencies. This is due to the fact that in the presence of compressive axial force after the initial deflection, the resultant moment pulls the beam further from its neutral position. Therefore the beam becomes more flexible and consequently the natural frequencies decrease. This decrease is more significant in the first natural frequencies (compared to the second and the third natural frequencies).
- By increasing the width-ratio for the width-tapered beam the natural frequencies increase for simply supported, clamped-clamped and free-clamped boundary conditions but they decrease for the clamped-free boundary condition. The reason is that by increasing the width-ratio, the additional material on the free side of the beam results in the corresponding changes in the stiffness and mass of the beam and consequently, decrease in natural frequencies. The thickness- and width-tapered beam shows a total decrease in natural frequencies (compared to width-tapered beam) but follows the same pattern.

- For the thickness-tapered beam, configuration C has the highest values of natural frequencies for all the boundary conditions. Configuration B has the second highest natural frequencies. Configuration D and configuration A come in third and fourth respectively. Because configuration A has the largest volume of resin compared to other configurations, it is less stiff and consequently has the lowest natural frequencies. Configuration D has less volume of resin than configuration A but much more than configurations B and C. Configuration C has the plies at a larger distance from the mid-plane and resin pockets at a smaller distance from the mid-plane, compared to configuration B and therefore has a slightly larger D_{11} value than configuration B and higher natural frequencies. Thickness- and width-tapered beam has slightly higher values of natural frequencies compared to the other two tapering types, but the effect of taper configuration on natural frequencies is the same.
- Overall, thickness-tapering has much more significant effect on natural frequencies than width-tapering. This comes from the fact that the difference between the natural frequencies of the thickness-tapered and the thickness- and width-tapered beams is not that significant. However, this difference is much more significant between the thickness-tapered and the width-tapered beams.
- For the uniform composite beam, clamped-free boundary condition has the largest amplitude of forced vibration response. Simply supported and clamped-clamped boundary conditions have the second and the third largest amplitudes of response respectively.
- For the thickness- and width-tapered composite beam (for all the taper configurations, laminate configurations and width-ratios) free-clamped boundary condition has the largest amplitude of response. Clamped-free and simply supported boundary conditions have the second

and the third largest amplitudes of response respectively. Clamped-clamped boundary condition has the smallest amplitude of response.

- For the thickness- and width-tapered composite beam, for all the boundary conditions taper configuration A has the largest amplitude of response. Configuration D and B have the second and the third largest amplitudes of responses and configuration C has the smallest amplitude of response.
- For the thickness- and width-tapered composite beam, for all the boundary conditions and taper configurations, by increasing the width-ratio, the amplitude of response decreases. The percentage of reduction is more significant for simply supported boundary condition compared to clamped-clamped and clamped-free boundary conditions.
- Addition of damping results in reduction of the amplitude of the response, especially near natural frequencies. The amount of reduction highly depends on the damping ratio (ξ) and therefore, the amount of reduction is larger for the second and the third natural frequencies (compared to the amount of reduction for the first natural frequencies).
- Also, clamped-clamped boundary condition has the largest damping ratio (ξ) among all boundary conditions. Simply supported, clamped-free and free-clamped boundary conditions have the second, the third and the fourth largest damping ratios respectively. Therefore the amount of reduction for the clamped-clamped boundary condition is the largest for all the taper configurations. Simply supported and clamped-free boundary conditions have the second and the third highest amounts of reduction of the amplitudes of the response. Free-clamped boundary condition has the smallest amount of reduction of the amplitude of the response.

5.3 Recommendations for future work

The presented study was an attempt to determine the effects of different material, geometrical and structural properties on the free vibration frequency response and the forced vibration response of the tapered composite beams. The author suggests the following as future work to complete the current study:

- Free and forced vibration analysis of the tapered composite beams considering the First order shear deformation theory (FSDT) using HFEM.
- Reliability analysis of the tapered composite beams by choosing the main parameters (that were studied in the present thesis) as random variables.
- Random vibration analysis of the tapered composite beams.

BIBLIOGRAPHY

- [1] O. O. Ochoa, J. N. Reddy, "Finite Element Analysis of Composite Laminates," Boston: Kluwer Academic Publishers, 1992.
- [2] Bhese. "Strategy Composite Materials & Structures".
Available at: <http://www.lr.tudelft.nl/?id=27470&L=1>
- [3] H. E. U. Ahmed, "Free and Forced Vibrations of Tapered Composite Beams Including the Effects of Axial Force and Damping," Montreal: Concordia University, 2008.
- [4] J. N. Reddy, "An Introduction to the Finite Element Method," New York: McGraw-Hill, 1993.
- [5] R. B. Abarcar and P. F. Cunniff, "The Vibration of Cantilever Beams of Fiber Reinforced Material," *Journal of Composite Materials*, vol. 6, pp. 504-517, 1972.
- [6] K. Chandrashekhara, K. Krishnamurthy and S. Roy, "Free Vibration of Composite Beams Including Rotary Inertia and Shear Deformation," *Composite Structures*, vol. 14, pp. 269-279, 1990.
- [7] A. K. Miller and D. F. Adams, "An Analytic Means of Determining the Flexural and Torsional Resonant Frequencies of Generally Orthotropic Beams," *Journal of Sound and Vibration*, vol. 41, pp. 433-449, 1975.
- [8] A. T. Chen and T. Y. Yang, "Static and Dynamic Formulation of a Symmetrically Laminated Beam Finite Element for a Microcomputer," *Journal of Composite Materials*, vol. 19, pp. 459-475, 1985.

- [9] J. R. Vinson, R. L. Sierakowski, and C. W. Bert, "The Behavior of Structures Composed of Composite Materials", *Journal of Applied Mechanics*, vol. 54, p. 249, 1987.
- [10] D. H. Hodges, A. R. Atilgan, C. E. S. Cesnik, and M. V. Fulton, "A Simplified Strain Energy Function for Geometrically Nonlinear Behaviour of Anisotropic Beams," *Composites Engineering*, vol. 2, pp. 513-526, 1992.
- [11] A. Khdeir, "Free Vibration of Cross-ply Laminated Beams with Arbitrary Boundary Conditions," *International Journal of Engineering Science*, vol. 32, pp. 1971-1980, 1994.
- [12] J. N. Reddy, "Mechanics of Laminated Composite Plates and Shells : Theory and Analysis," Boca Raton: CRC Press, 2004.
- [13] J. M. Bertholet, "Composite Materials : Mechanical Behavior and Structural Analysis," New York: Springer, 1999.
- [14] J. E. Whitney, "Structural Analysis of Laminated Anisotropic Plates," Lancaster, PA, U.S.A.: Technomic Pub. Co., 1987.
- [15] R. M. Jones, "Mechanics of Composite Materials," Philadelphia, PA: Taylor & Francis, 1999.
- [16] S. R. Marur and T. Kant , "Free Vibration Analysis of Fiber Reinforced Composite Beams using Higher-Order Theories and Finite Element Modelling," *Journal of Sound and Vibration*, vol. 194, pp. 337-351, 1996.
- [17] M. P. Singh and A. S. Abdelnaser, "Random Response of Symmetric Cross-ply Composite Beams with Arbitrary Boundary Conditions," *AIAA Journal*, vol. 30, pp. 1081-1088, 1992.
- [18] P. K. Roy and N. Ganesan, "Some Studies on the Response of a Tapered Beam," *Computers & Structures*, vol. 45, pp. 185-195, 1992.

- [19] K. He, S. V. Hoa, and R. Ganesan, "The Study of Tapered Laminated Composite Structures: A Review," *Composites Science and Technology*, vol. 60, pp. 2643-2657, 2000.
- [20] R. Ganesan and A. Zabihollah, "Vibration Analysis of Tapered Composite Beams using a Higher-Order Finite Element. Part I: Formulation," *Composite Structures*, vol. 77, pp. 306-318, 2007.
- [21] R. Ganesan and A. Zabihollah, "Vibration Analysis of Tapered Composite Beams using a Higher-Order Finite Element. Part II: Parametric Study," *Composite Structures*, vol. 77, pp. 319-330, 2007.
- [22] V. K. Badagi, "Dynamic Response of Width- and Thickness-Tapered Composite Beams using Rayleigh- Ritz Method and Modal Testing," Montreal: Concordia University, 2012.
- [23] S. H. Farghaly and R. M. Gadelrab, "Free Vibration of a Stepped Composite Timoshenko Cantilever Beam," *Journal of Sound and Vibration*, vol. 187, pp. 886-896, 1995.
- [24] O. C. Zienkiewicz, "The Finite Element Method," New York: McGraw-Hill, 1977.
- [25] R. D. Cook, D. S. Malkus and M. E. Plesha, "Concepts and Applications of Finite Element Analysis," New York: Wiley, 1989.
- [26] S. M. Ganesan and N. Nabi, "A Generalized Element for the Free Vibration Analysis of Composite Beams," *Computers and Structures*, vol. 51, pp. 607-610, 1994.
- [27] L. Chen, "Free Vibration Analysis of Tapered Composite Beams using Hierarchical Finite Element Method," Montreal: Concordia University, 2004.
- [28] A. W. Lees and D. L. Thomas, "Modal Hierarchical Timoshenko Beam Finite Elements," *Journal of Sound and Vibration*, vol. 99, pp. 455-461, 1985.

- [29] N. S. Bardell, "Free Vibration Analysis of a Flat Plate using the Hierarchical Finite Element Method," *Journal of Sound and Vibration*, vol. 151, pp. 263-289, 1991.
- [30] Z. Yu, X. Guo, and F. Chu, "A Multivariable Hierarchical Finite Element for Static and Dynamic Vibration Analysis of beams," *Finite Elements in Analysis and Design*, vol. 46, pp. 625-631, 2010.
- [31] P. Ribeiro and M. Petyt, "Non-linear Vibration of Composite Laminated Plates by the Hierarchical Finite Element Method," *Composite Structures*, vol. 46, pp. 197-208, 1999.
- [32] W. Han and M. Petyt, "Linear Vibration Analysis of Laminated Rectangular Plates using the Hierarchical Finite Element Method - I. Free Vibration Analysis," *Computers & Structures*, vol. 61, pp. 705-712, 1996.
- [33] W. Han and M. Petyt, "Linear Vibration Analysis of Laminated Rectangular Plates using the Hierarchical Finite Element Method - II. Forced Vibration Analysis," *Computers & Structures*, vol. 61, pp. 713-724, 1996.
- [34] <http://www.newportad.com/pdf/PL-NB-301.pdf>.
- [35] J. N. Reddy, "Mechanics of Laminated Composite Plates: Theory and Analysis," CRC Press, Inc., 1997.
- [36] P. Salajegheh, "Vibrations of Thickness-and-width Tapered Laminated Composite Beams with Rigid and Elastic Supports," Montreal: Concordia University, 2013.
- [37] M. D. Thomson and W. T. Dahleh, "Theory of Vibration with Applications," Upper Saddle River, N.J.: Prentice Hall, 1998.
- [38] http://www.totalhockey.com/product/11K_Tapered_Composite_Blade/itm/5472-41/
- [39] http://www.hockeyworld.com/index/page/product/product_id/10075

- [40] <http://airpigz.com/blog/2010/11/29/algie-composite-aircraft-lp1-385-mph-at-fl290-145-gph.html>
- [41] <http://www.fastcompany.com/1208530/nasa-invents-shape-shifting-helicopter-blade>
- [42] <http://blog.settleindenmark.com/siemens-tested-it-75m-long-rotor-blades-in-denmark/>

APPENDIX A

Table A.1 The first three natural frequencies of a width-tapered composite beam for different width ratios - A comparison between HFEM, HOFEM and R-R methods ($b_R/b_L = 0.01$)

b_R/b_L	0.01					
		R-R	HOFEM	HFEM	Difference (%) R-R	Difference (%) HOFEM
S-S	ω_1 (rad/s)	1198.5	1199.32	1199.49	0.08	0.01
	ω_2 (rad/s)	5055.5	5055.28	5056.53	0.02	0.02
	ω_3 (rad/s)	11438	11428.2	11433.65	0.04	0.05
C-C	ω_1 (rad/s)	2474.9	2439.11	2473.47	0.06	1.41
	ω_2 (rad/s)	7264.3	7159.2	7254.54	0.13	1.33
	ω_3 (rad/s)	14657	14504.74	14697.61	0.28	1.33
C-F	ω_1 (rad/s)	902.44	903.69	903.79	0.15	0.01
	ω_2 (rad/s)	3916.8	3921.75	3922.61	0.15	0.02
	ω_3 (rad/s)	9530.7	9541.81	9545.58	0.16	0.04
F-C	ω_1 (rad/s)	151.1	150.11	155.54	2.94	3.62
	ω_2 (rad/s)	2019.4	2014.95	2048.23	1.43	1.65
	ω_3 (rad/s)	6879.4	6868.19	6961.83	1.20	1.36

Table A.2 The first three natural frequencies of a width-tapered composite beam for different width ratios - A comparison between HFEM, HOFEM and R-R methods ($b_R/b_L = 0.02$)

b_R/b_L	0.02					
		R-R	HOFEM	HFEM	Difference (%) R-R	Difference (%) HOFEM
S-S	ω_1 (rad/s)	1203	1204.21	1204.38	0.11	0.01
	ω_2 (rad/s)	5062.9	5065.42	5066.74	0.08	0.03
	ω_3 (rad/s)	11446	11445.58	11451.45	0.05	0.05
C-C	ω_1 (rad/s)	2511.3	2494.86	2512.17	0.03	0.69
	ω_2 (rad/s)	7328.2	7273.14	7324.92	0.04	0.71
	ω_3 (rad/s)	14754	14679.47	14791.31	0.25	0.76
C-F	ω_1 (rad/s)	885.7	886.91	887	0.15	0.01
	ω_2 (rad/s)	3850.6	3855.48	3856.27	0.15	0.02
	ω_3 (rad/s)	9384.6	9395.68	9399.08	0.15	0.04
F-C	ω_1 (rad/s)	167.12	167.18	169.43	1.38	1.35
	ω_2 (rad/s)	2075	2076.36	2093.02	0.87	0.80
	ω_3 (rad/s)	6980.6	6985.16	7035.84	0.79	0.73

Table A.3 The first three natural frequencies of a width-tapered composite beam for different width ratios - A comparison between HFEM, HOFEM and R-R methods ($b_R/b_L = 0.05$)

b_R/b_L	0.05					
		R-R	HOFEM	HFEM	Difference (%) R-R	Difference (%) HOFEM
S-S	ω_1 (rad/s)	1214.1	1215.7	1215.8	0.14	0.01
	ω_2 (rad/s)	5077.3	5082.88	5083.77	0.13	0.02
	ω_3 (rad/s)	11460	11469.56	11474.17	0.12	0.04
C-C	ω_1 (rad/s)	2591.3	2590.94	2594.72	0.13	0.15
	ω_2 (rad/s)	7470.2	7462.21	7475.59	0.07	0.18
	ω_3 (rad/s)	14971	14958.4	14993.06	0.15	0.23
C-F	ω_1 (rad/s)	840.96	842.11	842.19	0.15	0.01
	ω_2 (rad/s)	3691.5	3696.27	3696.89	0.15	0.02
	ω_3 (rad/s)	9067.8	9079.05	9081.71	0.15	0.03
F-C	ω_1 (rad/s)	198.79	199.16	199.48	0.35	0.16
	ω_2 (rad/s)	2185.9	2189.56	2193.11	0.33	0.16
	ω_3 (rad/s)	7172.5	7184.04	7197	0.34	0.18

Table A.4 The first three natural frequencies of a width-tapered composite beam for different width ratios - A comparison between HFEM, HOFEM and R-R methods ($b_R/b_L = 0.1$)

b_R/b_L	0.1					
		R-R	HOFEM	HFEM	Difference (%) R-R	Difference (%) HOFEM
S-S	ω_1 (rad/s)	1227.4	1229.11	1229.15	0.14	0.00
	ω_2 (rad/s)	5087.8	5094.4	5094.81	0.14	0.01
	ω_3 (rad/s)	11464	11478.05	11481.09	0.15	0.03
C-C	ω_1 (rad/s)	2673.6	2676.97	2677.5	0.15	0.02
	ω_2 (rad/s)	7614.4	7620.69	7623.23	0.12	0.03
	ω_3 (rad/s)	15188	15177.87	15188.52	0.00	0.07
C-F	ω_1 (rad/s)	780.66	781.71	781.77	0.14	0.01
	ω_2 (rad/s)	3510.7	3515.27	3515.72	0.14	0.01
	ω_3 (rad/s)	8759.7	8770.84	8772.88	0.15	0.02
F-C	ω_1 (rad/s)	232.94	233.32	233.32	0.16	0.00
	ω_2 (rad/s)	2299.5	2303.09	2303.52	0.17	0.02
	ω_3 (rad/s)	7347.8	7359.31	7361.73	0.19	0.03

Table A.5 The first three natural frequencies of a width-tapered composite beam for different width ratios - A comparison between HFEM, HOFEM and R-R methods ($b_R/b_L = 0.4$)

b_R/b_L	0.4					
		R-R	HOFEM	HFEM	Difference (%) R-R	Difference (%) HOFEM
S-S	ω_1 (rad/s)	1259.9	1261.39	1261.4	0.12	0.00
	ω_2 (rad/s)	5085.7	5091.9	5092.02	0.12	0.00
	ω_3 (rad/s)	11439	11453.15	11455.45	0.14	0.02
C-C	ω_1 (rad/s)	2835.8	2839.29	2839.27	0.12	0.00
	ω_2 (rad/s)	7873.7	7883.45	7883.8	0.13	0.00
	ω_3 (rad/s)	15485	15504.47	15511.12	0.17	0.04
C-F	ω_1 (rad/s)	589.8	590.5	590.52	0.12	0.00
	ω_2 (rad/s)	3089.8	3093.44	3093.58	0.12	0.00
	ω_3 (rad/s)	8200.2	8209.93	8211.02	0.13	0.01
F-C	ω_1 (rad/s)	341.34	341.77	341.76	0.12	0.00
	ω_2 (rad/s)	2599.3	2602.53	2602.46	0.12	0.00
	ω_3 (rad/s)	7708.9	7718.54	7718.95	0.13	0.01

Table A.6 The first three natural frequencies of a width-tapered composite beam for different width ratios - A comparison between HFEM, HOFEM and R-R methods ($b_R/b_L = 0.6$)

b_R/b_L	0.6					
		R-R	HOFEM	HFEM	Difference (%) R-R	Difference (%) HOFEM
S-S	ω_1 (rad/s)	1266.5	1267.88	1267.88	0.11	0.00
	ω_2 (rad/s)	5081.5	5087.07	5087.18	0.11	0.00
	ω_3 (rad/s)	11432	11444.15	11446.53	0.13	0.02
C-C	ω_1 (rad/s)	2864.6	2867.75	2867.75	0.11	0.00
	ω_2 (rad/s)	7915.2	7923.87	7924.32	0.12	0.01
	ω_3 (rad/s)	15533	15549.98	15557.16	0.16	0.05
C-F	ω_1 (rad/s)	527.05	527.62	527.63	0.11	0.00
	ω_2 (rad/s)	2974.1	2977.28	2977.36	0.11	0.00
	ω_3 (rad/s)	8075.8	8084.5	8085.48	0.12	0.01
F-C	ω_1 (rad/s)	386.35	386.79	386.77	0.11	0.01
	ω_2 (rad/s)	2701.1	2704.12	2704.08	0.11	0.00
	ω_3 (rad/s)	7809.6	7818.32	7818.89	0.12	0.01

Table A.7 The first three natural frequencies of a width-tapered composite beam for different width ratios - A comparison between HFEM, HOFEM and R-R methods ($b_R/b_L = 0.8$)

b_R/b_L	0.8					
		R-R	HOFEM	HFEM	Difference (%) R-R	Difference (%) HOFEM
S-S	ω_1 (rad/s)	1269.2	1270.44	1270.44	0.10	0.00
	ω_2 (rad/s)	5079.9	5084.81	5084.92	0.10	0.00
	ω_3 (rad/s)	11429	11440.43	11442.84	0.12	0.02
C-C	ω_1 (rad/s)	2875.9	2878.71	2878.72	0.10	0.00
	ω_2 (rad/s)	7931.3	7938.96	7939.44	0.10	0.01
	ω_3 (rad/s)	15552	15566.62	15573.99	0.14	0.05
C-F	ω_1 (rad/s)	484.13	484.6	484.6	0.10	0.00
	ω_2 (rad/s)	2895.1	2897.87	2897.91	0.10	0.00
	ω_3 (rad/s)	7996.6	8004.25	8005.11	0.11	0.01
F-C	ω_1 (rad/s)	422.33	422.74	422.73	0.09	0.00
	ω_2 (rad/s)	2776	2778.65	2778.65	0.10	0.00
	ω_3 (rad/s)	7881.6	7889.28	7889.97	0.11	0.01

Table A.8 The first three natural frequencies of a width-tapered composite beam for different width ratios - A comparison between HFEM, HOFEM and R-R methods ($b_R/b_L = 1.0$)

b_R/b_L	1.0					
		R-R	HOFEM	HFEM	Difference (%) R-R	Difference (%) HOFEM
S-S	ω_1 (rad/s)	1270	1271.06	1271.06	0.08	0.00
	ω_2 (rad/s)	5080	5084.23	5084.34	0.09	0.00
	ω_3 (rad/s)	11430	11439.52	11441.93	0.10	0.02
C-C	ω_1 (rad/s)	2879	2881.34	2881.35	0.08	0.00
	ω_2 (rad/s)	7936	7942.54	7943.03	0.09	0.01
	ω_3 (rad/s)	15558	15570.55	15577.96	0.13	0.05
C-F	ω_1 (rad/s)	452.44	452.81	452.81	0.08	0.00
	ω_2 (rad/s)	2835.4	2837.71	2837.73	0.08	0.00
	ω_3 (rad/s)	7939.1	7945.68	7946.46	0.09	0.01
F-C	ω_1 (rad/s)	452.44	452.81	452.81	0.08	0.00
	ω_2 (rad/s)	2835.4	2837.71	2837.73	0.08	0.00
	ω_3 (rad/s)	7939.1	7945.68	7946.46	0.09	0.01

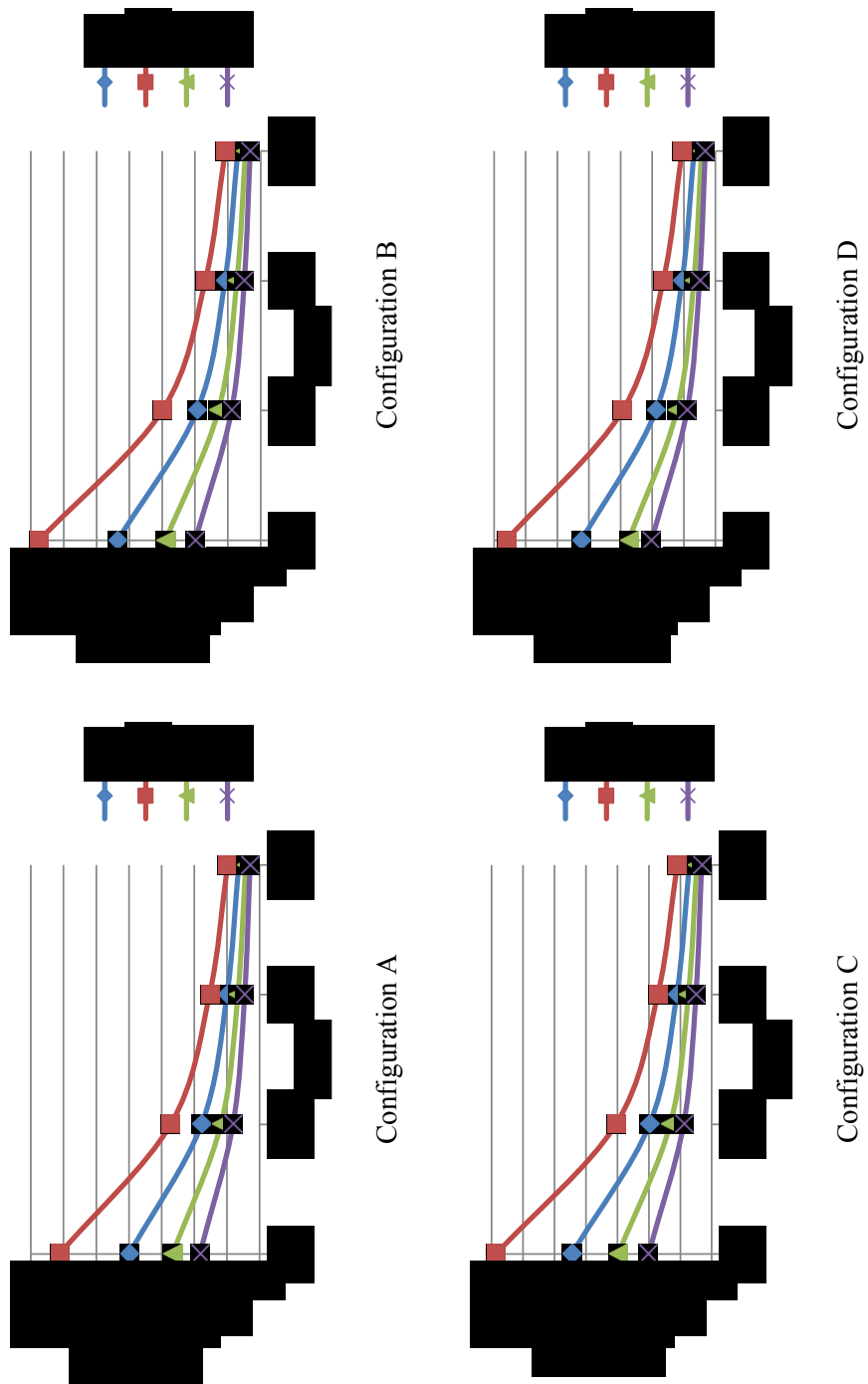


Figure A.0.1 Effect of the length on the second natural frequency of the thickness-tapered composite beam

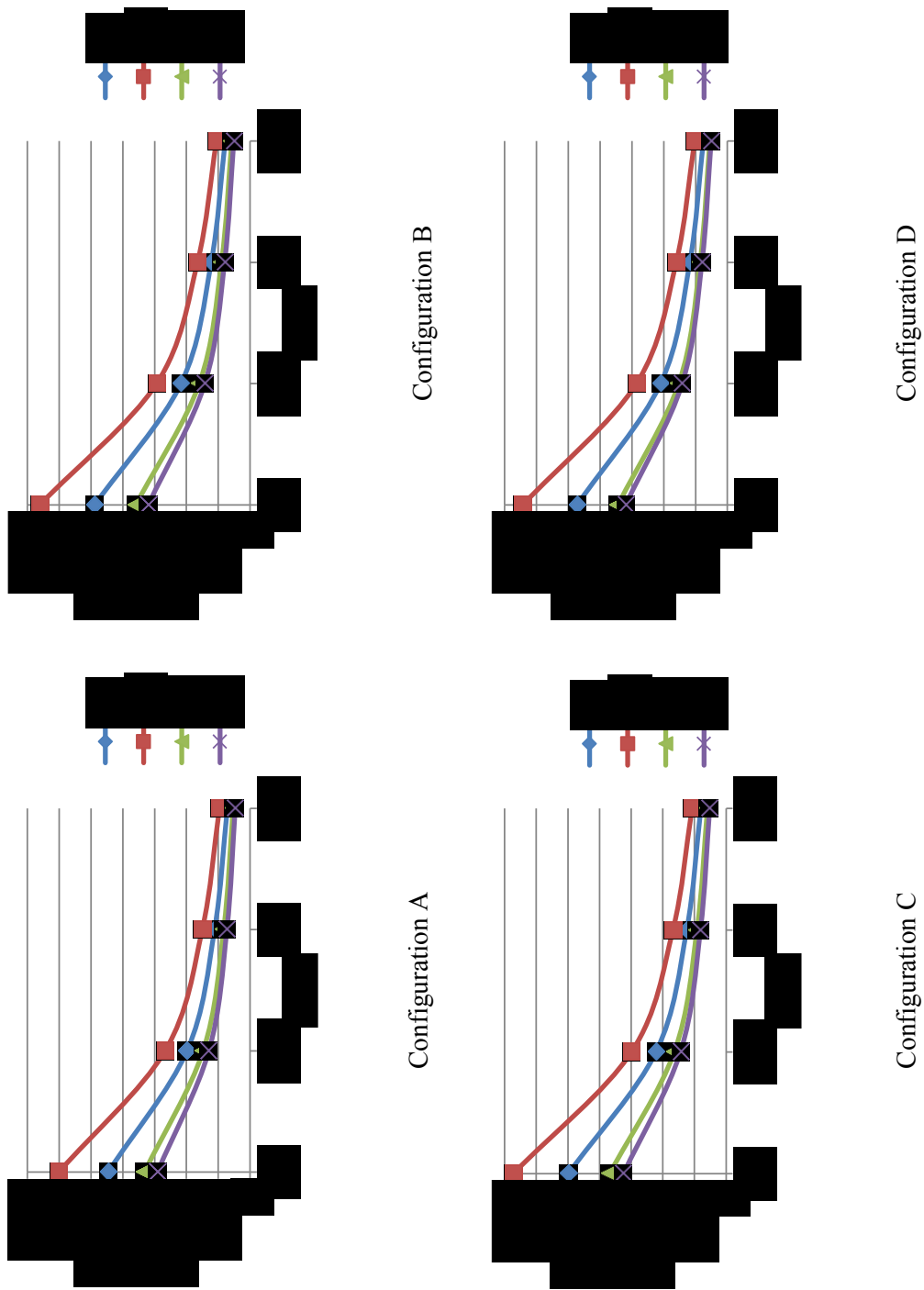


Figure A.0.2 Effect of the length on the third natural frequency of the thickness-tapered composite beam

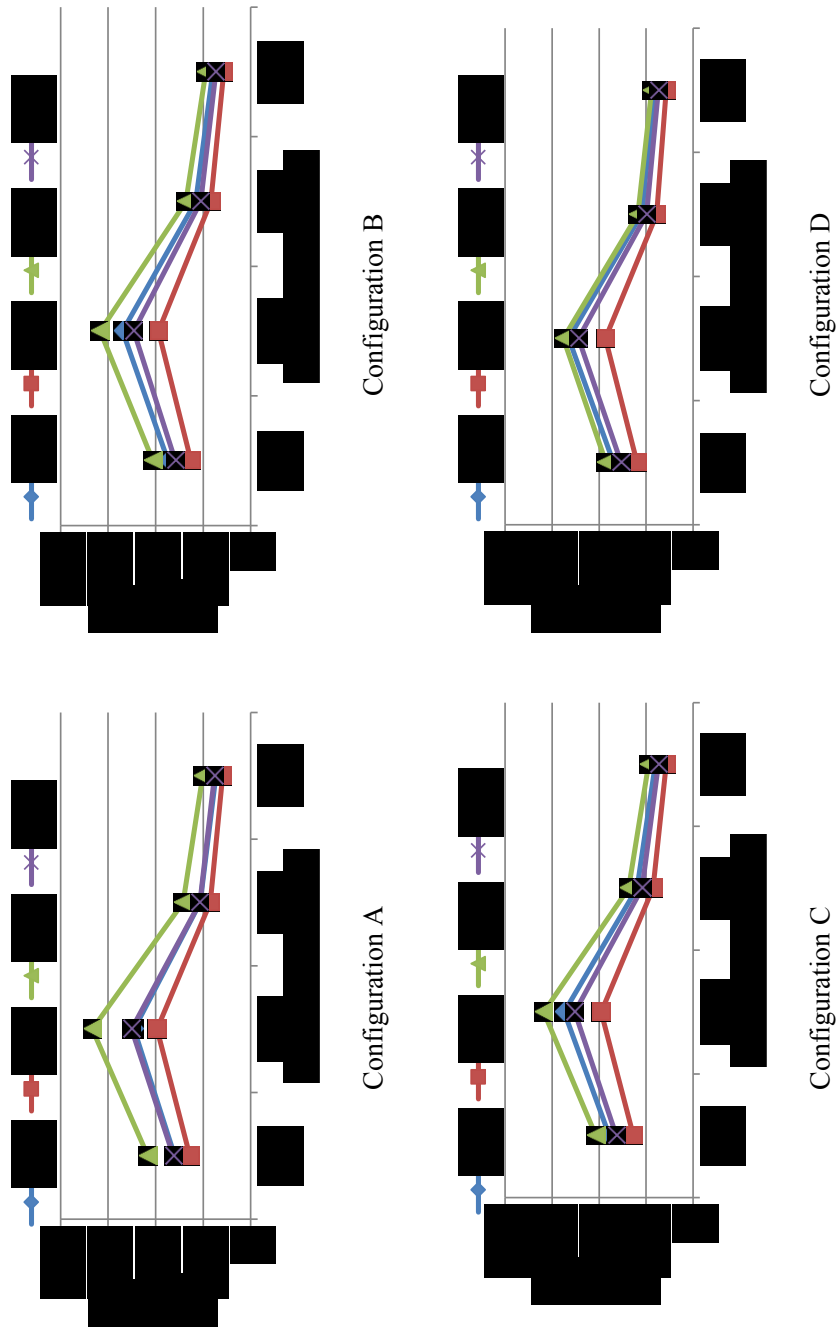


Figure A.0.3 Effect of the laminate configuration on the second natural frequency of the thickness-tapered composite beam

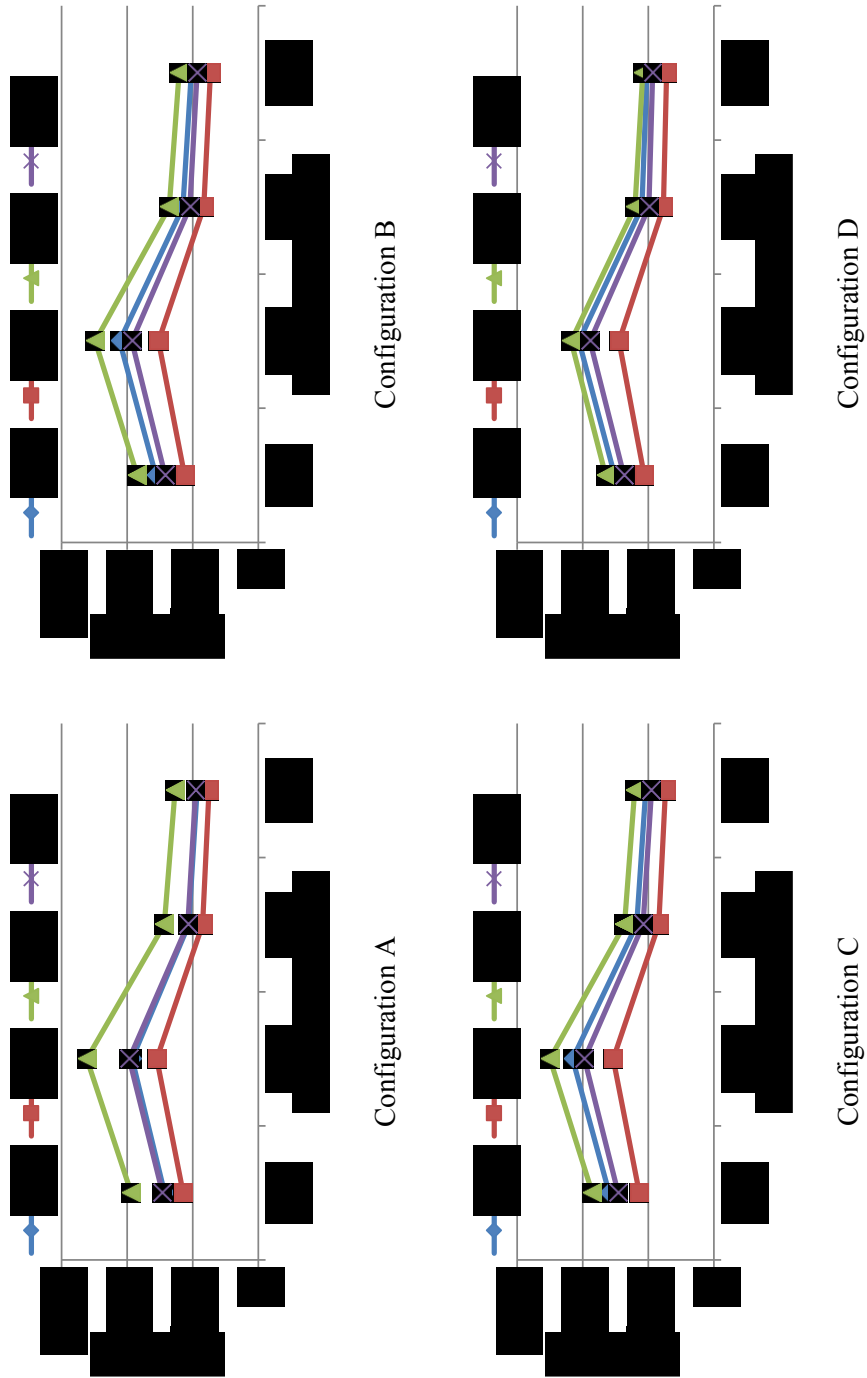


Figure A.0.4 Effect of the laminate configuration on the third natural frequency of the thickness-tapered composite beam

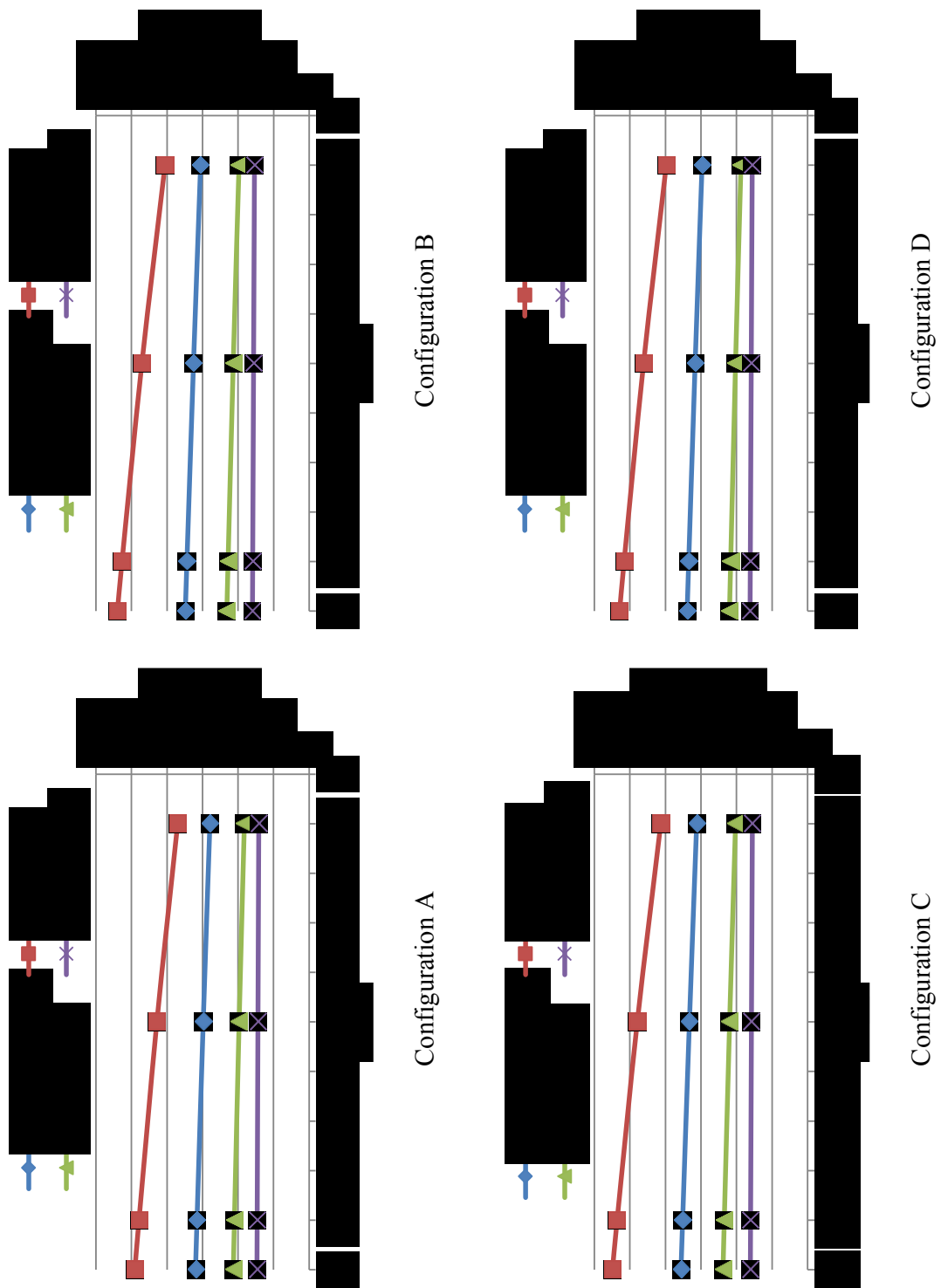


Figure A.0.5 Effect of compressive axial force on the second natural frequency of the thickness-tapered composite beam

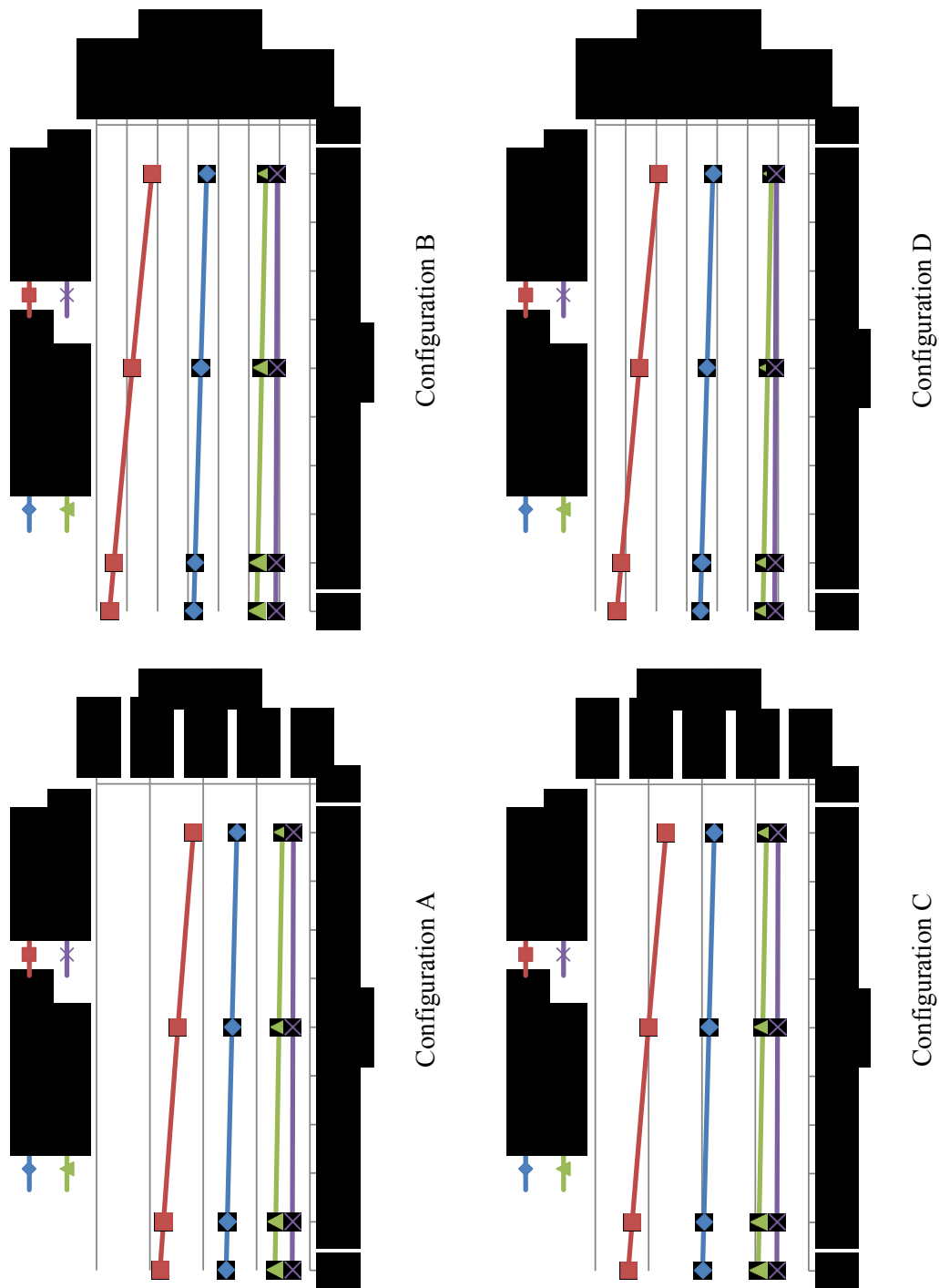


Figure A.0.6 Effect of compressive axial force on the third natural frequency thickness-tapered composite beam

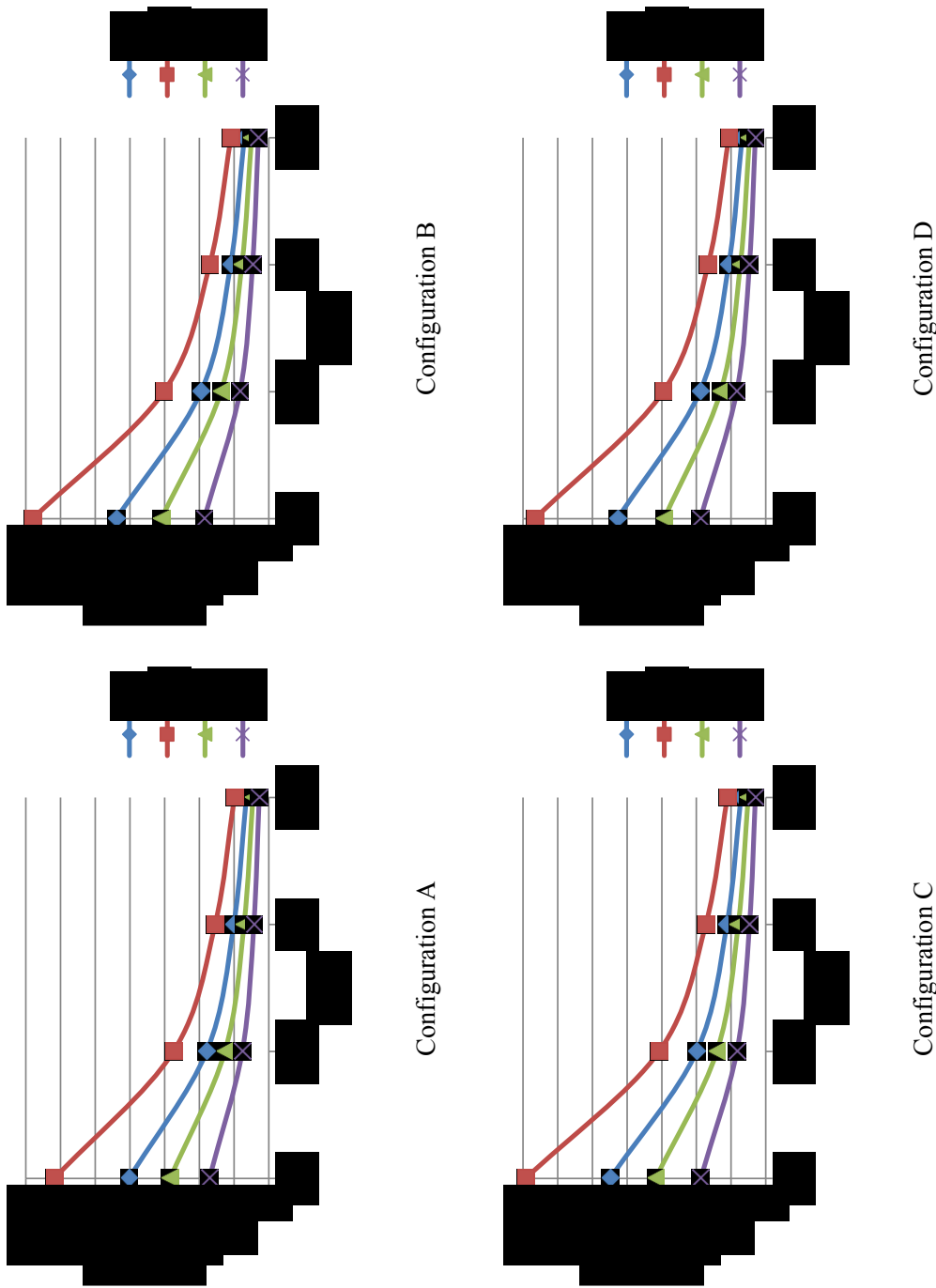


Figure A.0.7 Effect of the length on the second natural frequency of the thickness- and width-tapered composite beam

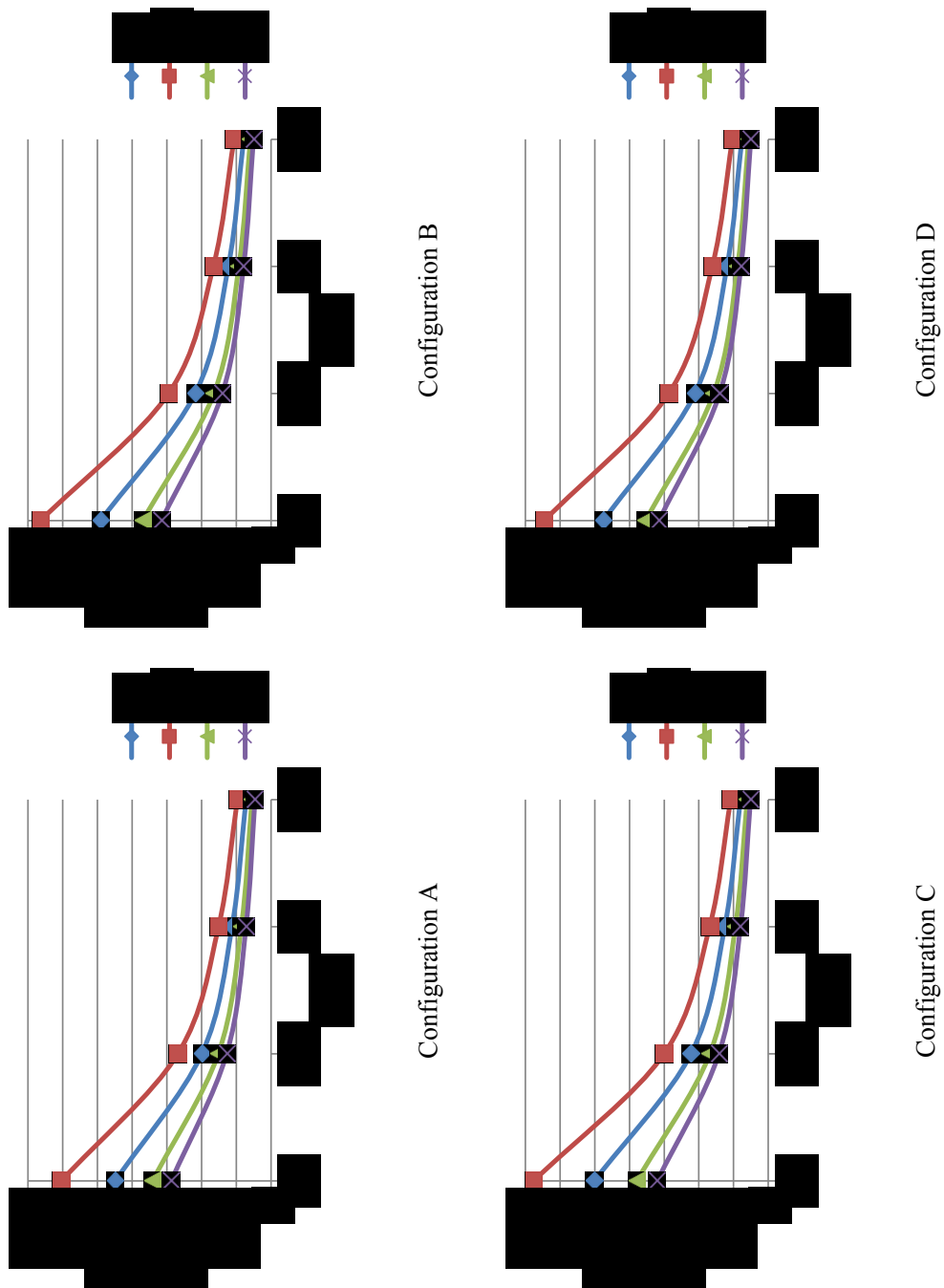


Figure A.0.8 Effect of the length on the third natural frequency of the thickness- and width-tapered composite beam

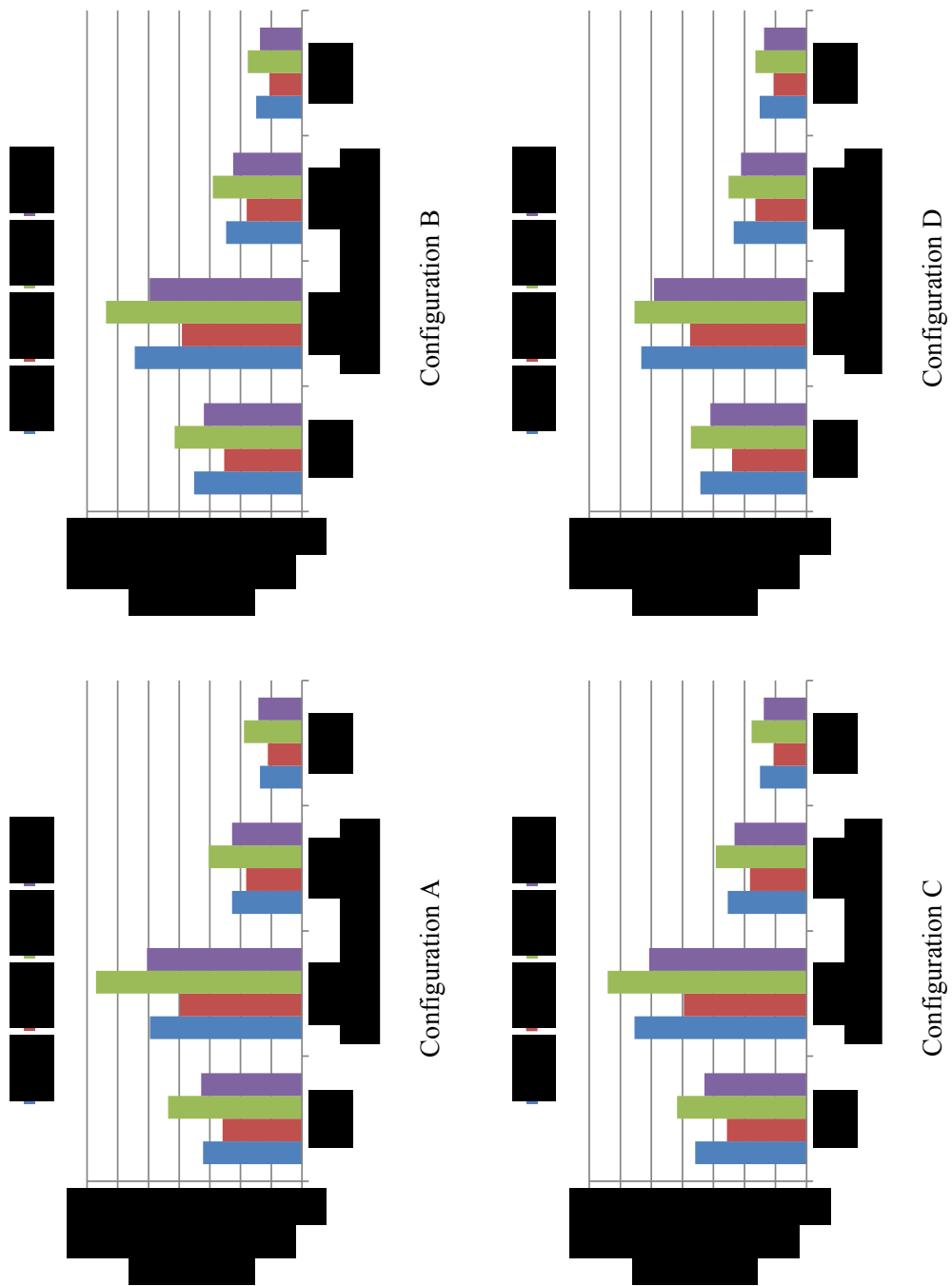


Figure A.0.9 Effect of laminate configuration on the second natural frequency of the thickness- and width-tapered composite beam

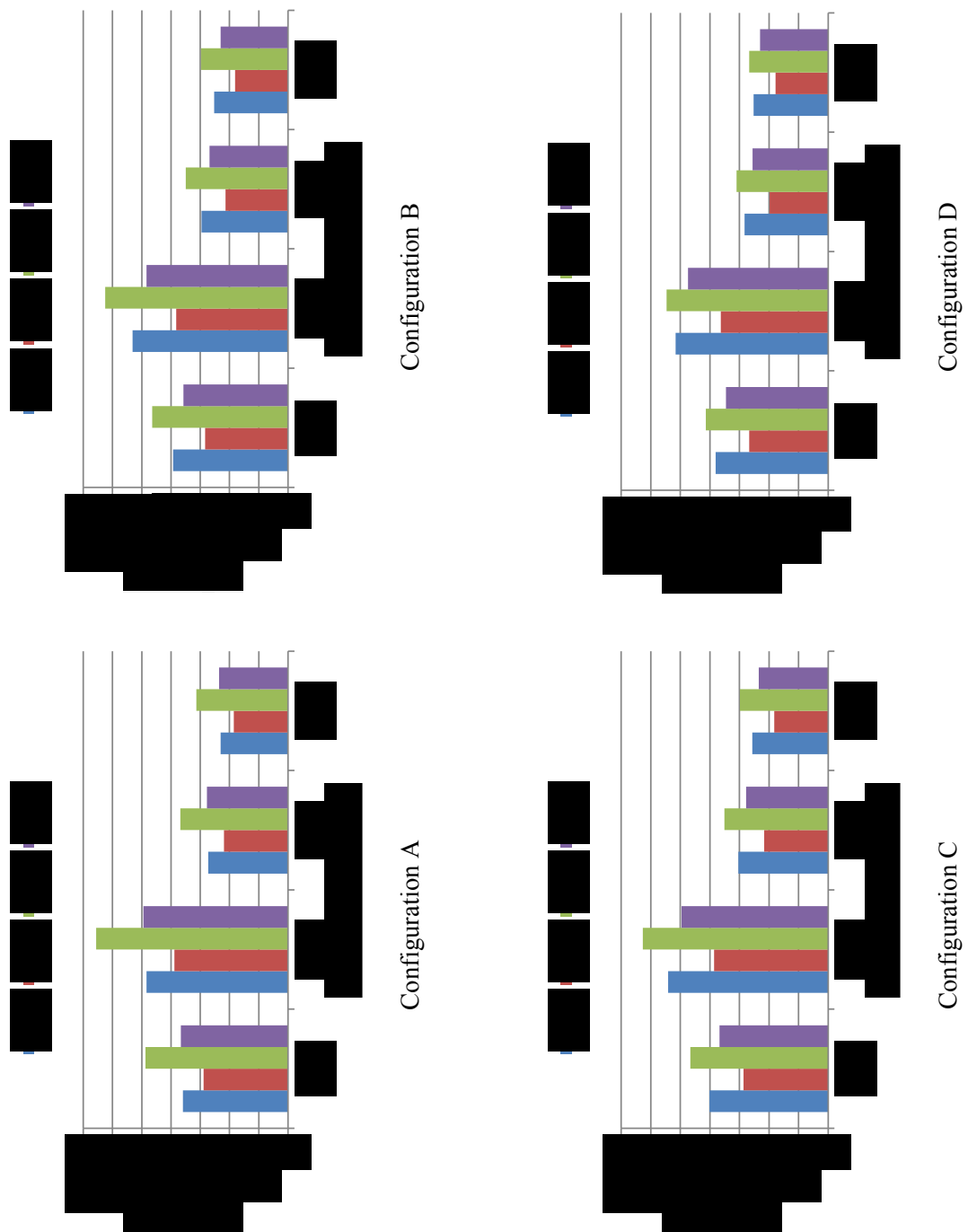


Figure A.0.10 Effect of laminate configuration on the third natural frequency of thickness- and width-tapered composite beam

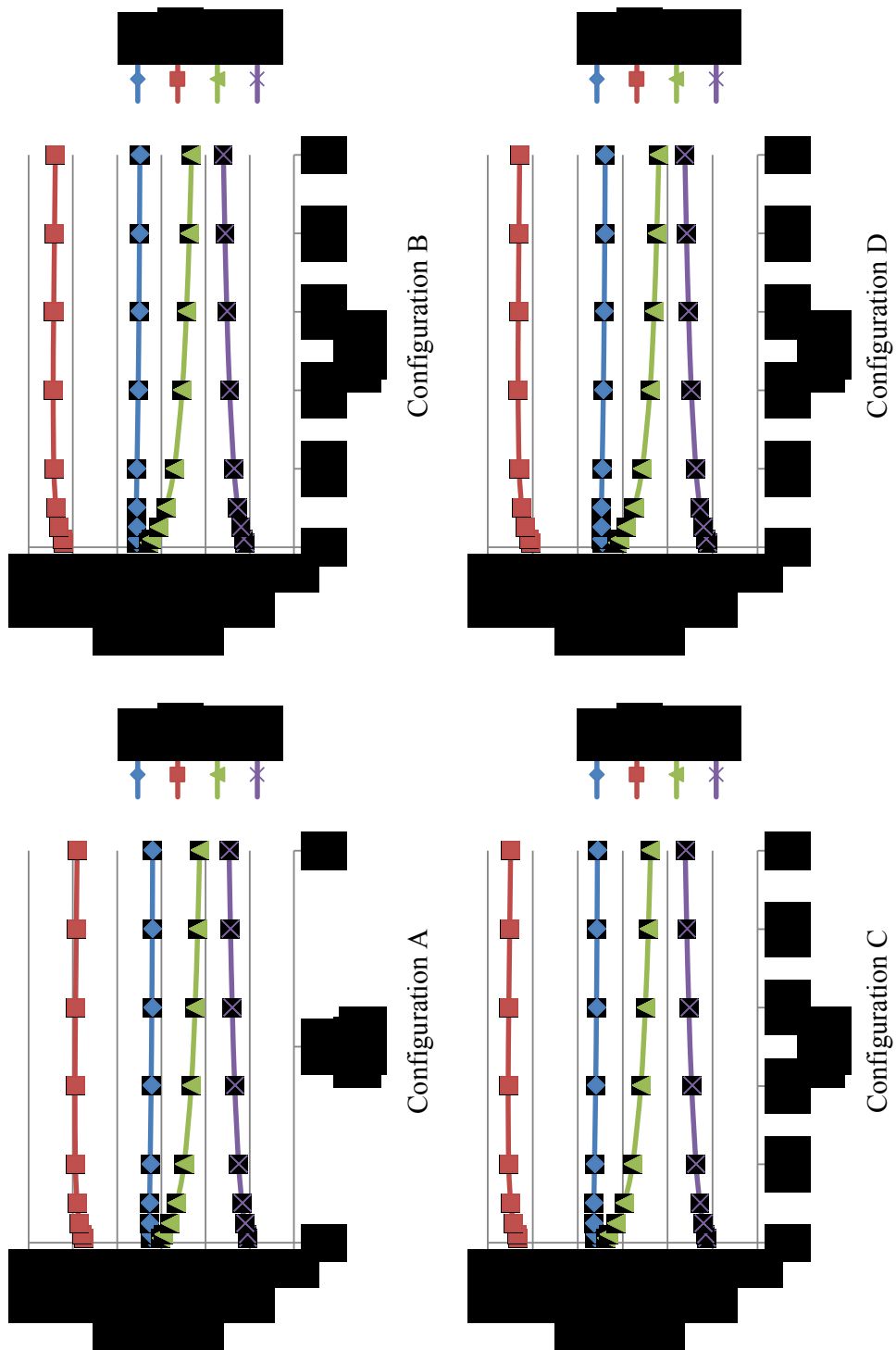


Figure A.0.11 Effect of width-ratio on the second natural frequency of the thickness- and width-tapered composite beam

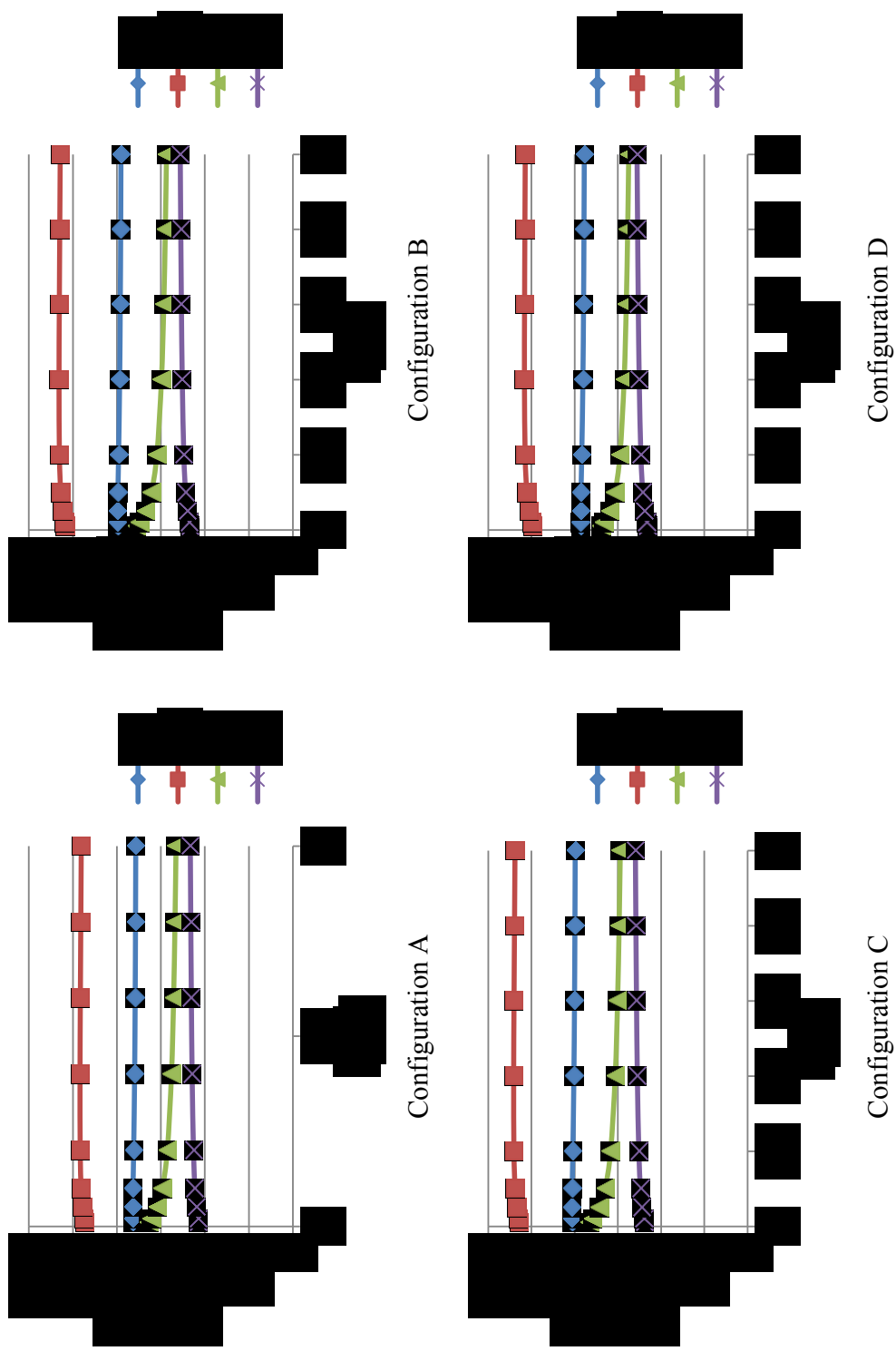


Figure A.0.12 Effect of width-ratio on the third natural frequency of the thickness- and width-tapered composite beam

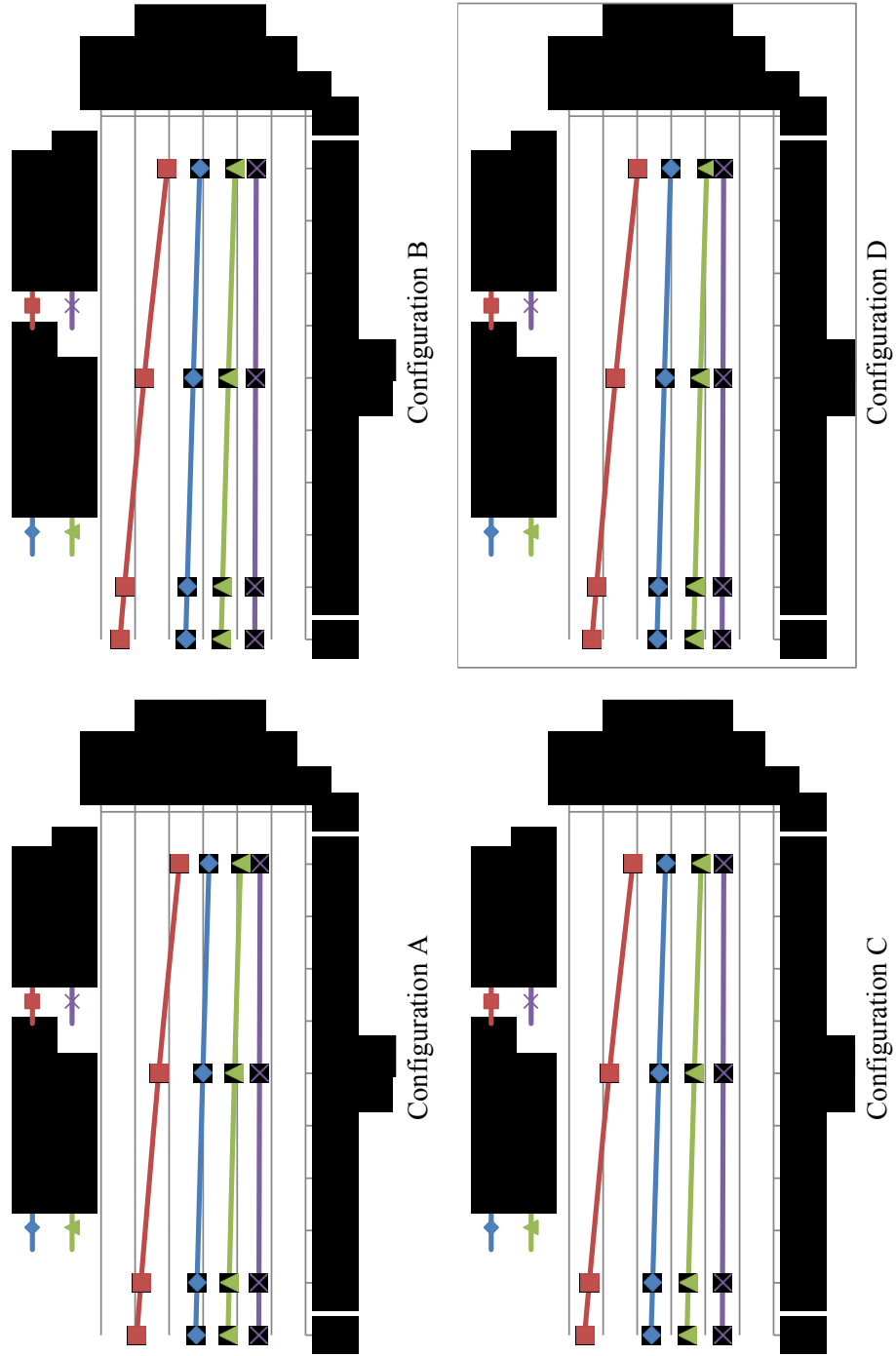


Figure A.0.13 Effect of compressive axial force on the second natural frequency of the thickness- and width-tapered composite beam

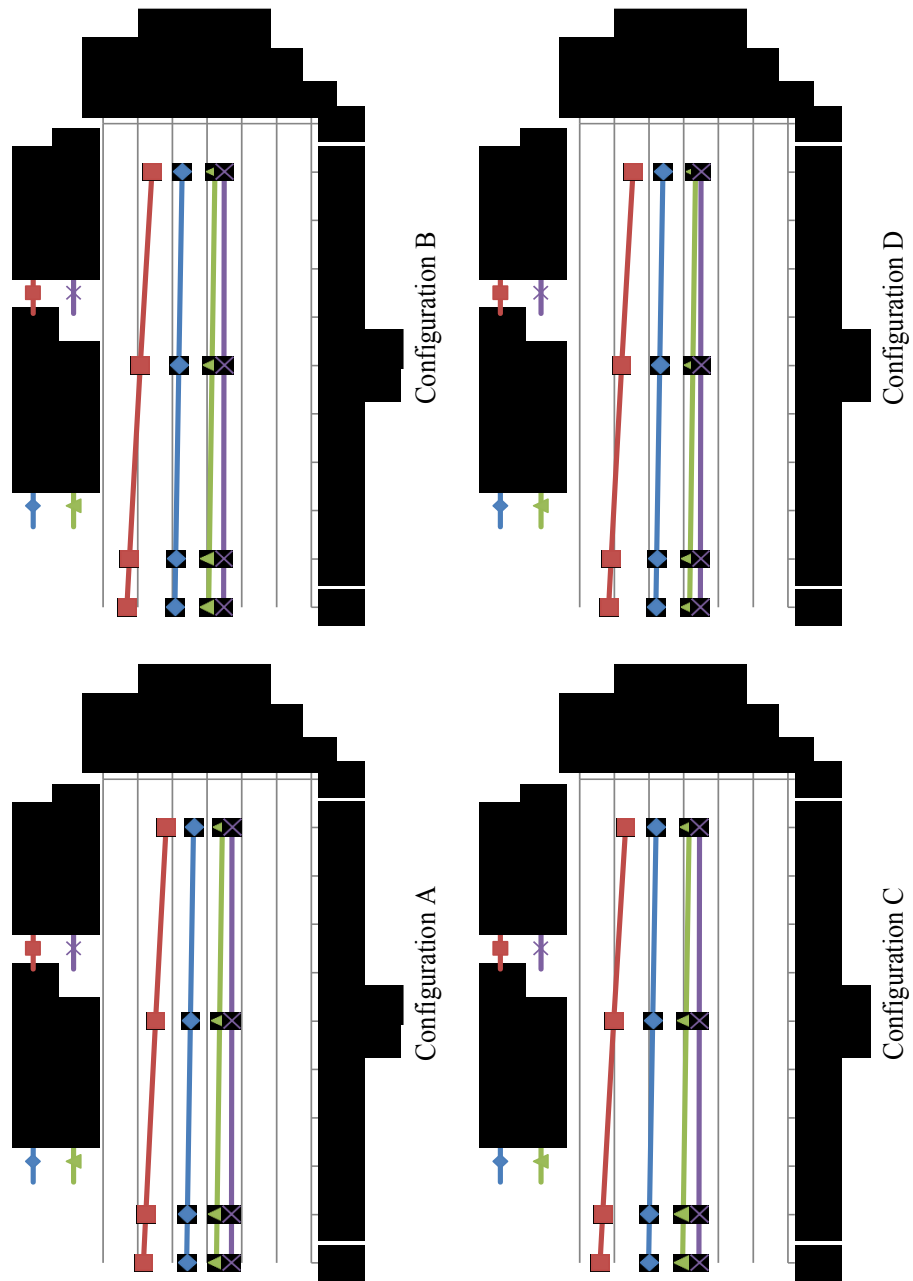


Figure A.0.14 Effect of compressive axial force on the third natural frequency of the thickness- and width-tapered composite beam

APPENDIX B

Table B.1 shows assembly algorithm of K and M matrices in CFEM for a composite beam divided into 6 elements. Each element has 2 nodes and each node has 2 degrees of freedom (w_i and θ_i). Each color represents an element's k or m matrix. In the areas that two matrices overlap, the two corresponding matrix elements are being added together.

Table B.1 Assembly algorithm of K and M matrices in CFEM

	1	2	3	4	5	6	7	8	9	10	11	12	13	14	
1															w_1
2															θ_1
3															w_2
4															θ_2
5															w_3
6															θ_3
7															w_4
8															θ_4
9															w_5
10															θ_5
11															w_6
12															θ_6
13															w_7
14															θ_7

In the hierarchical finite element method (HFEM) with one trigonometric term, each element's stiffness (k) or mass (m) matrix is a 5×5 matrix. The fifth row and the fifth column are the hierarchical terms corresponding to hierarchical non-physical degree of freedom (A_i) to complete the form of a square matrix. As it is shown in Table B.2 the global stiffness (K) and mass (M) matrices are assembled in the same manner as CFEM for the first four rows and columns. And the hierarchical terms fill the rest of the matrix.

Table B.2 Assembly algorithm of K and M matrices in HFEM with one hierarchical term

	1	2	3	4	5	6	7	8	9	10	11	12	13	14	15	16	17	18	19	20		
1	Blue	Blue	Blue	Blue											Blue						w_1	
2	Blue	Blue	Blue	Blue											Blue							θ_1
3	Blue	Blue	Red	Red	Red	Red									Blue	Red						w_2
4	Blue	Blue	Red	Red	Red	Red									Blue	Red						θ_2
5			Red	Red	Green	Green	Green	Green								Red	Green					w_3
6			Red	Red	Green	Green	Green	Green								Red	Green					θ_3
7					Green	Green	Dark Purple	Dark Purple	Purple	Purple							Green	Purple				w_4
8					Green	Green	Dark Purple	Dark Purple	Purple	Purple							Green	Purple				θ_4
9							Purple	Purple	Brown	Brown	Orange	Orange						Purple	Orange			w_5
10							Purple	Purple	Brown	Brown	Orange	Orange						Purple	Orange			θ_5
11									Orange	Orange	Dark Teal	Dark Teal	Teal	Teal					Orange	Teal		w_6
12									Orange	Orange	Dark Teal	Dark Teal	Teal	Teal					Orange	Teal		θ_6
13											Teal	Teal	Teal	Teal						Teal		w_7
14											Teal	Teal	Teal	Teal						Teal		θ_7
15	Blue	Blue	Blue	Blue											Blue							A_1
16			Red	Red	Red	Red										Red						A_2
17					Green	Green	Green	Green									Green					A_3
18							Purple	Purple	Purple	Purple								Purple				A_4
19									Orange	Orange	Orange	Orange							Orange			A_5
20											Teal	Teal	Teal	Teal						Teal		A_6